Spring 4-18-2013

Investigation Of The Rescue Of The Rubella Virus P150 Replicase Protein Q Domain By The Capsid Protein

Heather Mousa

INVESTIGATION OF THE RESCUE OF THE RUBELLA VIRUS P150 REPLICASE PROTEIN Q DOMAIN BY THE CAPSID PROTEIN

by

HEATHER MOUSA

Under the Direction of Teryl K. Frey

ABSTRACT

The rubella virus (RUB) capsid protein (C) is a multifunctional phosphoprotein with roles beyond encapsidation. It is able to rescue a large lethal deletion of the Q domain in the P150 replicase gene at a step in replication before detectable viral RNA synthesis, indicating a common function shared by RUB C and the Q domain. The goal of this dissertation was to use constructs containing the N-terminal 88 amino acids of RUB C, the region previously defined as the minimal region required for the rescue of Q domain mutants, to elucidate the function of RUB C in Q domain rescue and viral RNA synthesis. In the first specific aim, the rescue function of 1-88 RUB C and the importance of an arginine-rich cluster, R2, within 1-88 RUB C for rescue were confirmed. Rescue was not correlated with intracellular localization or phosphorylation

status of RUB C. In the second specific aim, the involvement of RUB C in early events post-transfection with RUB RNA was analyzed. RUB C specifically protected RUB transcripts early post-transfection and protection required R2. However, it was concluded the protection observed was due to the encapsidation function of RUB C and not related to Q domain rescue. No differences in the translation of the RUB nonstructural proteins in the presence or absence of RUB C were observed. Interactions of RUB C with host cell proteins were analyzed. Although the interaction of RUB C with cellular p32 required the R2 cluster, both wild type (does not require RUB C for replication) and R_QQ (requires RUB C for replication) Q domain bound p32, indicating interaction with this binding partner is not the basis of rescue. Using a human protein array phosphatidylinositol transfer protein alpha isoform (PITPα) was found to interact with RUB C but not its R2 mutant. However, co-immunoprecipitation experiments revealed that this protein binds both forms of RUB C. Although the mechanism behind the rescue of the RUB P150 Q domain by RUB C remains unknown, we propose a model that RUB C plays a role in generation of the virus replication complex in infected cells.

INDEX WORDS: Rubella virus, Capsid protein, Nonstructural roles of capsid, P150, Q domain, Replication

INVESTIGATION OF THE RESCUE OF THE RUBELLA VIRUS P150 REPLICASE PROTEIN Q DOMAIN BY THE CAPSID PROTEIN

by

HEATHER MOUSA

A Dissertation Submitted in Partial Fulfillment of the Requirements for the Degree of

Doctor of Philosophy

in the College of Arts and Sciences

Georgia State University

2013

INVESTIGATION OF THE RESCUE OF THE RUBELLA VIRUS P150 REPLICASE PROTEIN Q DOMAIN BY THE CAPSID PROTEIN

by

HEATHER MOUSA

Committee Chair: Teryl Frey

Committee: Margo Brinton

Susanna Greer

Electronic Version Approved:

Office of Graduate Studies

College of Arts and Sciences

Georgia State University

May 2013

DEDICATION

This dissertation is dedicated to my loving and supportive family. To my wonderful husband, Amro, who has provided constant encouragement and love throughout the highs and lows of attaining this degree. To my children, Noah Amro and Ada Joy, who inspire me to be the best version of myself everyday and fill my life with unconditional love and joy. To my parents, who fostered my love of learning and have always been two of my greatest fans. To my family-in-law and extended family, who have supported my goals throughout the years.

ACKNOWLEDGEMENTS

I would like to thank my mentor, Dr. Teryl Frey, for allowing me to work under his supervision to attain this degree. I thank him for his patience with me as I have grown as a scientist and his encouragement throughout my time in his lab. I would also like to thank my committee members, Dr. Margo Brinton and Dr. Susanna Greer, for their valuable input that has added to this work. I have enjoyed learning from both of these women in the context of my committee, coursework, and the MBD program. I would like to thank Dr. Tzeng for his efforts in spearheading this project and Dr. Yumei Zhou for her constant and patient assistance in the lab. I would also like to thank two previous students in the lab, Dr. Suganthi Suppiah and Dr. Jason Matthews, for their kind mentorship and encouragement. I would also like to thank Denise Ceron for her assistance carrying out experiments during her time in the Frey lab during her undergraduate career. I would like to thank the all of members of the Frey lab, both past and present, for their technical assistance, encouragement, and especially friendship. I would lastly like to thank my GSU friends, who have become like family to me. You have all have seen me through the highest and lowest moments of my personal and professional life and I am grateful for your friendship throughout it all.

TABLE OF CONTENTS

LIST OF TABLES

LIST OF FIGURES

1 INTRODUCTION

1.1 Disease

Rubella virus (RUB) is the causative agent of the disease rubella. This disease was first described in the 1750's by the German physicians de Bergan and Orlow (143), thus its alternate name German measles. RUB is a human pathogen with respiratory transmission causing a relatively mild disease that can range from asymptomatic to symptoms beginning with lymphadenopathy and later including rash, fever, conjunctivitis, sore throat, and arthralgia. From time of exposure to the appearance of a rash ranges from 14 to 22 days, with the rash normally lasting 3 days. Neutralizing antibodies can initially be found in the blood 2 to 3 days after the appearance of the rash and the exposed individual usually is then resistant to reinfection by RUB. Complications that can arise include acute polyarthralgia and arthritis, particularly in women, thrombocytopenic purpura, post-acute infection encephalitis, and rarely progressive rubella panencephalitis. The complication that has garnered the most public health interest is congenital rubella syndrome (CRS) (21, 66).

The connection between RUB and its nature as a teratogen was first made when Australian ophthalmologist Norman Gregg linked maternal RUB infection to an epidemic of congenital cataracts (29). Additional congenital defects were noted after a rubella epidemic in the United States in the 1960s in which it is estimated that upwards of 20,000 infants were born with CRS. Defects to the fetus are the most devastating when RUB infection occurs during the first trimester of pregnancy and infection during this time period also carries an elevated incidence of spontaneous abortion or stillbirth (21). Infants born with CRS may suffer from a host of defects including blindness, cataracts, deafness, mental retardation, and heart defects and are also at a

higher risk of infant mortality (21, 26). These children can shed virus for the first year of life but also have persistent neutralizing antibodies during this time as well (21). Currently there is no treatment for CRS.

It is important to understand how RUB replicates not only to further understand how this virus causes a mild disease in children and adults, but also how it causes devastating birth defects in an infected fetus as well, potentially drawing parallels with other viral teratogens. Discovering the mechanism behind RUB's ability to cause CRS has been of interest for decades. The virus crosses the placenta, infecting the placenta and fetus, and establishes a persistent infection. The pathology of CRS is thought to be attributed to decreased cellular growth and necrosis of established structures when infected with RUB (21). It was initially hypothesized that the pathogenesis of CRS could be attributed to RUB induced apoptosis that was demonstrated in cultures of cells derived from adult tissues (22, 23, 46, 87, 113). Later work in human embryonic fibroblasts (HEK) indicated this is likely not the case as RUB infection failed to induce apoptosis in this cell line and gene expression profiles in this cell line were anti-apoptotic when infected with RUB compared to adult cells (1, 2). This however, suggests a mechanism for the persistent infection in the fetal tissues.

The only preventative treatment for CRS is through vaccination for RUB, with vaccination efforts concentrating on children. RUB was isolated in 1962 (106, 142). The first vaccine was prepared from the HPV-77 strain grown in African green monkey kidney cells. Merck licensed the HPV-77/DE-5 rubella vaccine first in 1969. The rubella vaccine was combined with mumps (MR), which was approved by the FDA in 1970, and the measles-mumps-rubella (MMR) formulation was approved one year later. In 1979 Merck began using the RA27/3 strain attenuated in human lung fibroblast WI-38 cells for vaccine production (105). Since 1989, the MMR

vaccine strategy employed in the US is one dose at 12-15 months and a second dose at 5-10 years. In 2005, the MMRV (measles, mumps, rubella, varicella) was approved for use by the FDA in the United States (81). Vaccination with the MMRV vaccine is associated with a higher incidence of fever and fever-related seizures than when the MMR and varicella vaccines are given in two separate shots on the same day, so the MMR vaccine is still commonly given. Although the vaccination program has successfully controlled CRS in developed countries, RUB epidemics and CRS still occur in developing countries (9). In 2008, Global Alliance for Vaccines and Immunization (GAVI) identified rubella as a vaccine to include in their program that aids in the childhood vaccination efforts in underserved countries (98). The addition of the rubella vaccine to this program identifies rubella and its complication CRS as a major public health issues in developing countries. Support of vaccination against rubella in these underserved areas will not only aid in the elimination of rubella in these areas, but also decrease the number of cases imported to countries with vaccination programs in place. Additionally, RUB has remained of interest for the development of a vaccine vector for other pathogens (114). Therefore, it is important to further the understanding of RUB replication.

1.2 Rubella virus classification and related viruses

RUB is the sole member of the genus *Rubivirus*, which is in the family *Togaviridae*. The family *Togaviridae* contains a second genus, *Alphavirus*, which contains several viruses of clinical and economic significance for humans, mammals, and birds and its biology has been reviewed by Jose, Synder, and Kuhn (57). Alphaviruses are classified geographically into Old World and New World viruses. These arboviruses are maintained in a cycle between the arthropod vector (usually a mosquito) and the vertebrate host in which disease occurs. Disease symp-

toms can range from rash and fever with Old World viruses to encephalitis with New World viruses. Well studied alphaviruses include Sindbis virus (SINV), Semliki forest virus (SFV), Chikungunya virus (CHIKV), western equine encephalitis virus (WEEV), eastern equine encephalitis virus (EEEV), Venezuelan equine encephalitis virus (VEEV), and Ross River virus (RRV).

Alphaviruses enter the cell via receptor-mediated endocytosis and the nonstructural open reading frame (ORF) is translated from the genomic RNA into two polyproteins, P123 and P1234 (Figure 1). These polyproteins are cleaved to yield nsP1, nsP2, nsP3, and nsP4, which complex with host factors to form the replication complex (RC), the site of viral RNA replication. It is notable that the fully processed and intermediate nonstructural proteins play different roles in replication. The incoming genomic RNA is used as a template to generate a full-length negative-sense RNA that in turn serves as the template to produce both full-length positive-sense genomic RNA and a shorter positive-sense subgenomic RNA. The structural ORF is translated from the subgenomic RNA to give a polyprotein that is processed giving the capsid protein, glycoproteins E2 and E1, and 6K virion associated protein. The structural proteins package the newly synthesized genomic RNA and the virus buds from the plasma membrane obtaining its envelope and glycoproteins on the way. Due to the similarities in the coding strategies and viral life cycles between the two genera of *Togaviridae*, important parallels may be drawn between RUB and alphaviruses. However, there are differences in the coding strategies between alphaviruses and RUB. RUB P150 contains the viral protease while P90 contains the helicase and RNA dependent RNA polymerase (Figure 2) while in the alphaviruses nsP1 contains methyltransferase activity, nsp2 contains the helicase and protease domains, nsP3 contains the X domain, and nsP4 is the RNA dependent RNA polymerase.

1.3 Rubella virus life cycle and coding strategy

The RUB single-stranded genomic RNA has a 5' cap (99) and 3' poly-A tail (26), which serves as positive polarity mRNA allowing for immediate translation upon entry into the cytoplasm. The 9762 nucleotide genome contains two ORFs; the 5'-promimal ORF encodes for the nonstructural proteins while the 3'-proximal ORF encodes for the structural proteins (Figure 2.A). The genome also includes 5' and 3' *cis*-acting elements (CAEs) that are important for viral replication (12, 111).

The virus enters the cell through receptor-mediated endocytosis via its receptor, the myelin oligodendrocyte glycoprotein (19). The virion membrane fuses with the endosomal membrane and releases the genomic RNA into the cytoplasm after the lowering of the pH in the endosome. The first of the two ORFs in the viral genome is translated. The nonstructural ORF encodes the nonstructural protein precursor P200, which is cleaved into P150 and P90 (Figure 2.B) by the viral protease domain of P150, the only experimentally validated domain of P150 (83). The cysteine protease's catalytic dyad is composed of residues C1151 and H1272, which cleave P200 between residues G1301 and G1302 (11). Computer alignments of the RUB genome with sequences from other positive-sense RNA viruses predict that P150 also contains the following domains: methyl transferase, Y domain, proline hinge, and X domain (61). P150 also contains a hypervariable region (112). The function of the Y domain is unknown, but is also present in replicase proteins of hepatitis E virus (HEV) and beet necrotic yellow vein virus (BNYVV). The X domain, which is found in alphaviruses and coronaviruses in addition to HEV and BNYVV, shares homology with enzymes with ADP-ribose-1"-phosphatase activity. In coronaviruses, this domain has been shown to bind ADP-ribose (115) and has confirmed phosphatase activity (122). P90 contains domains for the helicase and the RNA-dependent RNA polymerase (RDRP) (61).

RNA replication (Figure 3) occurs in RCs created from modified lysosomes, which are morphologically termed cytopathic vacuoles (CPVs) (80). The processing of P200 into P150/P90 regulates the switch from the synthesis of negative-strand to positive-strand RNA (72). The minus-strand RNA is used as a template for the synthesis of two positive-strand RNA species: a full-length genomic RNA and a subgenomic RNA. The structural ORF is translated from the subgenomic RNA. The structural ORF encodes a polyprotein, p110, that produces the capsid (C) and the glycoproteins (E2 and E1) once cleaved (99, 101). p110 is targeted to the endoplasmic reticulum (ER) by signal peptides present in E2 and E1 (42, 45, 100) where it is cleaved by cellular signalase (82). Virion assembly occurs in the Golgi (26) and the encapsidation of the RUB genome involves the interaction of the region between nucleotides 347 and 375 of the viral RNA with residues 28 to 56 of RUB C (75).

1.4 Rubella replicons

A reverse genetics system for RUB based on an infectious cDNA clone has been available for nearly twenty years (140). This system is based on a cDNA copy of the virus genome contained within a plasmid from which infectious RNA transcripts can be produced *in vitro*. This system allows for modification of the RUB genome carried by the plasmid using standard recombinant DNA technology and subsequent generation of virus containing the modifications. Using the infectious cDNA clone, RUB "replicons" were developed in which the structural protein ORF was replaced with a reporter gene, usually green fluorescent protein (GFP) (Figure 2.A). Replicons express the P150 and P90 replicase proteins and thus these RNAs can be replicated following introduction into susceptible cells by transfection, but cannot spread from cell to cell because they lack the proteins necessary to form a virion. Using the GFP-expressing RUB

replicon (RUBrep/GFP) (132), replication can be assessed by monitoring GFP expression by fluorescence microscopy or the GFP-positive cell population of a sample can be quantified by flow cytometry.

1.5 Nonstructural functions of RUB C

RUB C has roles in the virus life cycle beyond the encapsidation of the viral genome. In addition to its localization to the Golgi for its role in virion assembly and budding (43, 44), RUB C is also associated with the mitochondria (67), P150 containing fibers (64), and CPVs (25), indicating additional functions. RUB C is a phosphoprotein and its phosphorylation negatively regulates RNA binding (65). The major phosphorylation site is S46, and mutants of this site that are hypophosphorylated yield decreased viral titers and cytopathic effect compared to wild type RUB C (65) (Figure 2.C). Another nonstructural function of RUB C is a role in modulating viral RNA synthesis. RUB C increases the amount of genomic RNA produced compared to the amount of subgenomic RNA produced (135). This enhancement was specific for RUB C and RUB RNAs and the region of RUB C required for this was mapped to the first 88 amino acids (135). The RUB C gene must be provided in *cis*, on the same viral RNA, to modulate viral RNA synthesis (135).

RUB C has also been implicated in modulating cell signaling pathways, including apoptotic pathways. It inhibits apoptosis by binding to Bax, which impairs the ability of Bax to form pores in the mitochondria. The region within RUB C required for this inhibition was mapped to an arginine cluster at the C terminus of the protein (49). This arginine cluster was also found to be important in a study of the growth kinetics of cell cultures harboring drug-selected RUB replicons. Drug-selected RUBrep/C-GFP/Neo-containing Vero cell cultures, in which the C pro-

tein is expressed, exhibit similar growth as Vero cells, while drug-selected RUBrep/GFP/Neo containing Vero cell cultures, lacking RUB C, exhibit impaired growth (137). The normal growth phenotype of RUBrep/C-GFP/Neo required this arginine cluster and it is thus thought that the inhibition of apoptosis is responsible for this increased cell survival, by allowing the time needed for the virus to replicate as RUB replicates relatively slowly.

RUB C has multiple cellular binding partners. The C-terminus of poly(A)-binding protein (PABP) interacts with the pool of RUB C associated with the mitochondria. RUB C acts to sequester PABP, resulting in impaired translation (50). Cellular binding partners that have been identified but not further investigated in the literature include Par-4 (6) and Y-box binding proteins (91). The most extensively studied RUB C cellular binding partner is p32, a multifunctional protein that has been identified as a component of the ASF/SF2 human splicing factor complex (63) as well as a mitochondrial resident protein (95) that plays a role in the maintenance of oxidative phosphorylation and phosphate transport (30, 109). Two yeast two-hybrid screens initially identified the interaction between p32 and RUB C, which was confirmed through both co-immunoprecipitation and colocalization studies (6, 91). This interaction occurs on the cytoplasmic side of the mitochondria (6). In the initial studies that identified binding of RUB C and p32, the N-terminus of RUB C was mapped as the p32-binding region. However, the minimal region required for this interaction was mapped to residues 46 to 89 of RUB C by one group (6) while another group mapped the minimal region for the interaction to the first 28 amino acids of RUB C (91). In a subsequent paper, the first group mapped the p32 binding region to amino acids 30 to 69, which contains two arginine clusters that are important for the binding of p32 (5). The region of p32 required for this interaction is the C-terminal 69 amino acids.

The importance of the interaction between RUB C and p32 to the RUB life cycle has been investigated by several groups. RUB infected p32-overexpressing Vero cell cultures had more cells that positively stained for RUB C than RUB infected Vero cultures (91), suggesting a positive role for p32 in the RUB replication cycle. We and others have observed reduced RUB viral titers in cells treated with p32-specific small interfering RNA (siRNA) (16, 127), further supporting the importance of p32 in RUB infection. Electroporation of *in vitro* transcribed RNA containing mutations of the two p32-binding arginine clusters in RUB C (to alanine) made in the RUB infectious clone resulted in no detectable virus released into culture medium, indicating the importance of the interaction between RUB C and p32 to RUB infection. Mutation of either arginine cluster individually within the context of the RUB infectious clone resulted in a decrease in the titer of secreted virus. Mutation of the first arginine cluster resulted in impaired production of subgenomic RNA and subsequently the expression of the RUB structural proteins compared to wild type virus.

Additionally, RUB C impacts mitochondrial distribution and function. RUB C reorganizes the mitochondria into perinuclear clusters and this reorganization is independent of the mitochondrial targeting sequence within p32 (5). Mitochondrial import is inhibited by RUB C and this inhibition is also independent of p32. Although RUB C with the first arginine cluster mutated associates with the mitochondria, mitochondrial import is not inhibited. RUB C was also found to bind cardiolipin, but this interaction is not required for the inhibition of mitochondrial import (51).

1.6 Nonstructural roles of other virus capsid proteins

1.6.1 Apoptosis and cell survival

Viruses can modulate the cell cycle and several viral capsid proteins have been found to play a role in that modulation. Often a role in apoptosis has been discovered when a pool of capsid protein produced by a virus that replicates in the cytoplasm is found in the nucleus, although the presence of capsid proteins in the nucleus can result in functions other than apoptosis such as the modulation of host gene expression or the innate immune response. Although West Nile virus (WNV; a member of the plus-strand RNA Flavivirus family) infection causes apoptosis in cell culture (107), this does not occur immediately and the role of the WNV capsid protein in this process is controversial. The WNV capsid protein, which is the first protein translated from the genomic RNA following infection, blocks apoptosis via the phosphatidylinositol 3-kinase pathway (138). WNV capsid protein also has been reported to stabilize and sequester HDM2 in the nucleolus, which allows stabilization of p53, which in turn induces apoptosis (146). The nucleoproteins of several coronaviruses (a family of plus-strand RNA viruses) (41, 144) and the capsid protein of human hepatitis B virus (HBV; a DNA virus in the family hepadnavirus) (97) also localize to the nucleolus where they are thought to impact the progression through the cell cycle, specifically by preventing cytokinesis. A portion of the severe acute respiratory syndrome-associated coronavirus (SARS-CoV) nucleocapsid protein localizes to the nucleus (131) and is able to induce apoptosis (129). The nucleocapsid protein of SARS-CoV has also been implicated in blocking the progression through S phase through its inhibition of cyclin-cyclin dependent kinase complex activity (128). Dengue virus (DENV; a flavivirus) capsid protein interacts with the nuclear pool of Daxx and this interaction is important for the induction of Fas-mediated apoptosis (96), although the exact pathway used has yet to be elucidated. Puumala virus (PUUV;

a negative-strand RNA bunyavirus) nucleocapsid protein also interacts with Daxx (71), but it is not known if this interaction is with the nuclear or cytoplasmic pool of Daxx and therefore the impact of this interaction on apoptosis signaling is currently unknown. Hepatitis C virus (HCV; a flavivirus) core protein does impact the cell cycle, although its exact role is controversial. There are examples in the literature that support its role in the induction of apoptosis (69, 92, 93, 120) as well as in supporting cell survival (55, 79, 103, 123).

1.6.2 Immune response

Viral capsid proteins have been found to inhibit the host cell immune response, presumably to promote viral replication. SARS-CoV nucleocapsid protein was found to be an interferon (IFN) antagonist through its inhibition of IRF3 and NF-κB (62). Further examination revealed that the inhibition of IFNβ production is dependent upon the RNA binding region of the nucleocapsid protein and occurs at an early stage of the induction pathway, suggesting the nucleocapsid protein may bind to the viral RNA, preventing its interaction with pattern recognition receptors (77). WEEV capsid protein is thought to play a role in cell survival and to promote viral replication though its suppression of pattern recognition receptor (PRR) signaling pathways at a step downstream of the activation of IRF3 in neuronal cell lines (108). EEEV capsid protein also inhibits the IFN response (3). The core protein of HCV blocks IFN signaling through its interaction with STAT1, resulting in STAT1 degradation (73, 74). The nucleoproteins of arenaviruses act as IFN antagonists by inhibiting the activation and nuclear translocation of IRF3 (85, 86). Closer examination of prototypical arenavirus lymphocytic choriomeningitis virus (LCMV) revealed that its nucleoprotein binds the kinase domain of IKKε, interfering with its ability to phosphorylate and activate IRF3 (116). The nucleoprotein of the arenavirus Lassa fever virus

(LAFV) contains a domain with 3'-5' exonuclease activity (36, 117). Interestingly, the IFN antagonist activity of this nucleoprotein has been mapped to this RNase domain (84, 117), which selectively cleaves pathogen-associated molecular pattern (PAMP) viral RNA ligands rather than cellular RNAs (117). The nucleoprotein of LCMV binds RIG-I and MDA5 (153), suggesting that its ability to cleave PAMP viral RNA could quench the activation of the pathways downstream of RIG-I or MDA5 (117). Alternatively, the binding of RIG-I and MDA5 by the LCMV nucleoprotein may serve to halt the signaling cascade initiated by the binding of viral RNA to these proteins (153). Bunyavirus severe fever with thrombocytopenia virus (SFTSV) also inhibits the IFN response though inhibition of the production of IFNβ and NF-κB signaling (118).

1.6.3 Roles in replication and viral events prior to packaging

Capsid proteins fulfill roles in the virus life cycle beyond entry, uncoating, encapsidation, and egress. It must be noted that viral proteins that form the capsid can associate with the genome differentially depending upon the structure of the capsid and this interaction with the packaged genome could impact the role of that capsid protein in viral replication. Helical capsids interlock around the viral genome, and therefore the capsid proteins that make up the capsid are in close association with the entire genome. An icosahedral capsid instead forms a shell around the genome. Among the viruses discussed below, TGEV, HCoV-229E, SARS-CoV, VSV, arenaviruses, SNV, CCHFV, and LAFV have helical capsids while BMV, HBV, HIV, HCV, WNV, and alphaviruses have icosahedral capsids. Brome mosaic virus (BMV; a plus-strand RNA virus of the bromovirus family) coat protein levels impact gene expression. Specifically, high coat protein levels result in decreased protein expression from viral RNA1 and RNA2, but not RNA3, and low coat protein levels increase protein expression from RNA1 and RNA2 (147). This re-

pression is due to the coat protein's influence on viral RNA accumulation as the overexpression of coat protein also inhibited RNA accumulation from RNA1 and RNA2 (148). The coat protein binds an RNA motif present in the 5'UTR of RNA1 and RNA2, the B Box (148). Interestingly, RNA1 and RNA2 contain the ORFs encoding proteins needed for RNA replication, while RNA3 contains the ORFs for the movement and coat proteins. Therefore, the coat protein is able to control the level of the viral replicase proteins by binding to the RNAs encoding these proteins. The BMV coat protein binds another RNA element that is thought to play a role in the coat protein's modulation of viral RNAs, a clamped adenine motif (CAM) (60). This motif is required for replication and binds the BMV replicase. It is hypothesized that high levels of coat protein out-compete the replicase and bind to this site to signal that RNA synthesis should end and encapsidation should begin.

Another viral capsid protein thought to play a role in viral replication is the capsid protein of HBV. This capsid protein was found to bind both RNA and DNA via one arginine-rich RNA binding repeat and three arginine-rich DNA binding repeats, respectively. While the binding of RNA was expected as the viral RNA is the moiety encapsidated, its ability to bind DNA suggests a role in replication with the reverse transcription of the encapsidated RNA into double-stranded DNA (37).

The nucleocapsid proteins of coronaviruses also play a role in viral replication (10, 18). Providing the nucleocapsid protein either in *cis* or in *trans* aids in efficient replication of transmissible gastroenteritis coronavirus (TGEV)-derived replicons (4). Moreover, human coronavirus 229E (HCoV-229E) vector RNAs that lack the nucleocapsid gene replicate less efficiently than ones that possess the gene (125). This increased efficiency of replication in the presence of the nucleocapsid can be attributed to increased transcription levels, specifically by its template

switching activity that is important for the discontinuous transcription of coronavirus RNA (154). The SARS-CoV nucleocapsid protein interacts with nsp3, a component of the viral replicase, and this interaction is important for the infectivity of the genomic RNA (48). It is thought that the nucleocapsid protein-nsp3 complex may act as a means of tethering the genomic RNA to the newly translated replicase early prior to its engagement with the replicase complex.

The nucleocapsid protein (NC) and capsid protein (CA) of human immunodeficiency virus type 1 (HIV-1; a retrovirus) have been implicated in several steps in the viral life cycle. The NC enhances genome reverse transcription (130) and progenome integration (8, 130) through its zinc-finger motifs. The CA binds the cyclophilin domain of Nup358/RanBP2, a component of the cell nuclear pore complex, and this interaction impacts the site of integration (124).

Capsid proteins also play a role in the replication of negative-sense RNA viruses. The nucleoprotein of arenaviruses is needed for RNA replication and transcription (35, 68, 76, 110). The nucleoprotein of vesicular stomatitis virus (VSV; a negative-strand RNA rhabdovirus) also plays a role in replication, specifically RNA synthesis. The nucleoprotein complexed with the genomic RNA is required for full processivity by the viral polymerase during RNA synthesis (94). The C-terminus of the nucleoprotein is important for RNA synthesis (38) and mutations in the C-terminal loop that impact the association of nucleoprotein monomers with one another result in increases in RNA replication but not in RNA transcription (34). The hydrogen bonding between the nucleoprotein and the genomic RNA is important to give the genome the proper structure to engage the viral polymerase for transcription and replication (119).

RNA chaperones are proteins that assist RNAs to achieve proper structures by either resolving or preventing unproductive misfolded states. Once an RNA has obtained its optimal conformation, the RNA chaperone is no longer required to maintain the proper folding (39).

Several viral capsid proteins have RNA chaperone activities that play a role in replication including the nucleocapsid proteins of TGEV and SARS-CoV (155), the core protein of HCV (20), the core protein of WNV (54), the nucleocapsid protein of Sin Nombre hantavirus (SNV) (89), and NC of HIV-1 (40). The TGEV nucleocapsid protein promotes the annealing of transcription regulating sequences (TRSs) within the genomic RNA, a step required for the transcription of the nested subgenomic RNAs that encode the viral proteins (155). The dimerization of HCV 3'UTR RNA is enhanced in the presence of HCV core protein, which has been proposed to aid in transitions in the viral replication cycle (20, 53). The core protein of WNV enhances the interaction and annealing of the 5' and 3' ends of the genomic RNA (52), and this cyclization is important for RNA synthesis (151). SNV nucleocapsid protein unwinds panhandles, double stranded RNA structures at the 5' and 3' ends of the viral genome, an activity important for the initiation of transcription (89). NC aids in the reverse transcription of the HIV-1 genome (70) through destabilizing secondary structures within the 5' UTR to prevent pausing or stalling of the reverse transcription machinery (121).

Some capsid proteins have unique alternative functions. The capsid proteins of alphaviruses possess autoprotease activity and are important in the processing of the structural polyprotein (32, 33). Bunyavirus Crimean–Congo hemorrhagic fever virus (CCHFV) nucleoprotein was found to have endonuclease activity, although the role of this activity in the viral life cycle has yet to be defined (31). The nucleoprotein of LAFV binds the m7GpppN cap structure of RNAs (117), suggesting that this nucleoprotein plays a role in the cap snatching characteristic of arenaviruses by binding the cap and then allowing the RNA to be digested either by the RNase activity of this nucleoprotein (117) or by cellular proteins. The hantavirus nucleocapsid protein binds capped RNAs and is associated with P bodies, suggesting a role in cap snatching by se-

questering capped RNAs needed for use in transcription initiation (88). The hantavirus SNV nucleocapsid protein has also been implicated in translation as it facilitates the translation of capped RNAs, both viral and cellular with a preference for viral sequences, with its translational initiation activities. The SNV nucleocapsid is able to bind capped RNAs, bind the 43S pre-initiation complex, and also can functionally replace the RNA helicase activity of eIF4A (90). Although this enhanced translation occurs for cellular messages as well, it does promote viral replication through its preference for capped viral sequences. The HCV core protein negatively regulates its HCV RNA synthesis by binding the viral RDRP (58). This core protein also negatively regulates viral replication of HBV through its interactions with its polymerase and X proteins (14).

1.6.4 Interaction with host cell proteins

Viral capsid proteins also interact with host cell proteins to modulate different activities to benefit the life cycle of their respective virus. DENV capsid protein binds histone proteins H2A, H2B, H3, and H4 to form heterodimers. This interaction prevents histone dimerization and the formation of nucleosomes. Additionally, DENV capsid protein can bind DNA (17). The purpose of these interactions are unknown, but it is hypothesized that they may play a role in altering host cell gene expression to create a favorable host environment for viral replication.

SARS-CoV nucleocapsid protein binds several host cell proteins. One binding partner is cellular B23 and the presence of the nucleocapsid protein inhibits the phosphorylation of B23 (150). This interaction may be of importance as B23 is involved in the duplication of the centrosome and the nucleocapsid protein does cause cell cycle arrest (128). Another binding partner is elongation factor 1-alpha, which the nucleocapsid protein aggregates, resulting in inhibition of translation and cytokinesis (152). This nucleocapsid protein also interacts with heterogeneous

nuclear ribonucleoprotein A1 (hnRNP A1) (78), a cellular protein that has been found to be important for the RNA synthesis of another coronavirus, mouse hepatitis virus (MHV), through its association with viral RNA, nucleocapsid protein, and polymerase (126).

WNV capsid protein also binds several cellular proteins. WNV capsid protein binds I_2^{PP2A}, an inhibitor of protein phosphatase 2A (PP2A), at the same area of the protein needed for its interaction with PP2A. PP2A inhibits the transcription factor AP1. Therefore, the binding of WNV capsid protein to I_2^{PP2A} ultimately results in decreased transcription of AP1 controlled genes, perhaps to also create a favorable host environment for viral replication (47). WNV capsid protein sequesters human Sec3 exocyst protein (hSec3p) and inhibits its antiviral action presumably to enhance the host environment for viral replication (7).

The HCV core protein interacts with various cellular proteins as well. Discussion of the interaction of this protein with host cell proteins that modulate the cell cycle are numerous, but will not be addressed here as the role of the core protein in apoptosis is controversial. The core protein interacts with Dicer, a component of the RNAi pathway, suppressing the antiviral response activated by the HCV replication (15, 141). DEAD box RNA helicase DDX3 interacts with HCV core protein (104), inhibiting the interaction between DDX3 and IPS-1 blocking the signaling for IFNβ production (102).

Tula hantavirus (TULV) nucleocapsid protein has been found to bind small ubiquitin-related modifier-1 (SUMO-1) (59). Although the exact role of this interaction is unknown, modulating posttranslational modifications could allow the TULV nucleocapsid protein to impact many cellular processes.

1.6.5 Modulating gene expression

Viral capsid proteins have been implicated in the modulation of host gene expression. SARS-CoV nucleocapsid protein upregulates proinflammatory protein COX-2 by binding to the NF-κB and C/EBP regulatory elements present at the COX-2 promoter (145). The core protein of HCV modulates gene expression differentially in different cells by activating or inhibiting NF-κB. In macrophages, the HCV core protein interacts with and suppresses of kinase activity of IKKβ, inhibiting NF-κB and ultimately down regulating COX-2 (56). The exact impact of this is unknown, but it is thought to aid viral persistence through the evasion of the innate immune response. However, in HeLa cells the expression of HCV core protein leads to the activation of NF-κB (149), suggesting the proinflammatory response perhaps plays a role in the development of hepatitis. The capsid proteins of two New World alphaviruses, VEEV and EEEV, inhibit host cell transcription and also cause translational shutoff (28), although overexpression of these proteins alone would produce artifacts. An additional study of the capsid protein of EEEV confirmed that it is a general inhibitor of host cell gene expression and can inhibit host cell translation, presumably as its expression also results in the phosphorylation of eukaryotic initiation factor 2 alpha (EIF2α) (3). VEEV capsid protein colocalizes with nuclear pore proteins, suggesting that the capsid protein may modulate host cell transcription by influencing the flow and ebb of transcription factors to the nucleus (27). SFV capsid protein expression results in the phosphorylation of protein kinase R (PKR), which in turn phosphorylates EIF2α, ultimately resulting in the inhibition of host cell translation (24). The WNV capsid protein expressed in isolation in neurons and astrocytes results in increased mRNA levels of neuroinflammatory genes (139).

1.7 The rescue of the RUB P150 Q domain by RUB C

In a study commenced in 2001 in our lab, serial deletions of the nonstructural ORF in the RUB replicon revealed that an in-frame deletion between two *Not*I sites (nt 1685-2192) in the P150 gene, which was lethal to the replicon (RUBrep/GFP-ΔNotI), could be rescued by wild type helper virus (132). Rescue is at an early step in replicon replication as no replicon RNA is synthesized by RUBrep/GFP-ΔNotI (133). When culture fluid from Vero cells transfected with RUBrep/GFP-ΔNotI and infected with RUB were passaged to fresh Vero cells, GFP positive cells were observed (132). It was initially assumed that the Δ*Not*I replicon was being rescued by P150 produced in *trans* by the helper virus. However, when the *Not*I deletion was introduced into the infectious cDNA clone (Robo402/ΔNotI), the resulting transcripts induced cytopathic effect (CPE) two to three days post transfection and produced virus (132). This indicated that a viral gene other than P150 was able to rescue the lethal *Not*I deletion. The difference between RUBrep/GFP-ΔNotI and Robo402/ΔNotI is the presence of the structural ORF in the virus; therefore, the structural proteins were examined to determine which RUB protein was responsible for the rescue of the *Not*I deletion. Different portions of the structural ORF were fused to GFP in RUBrep/GFP-ΔNotI, surprisingly, revealing that RUB C was the gene responsible for the rescue of the *Not*I deletion. Deletion mutants using this same replicon system mapped the region of RUB C required for rescue to amino acids 1-88 of RUB C as these residues were required for rescue when C was supplied in *trans* from an expression plasmid driven by the CMV promoter. The RUB C protein, rather than its RNA, was found to be responsible for rescue (133). The region of P150 that RUB C can rescue extends past the *Not*I sites to between nt 1529-2449 of the genome; this domain has been termed the capsid rescue-able or Q domain of P150. The Q do-

main spans from amino acids 497 to 803 and includes the polyproline hinge and hypervariable region within P150 (134).

In addition to its ability to rescue Q domain mutants, as shown using a cell line that constitutively expresses RUB C, it was found that RUB C also rescues replicons with mutations in both the 5' and 3' CAEs of the viral genome (13, 136). CAEs are necessary for virus replication, serving as recognition and control elements for translation, replication, and packaging. The RUB C also enhanced RNA replication by wild type RUB replicons during the first two days post-transfection, although RNA accumulation in the absence of RUB C was similar by three days post-transfection (136).

The rescue of RUB P150 Q domain mutants by RUB C suggests that a common function is shared by the RUB C and RUB P150 Q domain, and in proof of this hypothesis it was shown that replicons in which the Q domain was replaced by the 1-277 of the RUB C gene replicated, confirming this hypothesis. This portion of RUB C lacks the C terminal 23 amino acids that act as the E2 signal sequence, the presence of which resulted in a nonviable replicon when the complete C gene was used to replace the Q domain (134). When further mapped, it was found that the portion of RUB C that could be substituted for the Q domain and maintain viability was contained within amino acids 51 to 277 (134). Previously it had been shown that the first 88 amino acids of RUB C were required for complementation in *trans* (133), indicating that the region of RUB C required for rescue was between amino acids 51 and 88. The second arginine cluster within RUB C (R2) was the motif responsible for the rescue as introduction of a mutation in R2 into the replicon resulted in a loss of viability (134). When 1-277 RUB C was supplied in *trans*, mutation of the R2 to alanine (R2A) was not able to rescue the replication of RUBrep/GFP-ΔNotI (134), indicating the importance of the R2 in the complementation in *trans*. The P150 Q

domain also contains an arginine cluster between amino acids 731 and 735 (R_Q) that when mutated to glutamine (R_QQ), lysine (R_QK), or alanine (R_QA) did not generate viable virus (134). However, RUBrep-R_QA/GFP regains viability when wild type and R1A 1-277 RUB C sequences are inserted between the *Not*I sites, but not when the R2 or both arginine clusters of 1-277 RUB C are changed to alanines (134), further confirming the importance of the R2 cluster in C-mediated rescue of the Q domain.

1.8 Goal of this dissertation

The overarching goal of this dissertation is to identify the mechanism of RUB C rescue of the RUB P150 Q domain. This overarching goal is addressed in the two specific aims described below.

1.8.1 Specific Aim 1: Identify and characterize the region within the RUB C minimal region for rescue of the RUB P150 Q domain.

The minimal region of RUB C required for the rescue of RUBrep/GFP-ΔNotI replication has been mapped to the first 88 amino acids. This region includes two arginine clusters and the primary phosphorylation site and these were examined within the context of constructs containing amino acids 1-88 of C (1-88 RUB C) for their involvement in the rescue of P150 Q domain mutants. Once identified, rescuing and non-rescuing forms of 1-88 RUB C were characterized to find obvious differences between them, such as localization or phosphorylation that could elucidate the rescue mechanism.

1.8.2 Specific Aim 2: Determine the step in early replication at which RUB C functions in rescue.

The rescue of RUBrep/GFP-ΔNotI by RUB C occurs at an early stage of replication, specifically before the accumulation of viral RNA is detectable. Several early events in the replication of RUBrep/GFP-ΔNotI were studied to determine if they were enhanced by the presence of a rescuing form of RUB C. First, rescuing and non-rescuing forms of 1-88 RUB C were assayed for their ability to protect the incoming viral RNA from the host cell RNA decay machinery. Second, the translation of the nonstructural protein precursor, P200, from RUBrep/GFP-ΔNotI in the presence or absence of RUB C was analyzed. Finally, RUB C could also function in recruitment of cell proteins to the RC and/or in establishing the proper host environment for viral replication through its interactions with host proteins. Host proteins that bind to 1-88 RUB C were identified and examined to determine if any of these binding partners differentially bind rescuing and non-rescuing forms of 1-88 RUB C.

1.9 References

1. Adamo, M. P., M. Zapata, and T. K. Frey. 2008. Analysis of gene expression in fetal and adult cells infected with rubella virus. Virology 370:1-11.
2. Adamo, P., L. Asis, P. Silveyra, C. Cuffini, M. Pedranti, and M. Zapata. 2004. Rubella virus does not induce apoptosis in primary human embryo fibroblast cultures: a possible way of viral persistence in congenital infection. Viral Immunol 17:87-100.
3. Aguilar, P. V., S. C. Weaver, and C. F. Basler. 2007. Capsid protein of eastern equine encephalitis virus inhibits host cell gene expression. J Virol 81:3866-76.
4. Almazan, F., C. Galan, and L. Enjuanes. 2004. The nucleoprotein is required for efficient coronavirus genome replication. J Virol 78:12683-8.
5. Beatch, M. D., J. C. Everitt, L. J. Law, and T. C. Hobman. 2005. Interactions between rubella virus capsid and host protein p32 are important for virus replication. J Virol 79:10807-20.
6. Beatch, M. D., and T. C. Hobman. 2000. Rubella virus capsid associates with host cell protein p32 and localizes to mitochondria. J Virol 74:5569-76.
7. Bhuvanakantham, R., J. Li, T. T. Tan, and M. L. Ng. 2010. Human Sec3 protein is a novel transcriptional and translational repressor of flavivirus. Cell Microbiol 12:453-72.

8. Carteau, S., R. J. Gorelick, and F. D. Bushman. 1999. Coupled integration of human immunodeficiency virus type 1 cDNA ends by purified integrase in vitro: stimulation by the viral nucleocapsid protein. J Virol 73:6670-9.
9. CDC. 2010. Progress toward control of rubella and prevention of congenital rubella syndrome --- worldwide, 2009. MMWR Morb Mortal Wkly Rep 59:1307-10.
10. Chang, R. Y., R. Krishnan, and D. A. Brian. 1996. The UCUAAAC promoter motif is not required for high-frequency leader recombination in bovine coronavirus defective interfering RNA. J Virol 70:2720-9.
11. Chen, J. P., J. H. Strauss, E. G. Strauss, and T. K. Frey. 1996. Characterization of the rubella virus nonstructural protease domain and its cleavage site. J Virol 70:4707-13.
12. Chen, M. H., and T. K. Frey. 1999. Mutagenic analysis of the 3' cis-acting elements of the rubella virus genome. J Virol 73:3386-403.
13. Chen, M. H., and J. P. Icenogle. 2004. Rubella virus capsid protein modulates viral genome replication and virus infectivity. J Virol 78:4314-22.
14. Chen, S. Y., C. F. Kao, C. M. Chen, C. M. Shih, M. J. Hsu, C. H. Chao, S. H. Wang, L. R. You, and Y. H. Lee. 2003. Mechanisms for inhibition of hepatitis B virus gene expression and replication by hepatitis C virus core protein. J Biol Chem 278:591-607.
15. Chen, W., Z. Zhang, J. Chen, J. Zhang, J. Zhang, Y. Wu, Y. Huang, X. Cai, and A. Huang. 2008. HCV core protein interacts with Dicer to antagonize RNA silencing. Virus Res 133:250-8.
16. Claus, C., S. Chey, S. Heinrich, M. Reins, B. Richardt, S. Pinkert, H. Fechner, F. Gaunitz, I. Schafer, P. Seibel, and U. G. Liebert. 2011. Involvement of p32 and microtubules in alteration of mitochondrial functions by rubella virus. J Virol 85:3881-92.
17. Colpitts, T. M., S. Barthel, P. Wang, and E. Fikrig. 2011. Dengue virus capsid protein binds core histones and inhibits nucleosome formation in human liver cells. PLoS One 6:e24365.
18. Compton, S. R., D. B. Rogers, K. V. Holmes, D. Fertsch, J. Remenick, and J. J. McGowan. 1987. In vitro replication of mouse hepatitis virus strain A59. J Virol 61:1814-20.
19. Cong, H., Y. Jiang, and P. Tien. 2011. Identification of the myelin oligodendrocyte glycoprotein as a cellular receptor for rubella virus. J Virol 85:11038-47.
20. Cristofari, G., R. Ivanyi-Nagy, C. Gabus, S. Boulant, J. P. Lavergne, F. Penin, and J. L. Darlix. 2004. The hepatitis C virus Core protein is a potent nucleic acid chaperone that directs dimerization of the viral (+) strand RNA in vitro. Nucleic Acids Res 32:2623-31.
21. Dudgeon, J. A. 1967. Maternal rubella and its effect on the foetus. Arch Dis Child 42:110-25.
22. Duncan, R., A. Esmaili, L. M. Law, S. Bertholet, C. Hough, T. C. Hobman, and H. L. Nakhasi. 2000. Rubella virus capsid protein induces apoptosis in transfected RK13 cells. Virology 275:20-9.
23. Duncan, R., J. Muller, N. Lee, A. Esmaili, and H. L. Nakhasi. 1999. Rubella virus-induced apoptosis varies among cell lines and is modulated by Bcl-XL and caspase inhibitors. Virology 255:117-28.
24. Favre, D., E. Studer, and M. R. Michel. 1996. Semliki Forest virus capsid protein inhibits the initiation of translation by upregulating the double-stranded RNA-activated protein kinase (PKR). Biosci Rep 16:485-511.

25. Fontana, J., W. P. Tzeng, G. Calderita, A. Fraile-Ramos, T. K. Frey, and C. Risco. 2007. Novel replication complex architecture in rubella replicon-transfected cells. Cell Microbiol 9:875-90.
26. Frey, T. K. 1994. Molecular biology of rubella virus. Adv Virus Res 44:69-160.
27. Garmashova, N., S. Atasheva, W. Kang, S. C. Weaver, E. Frolova, and I. Frolov. 2007. Analysis of Venezuelan equine encephalitis virus capsid protein function in the inhibition of cellular transcription. J Virol 81:13552-65.
28. Garmashova, N., R. Gorchakov, E. Volkova, S. Paessler, E. Frolova, and I. Frolov. 2007. The Old World and New World alphaviruses use different virus-specific proteins for induction of transcriptional shutoff. J Virol 81:2472-84.
29. Gregg, N. M. 1941. Congenital cataract following German measles in the mother. Trans Ophthalmol Soc Aust 3:35-46.
30. Guerin, B., C. Bukusoglu, F. Rakotomanana, and H. Wohlrab. 1990. Mitochondrial phosphate transport. N-ethylmaleimide insensitivity correlates with absence of beef heart-like Cys42 from the Saccharomyces cerevisiae phosphate transport protein. J Biol Chem 265:19736-41.
31. Guo, Y., W. Wang, W. Ji, M. Deng, Y. Sun, H. Zhou, C. Yang, F. Deng, H. Wang, Z. Hu, Z. Lou, and Z. Rao. 2012. Crimean-Congo hemorrhagic fever virus nucleoprotein reveals endonuclease activity in bunyaviruses. Proc Natl Acad Sci U S A 109:5046-51.
32. Hahn, C. S., E. G. Strauss, and J. H. Strauss. 1985. Sequence analysis of three Sindbis virus mutants temperature-sensitive in the capsid protein autoprotease. Proc Natl Acad Sci U S A 82:4648-52.
33. Hahn, C. S., and J. H. Strauss. 1990. Site-directed mutagenesis of the proposed catalytic amino acids of the Sindbis virus capsid protein autoprotease. J Virol 64:3069-73.
34. Harouaka, D., and G. W. Wertz. 2009. Mutations in the C-terminal loop of the nucleocapsid protein affect vesicular stomatitis virus RNA replication and transcription differentially. J Virol 83:11429-39.
35. Hass, M., U. Golnitz, S. Muller, B. Becker-Ziaja, and S. Gunther. 2004. Replicon system for Lassa virus. J Virol 78:13793-803.
36. Hastie, K. M., C. R. Kimberlin, M. A. Zandonatti, I. J. MacRae, and E. O. Saphire. 2011. Structure of the Lassa virus nucleoprotein reveals a dsRNA-specific 3' to 5' exonuclease activity essential for immune suppression. Proc Natl Acad Sci U S A 108:2396-401.
37. Hatton, T., S. Zhou, and D. N. Standring. 1992. RNA- and DNA-binding activities in hepatitis B virus capsid protein: a model for their roles in viral replication. J Virol 66:5232-41.
38. Heinrich, B. S., B. Morin, A. A. Rahmeh, and S. P. Whelan. 2012. Structural properties of the C terminus of vesicular stomatitis virus N protein dictate N-RNA complex assembly, encapsidation, and RNA synthesis. J Virol 86:8720-9.
39. Herschlag, D. 1995. RNA chaperones and the RNA folding problem. J Biol Chem 270:20871-4.
40. Herschlag, D., M. Khosla, Z. Tsuchihashi, and R. L. Karpel. 1994. An RNA chaperone activity of non-specific RNA binding proteins in hammerhead ribozyme catalysis. Embo J 13:2913-24.
41. Hiscox, J. A., T. Wurm, L. Wilson, P. Britton, D. Cavanagh, and G. Brooks. 2001. The coronavirus infectious bronchitis virus nucleoprotein localizes to the nucleolus. J Virol 75:506-12.

42. Hobman, T. C., and S. Gillam. 1989. In vitro and in vivo expression of rubella virus glycoprotein E2: the signal peptide is contained in the C-terminal region of capsid protein. Virology 173:241-50.
43. Hobman, T. C., M. L. Lundstrom, and S. Gillam. 1990. Processing and intracellular transport of rubella virus structural proteins in COS cells. Virology 178:122-33.
44. Hobman, T. C., M. L. Lundstrom, C. A. Mauracher, L. Woodward, S. Gillam, and M. G. Farquhar. 1994. Assembly of rubella virus structural proteins into virus-like particles in transfected cells. Virology 202:574-85.
45. Hobman, T. C., R. Shukin, and S. Gillam. 1988. Translocation of rubella virus glycoprotein E1 into the endoplasmic reticulum. J Virol 62:4259-64.
46. Hofmann, J., M. W. Pletz, and U. G. Liebert. 1999. Rubella virus-induced cytopathic effect in vitro is caused by apoptosis. J Gen Virol 80 (Pt 7):1657-64.
47. Hunt, T. A., M. D. Urbanowski, K. Kakani, L. M. Law, M. A. Brinton, and T. C. Hobman. 2007. Interactions between the West Nile virus capsid protein and the host cell-encoded phosphatase inhibitor, I2PP2A. Cell Microbiol 9:2756-66.
48. Hurst, K. R., R. Ye, S. J. Goebel, P. Jayaraman, and P. S. Masters. 2010. An interaction between the nucleocapsid protein and a component of the replicase-transcriptase complex is crucial for the infectivity of coronavirus genomic RNA. J Virol 84:10276-88.
49. Ilkow, C. S., I. S. Goping, and T. C. Hobman. 2011. The Rubella virus capsid is an anti-apoptotic protein that attenuates the pore-forming ability of Bax. PLoS Pathog 7:e1001291.
50. Ilkow, C. S., V. Mancinelli, M. D. Beatch, and T. C. Hobman. 2008. Rubella virus capsid protein interacts with poly(a)-binding protein and inhibits translation. J Virol 82:4284-94.
51. Ilkow, C. S., D. Weckbecker, W. J. Cho, S. Meier, M. D. Beatch, I. S. Goping, J. M. Herrmann, and T. C. Hobman. 2010. The rubella virus capsid protein inhibits mitochondrial import. J Virol 84:119-30.
52. Ivanyi-Nagy, R., and J. L. Darlix. 2012. Core protein-mediated 5'-3' annealing of the West Nile virus genomic RNA in vitro. Virus Res 167:226-35.
53. Ivanyi-Nagy, R., I. Kanevsky, C. Gabus, J. P. Lavergne, D. Ficheux, F. Penin, P. Fosse, and J. L. Darlix. 2006. Analysis of hepatitis C virus RNA dimerization and core-RNA interactions. Nucleic Acids Res 34:2618-33.
54. Ivanyi-Nagy, R., J. P. Lavergne, C. Gabus, D. Ficheux, and J. L. Darlix. 2008. RNA chaperoning and intrinsic disorder in the core proteins of Flaviviridae. Nucleic Acids Res 36:712-25.
55. Jahan, S., S. Khaliq, M. H. Siddiqi, B. Ijaz, W. Ahmad, U. A. Ashfaq, and S. Hassan. Anti-apoptotic effect of HCV core gene of genotype 3a in Huh-7 cell line. Virol J 8:522.
56. Joo, M., Y. S. Hahn, M. Kwon, R. T. Sadikot, T. S. Blackwell, and J. W. Christman. 2005. Hepatitis C virus core protein suppresses NF-kappaB activation and cyclooxygenase-2 expression by direct interaction with IkappaB kinase beta. J Virol 79:7648-57.
57. Jose, J., J. E. Snyder, and R. J. Kuhn. 2009. A structural and functional perspective of alphavirus replication and assembly. Future Microbiol 4:837-56.
58. Kang, S. M., J. K. Choi, S. J. Kim, J. H. Kim, D. G. Ahn, and J. W. Oh. 2009. Regulation of hepatitis C virus replication by the core protein through its interaction with viral RNA polymerase. Biochem Biophys Res Commun 386:55-9.

59. Kaukinen, P., A. Vaheri, and A. Plyusnin. 2003. Non-covalent interaction between nucleocapsid protein of Tula hantavirus and small ubiquitin-related modifier-1, SUMO-1. Virus Res 92:37-45.
60. Kim, C. H., and I. Tinoco, Jr. 2001. Structural and thermodynamic studies on mutant RNA motifs that impair the specificity between a viral replicase and its promoter. J Mol Biol 307:827-39.
61. Koonin, E. V., A. E. Gorbalenya, M. A. Purdy, M. N. Rozanov, G. R. Reyes, and D. W. Bradley. 1992. Computer-assisted assignment of functional domains in the nonstructural polyprotein of hepatitis E virus: delineation of an additional group of positive-strand RNA plant and animal viruses. Proc Natl Acad Sci U S A 89:8259-63.
62. Kopecky-Bromberg, S. A., L. Martinez-Sobrido, M. Frieman, R. A. Baric, and P. Palese. 2007. Severe acute respiratory syndrome coronavirus open reading frame (ORF) 3b, ORF 6, and nucleocapsid proteins function as interferon antagonists. J Virol 81:548-57.
63. Krainer, A. R., A. Mayeda, D. Kozak, and G. Binns. 1991. Functional expression of cloned human splicing factor SF2: homology to RNA-binding proteins, U1 70K, and Drosophila splicing regulators. Cell 66:383-94.
64. Kujala, P., T. Ahola, N. Ehsani, P. Auvinen, H. Vihinen, and L. Kaariainen. 1999. Intracellular distribution of rubella virus nonstructural protein P150. J Virol 73:7805-11.
65. Law, L. M., J. C. Everitt, M. D. Beatch, C. F. Holmes, and T. C. Hobman. 2003. Phosphorylation of rubella virus capsid regulates its RNA binding activity and virus replication. J Virol 77:1764-71.
66. Lee, J. Y., and D. S. Bowden. 2000. Rubella virus replication and links to teratogenicity. Clin Microbiol Rev 13:571-87.
67. Lee, J. Y., J. A. Marshall, and D. S. Bowden. 1999. Localization of rubella virus core particles in vero cells. Virology 265:110-9.
68. Lee, K. J., I. S. Novella, M. N. Teng, M. B. Oldstone, and J. C. de La Torre. 2000. NP and L proteins of lymphocytic choriomeningitis virus (LCMV) are sufficient for efficient transcription and replication of LCMV genomic RNA analogs. J Virol 74:3470-7.
69. Lee, S. K., S. O. Park, C. O. Joe, and Y. S. Kim. 2007. Interaction of HCV core protein with 14-3-3epsilon protein releases Bax to activate apoptosis. Biochem Biophys Res Commun 352:756-62.
70. Levin, J. G., J. Guo, I. Rouzina, and K. Musier-Forsyth. 2005. Nucleic acid chaperone activity of HIV-1 nucleocapsid protein: critical role in reverse transcription and molecular mechanism. Prog Nucleic Acid Res Mol Biol 80:217-86.
71. Li, X. D., T. P. Makela, D. Guo, R. Soliymani, V. Koistinen, O. Vapalahti, A. Vaheri, and H. Lankinen. 2002. Hantavirus nucleocapsid protein interacts with the Fas-mediated apoptosis enhancer Daxx. J Gen Virol 83:759-66.
72. Liang, Y., and S. Gillam. 2001. Rubella virus RNA replication is cis-preferential and synthesis of negative- and positive-strand RNAs is regulated by the processing of nonstructural protein. Virology 282:307-19.
73. Lin, W., W. H. Choe, Y. Hiasa, Y. Kamegaya, J. T. Blackard, E. V. Schmidt, and R. T. Chung. 2005. Hepatitis C virus expression suppresses interferon signaling by degrading STAT1. Gastroenterology 128:1034-41.
74. Lin, W., S. S. Kim, E. Yeung, Y. Kamegaya, J. T. Blackard, K. A. Kim, M. J. Holtzman, and R. T. Chung. 2006. Hepatitis C virus core protein blocks interferon signaling by interaction with the STAT1 SH2 domain. J Virol 80:9226-35.

75. Liu, Z., D. Yang, Z. Qiu, K. T. Lim, P. Chong, and S. Gillam. 1996. Identification of domains in rubella virus genomic RNA and capsid protein necessary for specific interaction. J Virol 70:2184-90.
76. Lopez, N., R. Jacamo, and M. T. Franze-Fernandez. 2001. Transcription and RNA replication of tacaribe virus genome and antigenome analogs require N and L proteins: Z protein is an inhibitor of these processes. J Virol 75:12241-51.
77. Lu, X., J. Pan, J. Tao, and D. Guo. 2010. SARS-CoV nucleocapsid protein antagonizes IFN-beta response by targeting initial step of IFN-beta induction pathway, and its C-terminal region is critical for the antagonism. Virus Genes 42:37-45.
78. Luo, H., Q. Chen, J. Chen, K. Chen, X. Shen, and H. Jiang. 2005. The nucleocapsid protein of SARS coronavirus has a high binding affinity to the human cellular heterogeneous nuclear ribonucleoprotein A1. FEBS Lett 579:2623-8.
79. Machida, K., K. Tsukiyama-Kohara, E. Seike, S. Tone, F. Shibasaki, M. Shimizu, H. Takahashi, Y. Hayashi, N. Funata, C. Taya, H. Yonekawa, and M. Kohara. 2001. Inhibition of cytochrome c release in Fas-mediated signaling pathway in transgenic mice induced to express hepatitis C viral proteins. J Biol Chem 276:12140-6.
80. Magliano, D., J. A. Marshall, D. S. Bowden, N. Vardaxis, J. Meanger, and J. Y. Lee. 1998. Rubella virus replication complexes are virus-modified lysosomes. Virology 240:57-63.
81. Marin, M., K. R. Broder, J. L. Temte, D. E. Snider, and J. F. Seward. 2010. Use of combination measles, mumps, rubella, and varicella vaccine: recommendations of the Advisory Committee on Immunization Practices (ACIP). MMWR Recomm Rep 59:1-12.
82. Marr, L. D., A. Sanchez, and T. K. Frey. 1991. Efficient in vitro translation and processing of the rubella virus structural proteins in the presence of microsomes. Virology 180:400-5.
83. Marr, L. D., C. Y. Wang, and T. K. Frey. 1994. Expression of the rubella virus nonstructural protein ORF and demonstration of proteolytic processing. Virology 198:586-92.
84. Martinez-Sobrido, L., S. Emonet, P. Giannakas, B. Cubitt, A. Garcia-Sastre, and J. C. de la Torre. 2009. Identification of amino acid residues critical for the anti-interferon activity of the nucleoprotein of the prototypic arenavirus lymphocytic choriomeningitis virus. J Virol 83:11330-40.
85. Martinez-Sobrido, L., P. Giannakas, B. Cubitt, A. Garcia-Sastre, and J. C. de la Torre. 2007. Differential inhibition of type I interferon induction by arenavirus nucleoproteins. J Virol 81:12696-703.
86. Martinez-Sobrido, L., E. I. Zuniga, D. Rosario, A. Garcia-Sastre, and J. C. de la Torre. 2006. Inhibition of the type I interferon response by the nucleoprotein of the prototypic arenavirus lymphocytic choriomeningitis virus. J Virol 80:9192-9.
87. Megyeri, K., K. Berencsi, T. D. Halazonetis, G. C. Prendergast, G. Gri, S. A. Plotkin, G. Rovera, and E. Gonczol. 1999. Involvement of a p53-dependent pathway in rubella virus-induced apoptosis. Virology 259:74-84.
88. Mir, M. A., W. A. Duran, B. L. Hjelle, C. Ye, and A. T. Panganiban. 2008. Storage of cellular 5' mRNA caps in P bodies for viral cap-snatching. Proc Natl Acad Sci U S A 105:19294-9.
89. Mir, M. A., and A. T. Panganiban. 2006. Characterization of the RNA chaperone activity of hantavirus nucleocapsid protein. J Virol 80:6276-85.

90. Mir, M. A., and A. T. Panganiban. 2008. A protein that replaces the entire cellular eIF4F complex. Embo J 27:3129-39.
91. Mohan, K. V., B. Ghebrehiwet, and C. D. Atreya. 2002. The N-terminal conserved domain of rubella virus capsid interacts with the C-terminal region of cellular p32 and overexpression of p32 enhances the viral infectivity. Virus Res 85:151-61.
92. Mohd-Ismail, N. K., L. Deng, S. K. Sukumaran, V. C. Yu, H. Hotta, and Y. J. Tan. 2009. The hepatitis C virus core protein contains a BH3 domain that regulates apoptosis through specific interaction with human Mcl-1. J Virol 83:9993-10006.
93. Moorman, J. P., D. Praither, D. McVay, Y. S. Hahn, and C. S. Hahn. 2003. The C-terminal region of hepatitis C core protein is required for Fas-ligand independent apoptosis in Jurkat cells by facilitating Fas oligomerization. Virology 312:320-9.
94. Morin, B., A. A. Rahmeh, and S. P. Whelan. 2012. Mechanism of RNA synthesis initiation by the vesicular stomatitis virus polymerase. Embo J 31:1320-9.
95. Muta, T., D. Kang, S. Kitajima, T. Fujiwara, and N. Hamasaki. 1997. p32 protein, a splicing factor 2-associated protein, is localized in mitochondrial matrix and is functionally important in maintaining oxidative phosphorylation. J Biol Chem 272:24363-70.
96. Netsawang, J., S. Noisakran, C. Puttikhunt, W. Kasinrerk, W. Wongwiwat, P. Malasit, P. T. Yenchitsomanus, and T. Limjindaporn. 2010. Nuclear localization of dengue virus capsid protein is required for DAXX interaction and apoptosis. Virus Res 147:275-83.
97. Ning, B., and C. Shih. 2004. Nucleolar localization of human hepatitis B virus capsid protein. J Virol 78:13653-68.
98. Nossal, G. J. 2011. Vaccines and future global health needs. Philos Trans R Soc Lond B Biol Sci 366:2833-40.
99. Oker-Blom, C. 1984. The gene order for rubella virus structural proteins is NH2-C-E2-E1-COOH. J Virol 51:354-8.
100. Oker-Blom, C., D. L. Jarvis, and M. D. Summers. 1990. Translocation and cleavage of rubella virus envelope glycoproteins: identification and role of the E2 signal sequence. J Gen Virol 71 (Pt 12):3047-53.
101. Oker-Blom, C., N. Kalkkinen, L. Kaariainen, and R. F. Pettersson. 1983. Rubella virus contains one capsid protein and three envelope glycoproteins, E1, E2a, and E2b. J Virol 46:964-73.
102. Oshiumi, H., M. Ikeda, M. Matsumoto, A. Watanabe, O. Takeuchi, S. Akira, N. Kato, K. Shimotohno, and T. Seya. 2010. Hepatitis C virus core protein abrogates the DDX3 function that enhances IPS-1-mediated IFN-beta induction. PLoS One 5:e14258.
103. Otsuka, M., N. Kato, K. Lan, H. Yoshida, J. Kato, T. Goto, Y. Shiratori, and M. Omata. 2000. Hepatitis C virus core protein enhances p53 function through augmentation of DNA binding affinity and transcriptional ability. J Biol Chem 275:34122-30.
104. Owsianka, A. M., and A. H. Patel. 1999. Hepatitis C virus core protein interacts with a human DEAD box protein DDX3. Virology 257:330-40.
105. Parkman, P. D. 1999. Making vaccination policy: the experience with rubella. Clin Infect Dis 28 Suppl 2:S140-6.
106. Parkman, P. D., E. L. Buescher, and M. S. Artenstein. 1962. Recovery of rubella virus from army recruits. Proc Soc Exp Biol Med 111:225-30.
107. Parquet, M. C., A. Kumatori, F. Hasebe, K. Morita, and A. Igarashi. 2001. West Nile virus-induced bax-dependent apoptosis. FEBS Lett 500:17-24.

108. Peltier, D. C., H. M. Lazear, J. R. Farmer, M. S. Diamond, and D. J. Miller. 2013. Neurotropic arboviruses induce interferon regulatory factor 3-mediated neuronal responses that are cytoprotective, interferon independent, and inhibited by Western equine encephalitis virus capsid. J Virol 87:1821-33.
109. Phelps, A., C. T. Schobert, and H. Wohlrab. 1991. Cloning and characterization of the mitochondrial phosphate transport protein gene from the yeast Saccharomyces cerevisiae. Biochemistry 30:248-52.
110. Pinschewer, D. D., M. Perez, and J. C. de la Torre. 2003. Role of the virus nucleoprotein in the regulation of lymphocytic choriomeningitis virus transcription and RNA replication. J Virol 77:3882-7.
111. Pogue, G. P., X. Q. Cao, N. K. Singh, and H. L. Nakhasi. 1993. 5' sequences of rubella virus RNA stimulate translation of chimeric RNAs and specifically interact with two host-encoded proteins. J Virol 67:7106-17.
112. Pugachev, K. V., E. S. Abernathy, and T. K. Frey. 1997. Improvement of the specific infectivity of the rubella virus (RUB) infectious clone: determinants of cytopathogenicity induced by RUB map to the nonstructural proteins. J Virol 71:562-8.
113. Pugachev, K. V., and T. K. Frey. 1998. Rubella virus induces apoptosis in culture cells. Virology 250:359-70.
114. Pugachev, K. V., W. P. Tzeng, and T. K. Frey. 2000. Development of a rubella virus vaccine expression vector: use of a picornavirus internal ribosome entry site increases stability of expression. J Virol 74:10811-5.
115. Putics, A., J. Slaby, W. Filipowicz, A. E. Gorbalenya, and J. Ziebuhr. 2006. ADP-ribose-1"-phosphatase activities of the human coronavirus 229E and SARS coronavirus X domains. Adv Exp Med Biol 581:93-6.
116. Pythoud, C., W. W. Rodrigo, G. Pasqual, S. Rothenberger, L. Martinez-Sobrido, J. C. de la Torre, and S. Kunz. 2012. Arenavirus nucleoprotein targets interferon regulatory factor-activating kinase IKKepsilon. J Virol 86:7728-38.
117. Qi, X., S. Lan, W. Wang, L. M. Schelde, H. Dong, G. D. Wallat, H. Ly, Y. Liang, and C. Dong. 2010. Cap binding and immune evasion revealed by Lassa nucleoprotein structure. Nature 468:779-83.
118. Qu, B., X. Qi, X. Wu, M. Liang, C. Li, C. J. Cardona, W. Xu, F. Tang, Z. Li, B. Wu, K. Powell, M. Wegner, D. Li, and Z. Xing. 2012. Suppression of the interferon and NF-kappaB responses by severe fever with thrombocytopenia syndrome virus. J Virol 86:8388-401.
119. Rainsford, E. W., D. Harouaka, and G. W. Wertz. 2010. Importance of hydrogen bond contacts between the N protein and RNA genome of vesicular stomatitis virus in encapsidation and RNA synthesis. J Virol 84:1741-51.
120. Realdon, S., M. Gerotto, F. Dal Pero, O. Marin, A. Granato, G. Basso, M. Muraca, and A. Alberti. 2004. Proapoptotic effect of hepatitis C virus CORE protein in transiently transfected cells is enhanced by nuclear localization and is dependent on PKR activation. J Hepatol 40:77-85.
121. Rodriguez-Rodriguez, L., Z. Tsuchihashi, G. M. Fuentes, R. A. Bambara, and P. J. Fay. 1995. Influence of human immunodeficiency virus nucleocapsid protein on synthesis and strand transfer by the reverse transcriptase in vitro. J Biol Chem 270:15005-11.
122. Saikatendu, K. S., J. S. Joseph, V. Subramanian, T. Clayton, M. Griffith, K. Moy, J. Velasquez, B. W. Neuman, M. J. Buchmeier, R. C. Stevens, and P. Kuhn. 2005. Structural

basis of severe acute respiratory syndrome coronavirus ADP-ribose-1"-phosphate dephosphorylation by a conserved domain of nsP3. Structure 13:1665-75.
123. Saito, K., K. Meyer, R. Warner, A. Basu, R. B. Ray, and R. Ray. 2006. Hepatitis C virus core protein inhibits tumor necrosis factor alpha-mediated apoptosis by a protective effect involving cellular FLICE inhibitory protein. J Virol 80:4372-9.
124. Schaller, T., K. E. Ocwieja, J. Rasaiyaah, A. J. Price, T. L. Brady, S. L. Roth, S. Hue, A. J. Fletcher, K. Lee, V. N. KewalRamani, M. Noursadeghi, R. G. Jenner, L. C. James, F. D. Bushman, and G. J. Towers. 2011. HIV-1 capsid-cyclophilin interactions determine nuclear import pathway, integration targeting and replication efficiency. PLoS Pathog 7:e1002439.
125. Schelle, B., N. Karl, B. Ludewig, S. G. Siddell, and V. Thiel. 2005. Selective replication of coronavirus genomes that express nucleocapsid protein. J Virol 79:6620-30.
126. Shi, S. T., P. Huang, H. P. Li, and M. M. Lai. 2000. Heterogeneous nuclear ribonucleoprotein A1 regulates RNA synthesis of a cytoplasmic virus. Embo J 19:4701-11.
127. Suppiah, S., H. A. Mousa, W. P. Tzeng, J. D. Matthews, and T. K. Frey. 2012. Binding of cellular p32 protein to the rubella virus P150 replicase protein via PxxPxR motifs. J Gen Virol 93:807-16.
128. Surjit, M., B. Liu, V. T. Chow, and S. K. Lal. 2006. The nucleocapsid protein of severe acute respiratory syndrome-coronavirus inhibits the activity of cyclin-cyclin-dependent kinase complex and blocks S phase progression in mammalian cells. J Biol Chem 281:10669-81.
129. Surjit, M., B. Liu, S. Jameel, V. T. Chow, and S. K. Lal. 2004. The SARS coronavirus nucleocapsid protein induces actin reorganization and apoptosis in COS-1 cells in the absence of growth factors. Biochem J 383:13-8.
130. Thomas, J. A., T. D. Gagliardi, W. G. Alvord, M. Lubomirski, W. J. Bosche, and R. J. Gorelick. 2006. Human immunodeficiency virus type 1 nucleocapsid zinc-finger mutations cause defects in reverse transcription and integration. Virology 353:41-51.
131. Timani, K. A., Q. Liao, L. Ye, Y. Zeng, J. Liu, Y. Zheng, L. Ye, X. Yang, K. Lingbao, J. Gao, and Y. Zhu. 2005. Nuclear/nucleolar localization properties of C-terminal nucleocapsid protein of SARS coronavirus. Virus Res 114:23-34.
132. Tzeng, W. P., M. H. Chen, C. A. Derdeyn, and T. K. Frey. 2001. Rubella virus DI RNAs and replicons: requirement for nonstructural proteins acting in cis for amplification by helper virus. Virology 289:63-73.
133. Tzeng, W. P., and T. K. Frey. 2003. Complementation of a deletion in the rubella virus p150 nonstructural protein by the viral capsid protein. J Virol 77:9502-10.
134. Tzeng, W. P., and T. K. Frey. 2009. Functional replacement of a domain in the rubella virus p150 replicase protein by the virus capsid protein. J Virol 83:3549-55.
135. Tzeng, W. P., and T. K. Frey. 2005. Rubella virus capsid protein modulation of viral genomic and subgenomic RNA synthesis. Virology 337:327-34.
136. Tzeng, W. P., J. D. Matthews, and T. K. Frey. 2006. Analysis of rubella virus capsid protein-mediated enhancement of replicon replication and mutant rescue. J Virol 80:3966-74.
137. Tzeng, W. P., J. Xu, and T. K. Frey. 2012. Characterization of cell lines stably transfected with rubella virus replicons. Virology 429:29-36.

138. Urbanowski, M. D., and T. C. Hobman. 2013. The West Nile Virus Capsid Protein Blocks Apoptosis through a Phosphatidylinositol 3-Kinase-Dependent Mechanism. J Virol 87:872-81.
139. van Marle, G., J. Antony, H. Ostermann, C. Dunham, T. Hunt, W. Halliday, F. Maingat, M. D. Urbanowski, T. Hobman, J. Peeling, and C. Power. 2007. West Nile virus-induced neuroinflammation: glial infection and capsid protein-mediated neurovirulence. J Virol 81:10933-49.
140. Wang, C. Y., G. Dominguez, and T. K. Frey. 1994. Construction of rubella virus genome-length cDNA clones and synthesis of infectious RNA transcripts. J Virol 68:3550-7.
141. Wang, Y., N. Kato, A. Jazag, N. Dharel, M. Otsuka, H. Taniguchi, T. Kawabe, and M. Omata. 2006. Hepatitis C virus core protein is a potent inhibitor of RNA silencing-based antiviral response. Gastroenterology 130:883-92.
142. Weller, T. H., and F. A. Neva. 1962. Propagation in tissue culture of cytopathic agents from patients with rubella-like illness. Proc Soc Exp Biol Med 111:215-225.
143. Wesselhoeft, C. 1947. Rubella (German measles). N Engl J Med 236:978-88.
144. Wurm, T., H. Chen, T. Hodgson, P. Britton, G. Brooks, and J. A. Hiscox. 2001. Localization to the nucleolus is a common feature of coronavirus nucleoproteins, and the protein may disrupt host cell division. J Virol 75:9345-56.
145. Yan, X., Q. Hao, Y. Mu, K. A. Timani, L. Ye, Y. Zhu, and J. Wu. 2006. Nucleocapsid protein of SARS-CoV activates the expression of cyclooxygenase-2 by binding directly to regulatory elements for nuclear factor-kappa B and CCAAT/enhancer binding protein. Int J Biochem Cell Biol 38:1417-28.
146. Yang, M. R., S. R. Lee, W. Oh, E. W. Lee, J. Y. Yeh, J. J. Nah, Y. S. Joo, J. Shin, H. W. Lee, S. Pyo, and J. Song. 2008. West Nile virus capsid protein induces p53-mediated apoptosis via the sequestration of HDM2 to the nucleolus. Cell Microbiol 10:165-76.
147. Yi, G., K. Gopinath, and C. C. Kao. 2007. Selective repression of translation by the brome mosaic virus 1a RNA replication protein. J Virol 81:1601-9.
148. Yi, G., E. Letteney, C. H. Kim, and C. C. Kao. 2009. Brome mosaic virus capsid protein regulates accumulation of viral replication proteins by binding to the replicase assembly RNA element. Rna 15:615-26.
149. Yoshida, H., N. Kato, Y. Shiratori, M. Otsuka, S. Maeda, J. Kato, and M. Omata. 2001. Hepatitis C virus core protein activates nuclear factor kappa B-dependent signaling through tumor necrosis factor receptor-associated factor. J Biol Chem 276:16399-405.
150. Zeng, Y., L. Ye, S. Zhu, H. Zheng, P. Zhao, W. Cai, L. Su, Y. She, and Z. Wu. 2008. The nucleocapsid protein of SARS-associated coronavirus inhibits B23 phosphorylation. Biochem Biophys Res Commun 369:287-91.
151. Zhang, B., H. Dong, D. A. Stein, P. L. Iversen, and P. Y. Shi. 2008. West Nile virus genome cyclization and RNA replication require two pairs of long-distance RNA interactions. Virology 373:1-13.
152. Zhou, B., J. Liu, Q. Wang, X. Liu, X. Li, P. Li, Q. Ma, and C. Cao. 2008. The nucleocapsid protein of severe acute respiratory syndrome coronavirus inhibits cell cytokinesis and proliferation by interacting with translation elongation factor 1alpha. J Virol 82:6962-71.
153. Zhou, S., A. M. Cerny, A. Zacharia, K. A. Fitzgerald, E. A. Kurt-Jones, and R. W. Finberg. 2010. Induction and inhibition of type I interferon responses by distinct components of lymphocytic choriomeningitis virus. J Virol 84:9452-62.

154. Zuniga, S., J. L. Cruz, I. Sola, P. A. Mateos-Gomez, L. Palacio, and L. Enjuanes. 2010. Coronavirus nucleocapsid protein facilitates template switching and is required for efficient transcription. J Virol 84:2169-75.
155. Zuniga, S., I. Sola, J. L. Moreno, P. Sabella, J. Plana-Duran, and L. Enjuanes. 2007. Coronavirus nucleocapsid protein is an RNA chaperone. Virology 357:215-27.

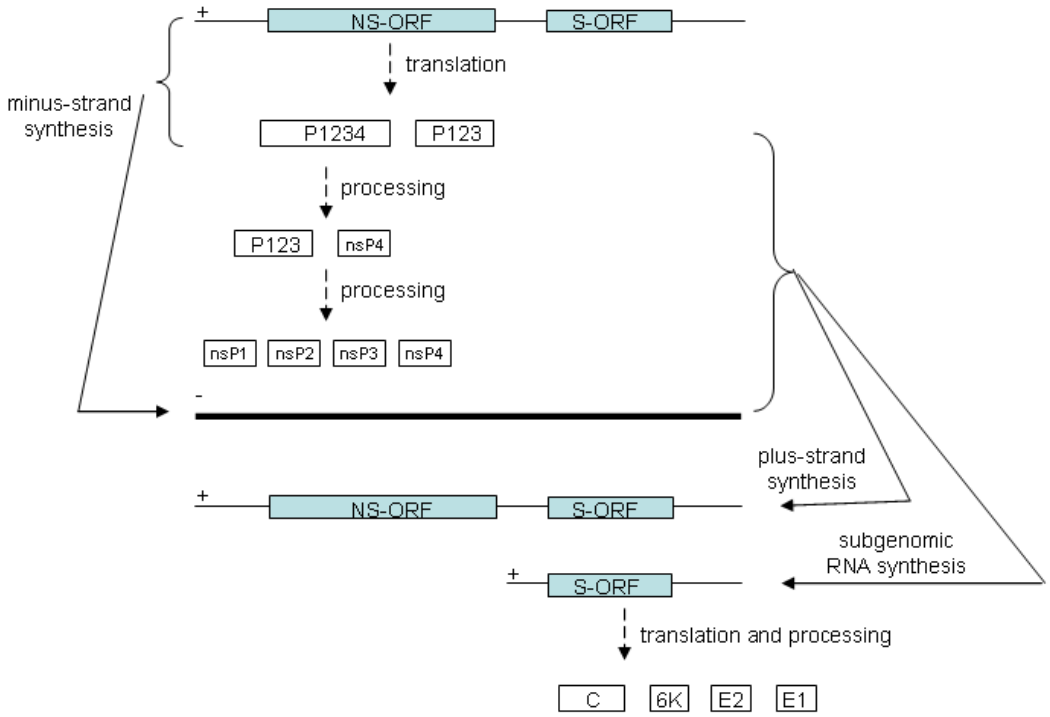

Figure 1. Alphavirus replication cycle
The nonstructural ORF is translated from the genomic RNA into two polyproteins, P123 and P1234. These polyproteins are cleaved to yield nsP1, nsP2, nsP3, and nsP4, which complex with host factors to form the RC. The incoming genomic RNA is used as a template to generate negative-sense RNA that in turn serves as the template to produce both genomic RNA and subgenomic RNA. The structural ORF is translated from the subgenomic RNA to give a polyprotein that is processed giving the capsid protein, glycoproteins E2 and E1, and 6K protein.

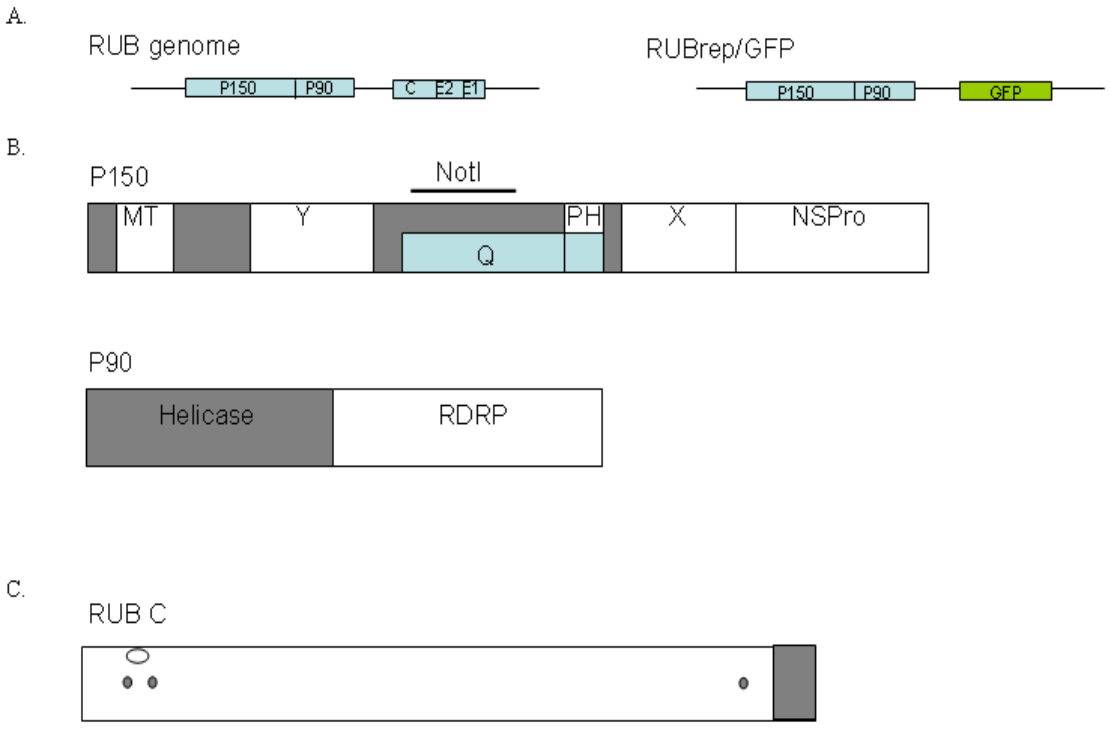

Figure 2. Rubella virus genome, replicon, and features of P150, P90 and the capsid protein A) RUB genome (left) containing the nonstructural proteins P150 and P90 translated from the NS-ORF and the structural proteins C, E2, and E1 from the S-OFR and RUB replicon with GFP replacing the S-ORF (right). B) Domain map of RUB P150 including methyl transferase (MT), Y, proline hinge (PH), X, protease (NSPro), and Q domain (Q) regions. The *Not*I region is also highlighted. Domain map of RUB P90 including helicase and RDRP. C) Map of RUB C (300 aa in length) showing the two arginine clusters (gray circles), S46 primary phosphorylation site (white circle), and C-terminal E2 signal sequence (gray box).

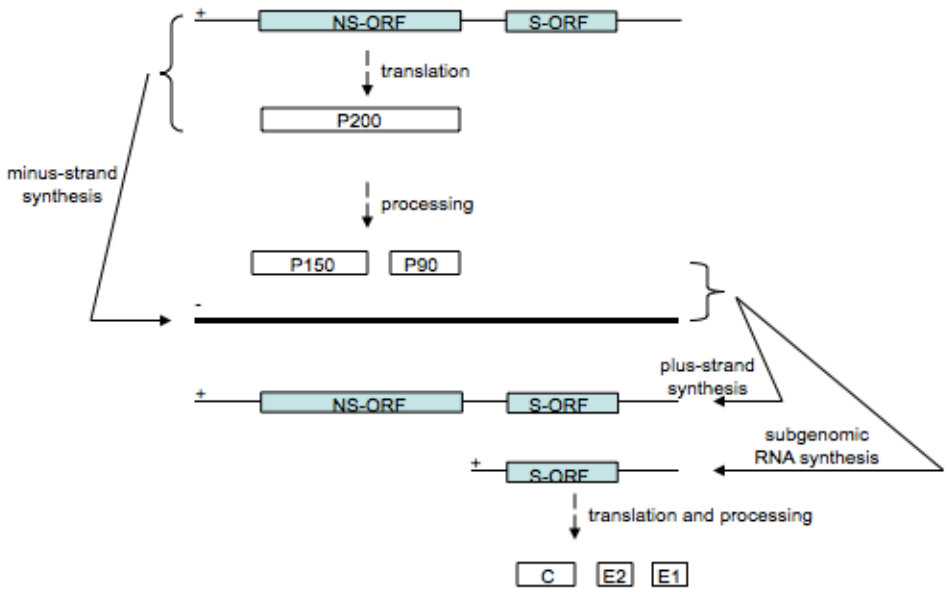

Figure 3. Rubella virus replication cycle
The nonstructural ORF is translated and processed from the genomic RNA into yield P150 and P90, which use the incoming genomic RNA is as a template to generate negative-sense RNA that in turn serves as the template to produce both genomic RNA and subgenomic RNA. The structural ORF is translated and processed from the subgenomic RNA to give C, E2, and E1.

2 SPECIFIC AIM 1: IDENTIFY AND CHARACTERIZE THE REGION WITHIN THE RUB C MINIMAL REGION FOR RESCUE OF THE RUB P150 Q DOMAIN.

2.1 Introduction

RUB C contains several characterized landmarks, many of which fall within the first 88 amino acids, the minimal region required for the rescue of the RUB P150 Q domain (Figure 4. A). The primary phosphorylation site of RUB C is at serine 46. Nonphosphorylated capsid has a higher affinity for genomic RNA, suggesting that the phosphorylation negatively regulates the RNA binding activity of this protein (4). The negative charge of the phosphate group on serine 46 in the RNA binding region may prevent nonspecific electrostatic interaction with RNA or the phosphate group may alter conformation in a manner to inhibit RNA binding. It has also been postulated to serve as a regulatory phosphorylation site governing phosphorylation of several nearby serine and threonine residues (3). There are also two arginine clusters; the first arginine cluster (R1) is located between amino acids 35 through 43 and the second arginine cluster (R2) is located between amino acids 54 through 68; the R2 cluster is required for RUB C binding of RNA (1). A 2000 study by the Hobman lab mapped the p32 binding region of RUB C to amino acids 46-89 (2), a region that does not include the R1 cluster. However, in a later 2005 study, the Hobman lab reported that the region of RUB C that binds p32 is found between amino acids 30-69, a region that includes both R1 and R2, and found that both R1 and R2 were necessary for p32 binding (2). In Chapter 3, we provide evidence that R2, but not R1, is necessary for p32 binding, at least within the context of the 1-88 RUB C construct.

This study sought to identify the specific landmarks within the first 88 amino acids of RUB C required for the rescue of the RUB P150 Q domain. Previous studies indicated that the R2 cluster is required for the rescue of RUBrep/GFP-ΔNotI when 1-277 RUB C was provided in

trans from a plasmid vector (6). However, we wanted to re-examine mutations in this cluster in the context of the 1-88 construct as we planned to use this truncated version of RUB C in cell protein binding experiments proposed in Specific Aim 2. We began by examining the arginine clusters and primary phosphorylation site within the context of 1-88 RUB C provided in *trans* from a plasmid vector to determine if these regions were important for the rescue of RU-Brep/GFP-ΔNotI. After identification, rescuing and non-rescuing 1-88 RUB C mutants as well as wild type 1-88 RUB C were studied for differences in phosphorylation and intracellular local-ization.

2.2 Results

2.2.1 Generation of 1-88 RUB C mutants

A series of mutations in the phosphorylation site and arginine clusters that had been previously reported in the literature were introduced into a FLAG-tagged 1-88 RUB C plasmid-based expression construct (expressed from a CMV promoter), further referred to as 1-88 RUB C, to determine if any of these landmarks were important for the rescue of RUBrep/GFP-ΔNotI replication (Figure 4.A). Arginines in the two arginine clusters were changed to alanines either in the individual clusters (R1A, R2A) or together (2RA). The primary phosphorylation site, S46, was changed to aspartic acid (S46D) or glutamic acid (S46E) to mimic phosphorylation. Expres-sion of 1-88 RUB C and all of its mutants in transfected cells was detectable by Western blot (Figure 4.B).

2.2.2 Optimization of RUBrep/GFP-ΔNotI rescue assay

Prior to the examination of the 1-88 RUB C mutant panel, the RUBrep/GFP-ΔNotI rescue assay was optimized to determine the timeline of transfection of wild type 1-88 RUB C and RUBrep/GFP-ΔNotI RNA that would yield the most robust GFP signal. The premise behind the rescue assay is to cotransfect a plasmid expressing RUB C and *in vitro* RUBrep/GFP-ΔNotI transcripts into Vero cells and then observe whether or not the form of RUB C used was able to rescue the replication of the replicon through the detection of GFP positive cells (Figure 5). On day 1, 1-88 RUB C was transfected into Vero cells and *in vitro* RUBrep/GFP-ΔNotI RNA transcripts were transfected on day 1, day 2, or day 3. GFP expression was observed in live cells using fluorescence microscopy and scored for intensity on day 2, day 3, and day 4. GFP was first observed in all cultures examined at day 3, but the highest GFP levels were observed on day 4 when RUBrep/GFP-ΔNotI RNA was transfected on day 2 (Figure 6.A). The expression of 1-88 RUB C was evident in each cell lysate sample at day 4 (Figure 6.B). Based on the results of this pilot experiment, 1-88 RUB C and its mutants were transfected on day 1, RUBrep/GFP-ΔNotI RNA was transfected on day 2, and GFP expression was examined on day 4 during subsequent experimentation.

2.2.3 Second arginine cluster of 1-88 RUB C is necessary for the rescue of RUBrep/GFP-ΔNotI by 1-88 RUB C

The 1-88 RUB C mutant panel was next screened for the ability to rescue RUBrep/GFP-ΔNotI using the experimental timeline established for wild type 1-88 RUB C. RUBrep/GFP-ΔNotI replication was rescued by wild type 1-88 RUB C as well as the S46D, S46E, and R1A mutants as evidenced by the presence of GFP positive cells observed using fluores-

cence microscopy, while no GFP positive cells, and therefore no rescue, were observed with the 1-88 RUB C R2A and 2RA mutants as well as in mock transfected cells (Figure 7). These results are consistent with results previously found with a similar mutant panel in the context of FLAG-tagged 1-277 RUB C expressed from the same vector (6).

Quantification of the GFP positive cell population by FACS analysis confirmed the observations made by fluorescence microscopy. The percentage of GFP positive cells was significantly reduced following transfection with the 1-88 RUB C R2A and 2RA mutants compared with wild type 1-277 RUB C or wild type 1-88 RUB C (Figure 8). Western blot analysis of the expression of the wild type 1-88 RUB C and mutant panel C proteins in an aliquot of the same cells used for cytometry quantification confirmed expression of the various constructs during this experiment. Thus, lack of GFP positive cells could not be attributed to poor expression of the non-rescuing 1-88 RUB C mutants. The data showed that the second arginine cluster of 1-88 RUB C, which is mutated in both the R2A and 2RA mutants, is important for the rescue RUBrep/GFP-ΔNotI.

2.2.4 Localization of 1-88 RUB C panel does not differ between rescuing and non-rescuing mutants

The localization of wild type 1-88 RUB C and its mutants was next examined to determine if rescuing and non-rescuing forms of 1-88 RUB C have different cellular locations. RUB C localizes to the mitochondria and is known to associate with mitochondrial matrix protein p32 (2). A nuclear and perinuclear distribution can be seen for all forms of 1-88 RUB C. The perinuclear distribution of the 1-88 RUB C proteins overlaps with the mitochondria as seen with staining with anti-p32 antibodies. Representative images for a rescuing (1-88 RUB C S46D)

and non-rescuing (1-88 RUB C R2A) 1-88 RUB C are shown (Figure 9). This same pattern was observed when the mitochondria were stained using MitoTracker® (data not shown). The differential ability of the 1-88 RUB C proteins to rescue the *Not*I deletion in RUB P150 cannot be explained by differences in intracellular localization between rescuing and non-rescuing forms of 1-88 RUB C proteins.

2.2.5 Phosphorylation states of 1-88 RUB C and its mutants cannot explain rescue phenomenon

We next examined the phosphorylation status of wild type 1-88 RUB C and its mutants to determine if this modification regulates the ability of 1-88 RUB C to rescue RUBrep/GFP-ΔNotI. Treatment with calf intestinal phosphatase (CIP) resulted in a downward shift in the bands for wild type 1-88 RUB C, R2A, S46D, and S46E while there was no change in mobility for 1-88 RUB C R1A and 2RA (Figure 10). This indicates that wild type RUB C 1-88, R2A, S46D, and S46E are phosphorylated, while RUB C 1-88 R1A and 2RA are not phosphorylated and thus the phosphorylation status of 1-88 RUB C cannot explain the rescue phenomenon. This result also suggests that the R1 cluster is important in phosphorylation of RUB C.

2.3 Methods

2.3.1 Cells and replicons

African green monkey kidney cells (Vero) were maintained in DMEM containing 5% FBS and gentamycin (10 μg/ml) at 35ºC and 5% CO_2. The rubella replicon RUBrep/GFP-ΔNotI (5) was used in this study. *In vitro* transcription of linearized replicon DNA templates was car-

ried out in a 25 µl reaction containing 5 µl 5X transcription buffer (40 mM Tris-HCl (pH7.5), 6 mM $MgCl_2$, 2 mM spermidine) (Epicentre), 2.5 µl 100 mM DTT, 40U RNasin Ribonuclease Inhibitors (Promega), 1 µl 25mM NTPs (Amersham), 5 µl 10mM cap analogue ($m^7G(5')ppp(5')G$) (New England BioLabs), 50U SP6 DNA dependent RNA polymerase (Epicentre), and 2 µl 250 ng/µl linearized template incubated at 37ºC for 1 hr. The quality of the *in vitro* transcript was assayed by electrophoresing the product through a 1% agarose gel followed by staining with ethidium bromide.

2.3.2 Antibodies

The following antibodies were used in this study: monoclonal mouse M2 anti-FLAG (Sigma), rabbit anti-calnexin (Sigma), and polyclonal rabbit anti-32 (Santa Cruz). Secondary antibodies were AP-conjugated goat or donkey anti-mouse IgG, AP-conjugated goat or donkey anti-rabbit IgG (Promega), and FITC- or TRITC-conjugated goat antibodies against mouse or rabbit IgG (Sigma).

2.3.3 Generation of expression constructs

A series of RUB C mutants were generated such that the mutation of interest was in the context of the first 88 amino acids of a FLAG-tagged RUB C expressed from the vector pcDNA. The mutants in this region were S46D (GAC), S46E (GAA), R1A, R2A, and 2RA. The 1-88 RUB C sequence was amplified from the corresponding FLAG-tagged 1-277 RUB C mutant construct (6). This was accomplished in a 50 µl reaction containing 25 µl 2X GC buffer (Takara), 8 µl 2.5mM dNTPs, 1 µl 200 ng/µl forward primer including a *Eco*RV restriction site and 2X FLAG tag in front of the 5' terminus of the RUB C gene (5' TAAGATATCCATGGACT

ATAAGGACGACGACGACAAGGACTATAAGGACGACGACGACAAGGCTTCTACTACC CCCATCACCATGGAG 3'), 1 µl of 200 ng/µl of reverse primer including a *Xba*I restriction site, translation termination codon, and sequences complementary to the RUB C gene starting at codon 88 (5' GTACTCTAGACTAGCGAGTTTCTTGCCGC 3'), 5U Ex Taq DNA polymerase (Takara), and 0.5 µl the appropriate 1-277 RUB C template in pcDNA. The PCR protocol used was 36 cycles of 98ºC for 30 sec, 55ºC for 20 sec, and 72ºC for 1 min followed by incubation at 72ºC for 1 min. pcDNA and purified PCR products underwent digestion using *Eco*RV and *Xba*I restriction enzymes (New England BioLabs), followed by gel purification using QIAquick gel extraction kit (QIAGEN) and these fragments were ligated together using T4 DNA ligase (New England BioLabs) for 1 hour at room temperature. The ligation reactions were then transformed into competent DH5α *E. coli*. Resulting colonies were picked for miniprep plasmid DNA isolation that was then screened for the presence of both the insert and the vector using restriction digestion on *Eco*RV and *Xba*I sites. Positive colonies were then sequenced. The resulting constructs were termed 1-88 RUB C wt, R1A, R2A, 2RA, S46D, or S46E.

2.3.4 Optimization of RUBrep/GFP-ΔNotI rescue assay

Parameters for the assay of the rescue of RUBrep/GFP-ΔNotI replication by RUB C were optimized using wild type 1-88 RUB C. Vero cells were plated in 60 mm plates and allowed to grow overnight. The plates were divided into the following groups: transfected with wild type 1-88 RUB C and RUBrep/GFP-ΔNotI 1 day after plating (day 1), transfected with wild type 1-88 RUB C on day 1 and RUBrep/GFP-ΔNotI 2 days after plating (day 2), and transfected with wild type 1-88 RUB C on day 1 and RUBrep/GFP-ΔNotI 3 days after plating (day 3). The cells were transfected using Lipofectamine 2000 (Invitrogen) according to manufacturer's rec-

ommendations with 10 μg of cDNA and/or 6 μl of *in vitro* transcribed RNA. Transfection reagents were incubated on cell cultures for at least 4 hours before removal and addition of growth medium. Living cells on these plates were observed for expression of GFP using a Zeiss Axionplan 2 Imaging microscope beginning the day after the transfection of RUBrep/GFP-ΔNotI through day 4. Following microscopy on day 4, the cells were lysed to assay the expression of wild type 1-88 RUB C levels using Western blot.

2.3.5 Analysis of 1-88 RUB C mutant panel using RUBrep/GFP-ΔNotI rescue assay

Screening of the 1-88 RUB C mutant panel for RUBrep/GFP-ΔNotI GFP rescue was done as follows. Vero cells were plated in 60 mm plates and allowed to grow overnight. The cells were transfected with 1-88 RUB C wt or mutant panel DNA 1 day after plating and then transfected with *in vitro* transcribed RUBrep/GFP-ΔNotI RNA 2 days after plating. The cells were transfected using Lipofectamine 2000 (Invitrogen) according to manufacturer's recommendations with 10 μg of cDNA or 6 μl of *in vitro* transcribed RNA. Transfection reagents were allowed to incubate on cell cultures for at least 4 hours before removal and addition of growth medium. Plates were observed for expression of GFP using a Zeiss Axionplan 2 Imaging microscope followed by cell lysis for analysis of 1-88 RUB C levels using Western blot on day 4.

2.3.6 Flow cytometry of RUBrep/GFP-ΔNotI rescue by 1-88 RUB C mutant panel

Quantification of the number of GFP positive cells present during rescue was done as follows. Vero cells were plated in 60 mm plates and allowed to grow overnight. The cells were transfected with the 1-88 RUB C wt or mutant panel cDNA 1 day after plating and then transfected with *in vitro* transcribed RUBrep/GFP-ΔNotI RNA 2 days after plating. The cells were

transfected using Lipofectamine 2000 (Invitrogen) according to manufacturer's recommendations with 10 µg cDNA or 6 µl of *in vitro* transcribed RNA. Transfection reagents were allowed to incubate on cell cultures for at least 4 hours before removal and addition of growth medium. Cell cultures were observed for expression of GFP using fluorescence microscopy and then cells were either quantified using FACS analysis or processed by cell lysis for analysis of 1-88 RUB C levels using Western blot 4 days after plating.

The plates were prepared for FACS analysis by decanting the media, adding 0.5 ml of trypsin solution, and allowing the plates to incubate at 35°C for 10 minutes until cell detachment occurred. Next, 1.5 ml PBS was added to each plate to resuspend the cells; 1 ml of this suspension was used for FACS and 1 ml was lysed for Western blot analysis.

2.3.7 Immunofluorescence assay

In order to observe the intracellular localization of 1-88 RUB C and its mutants, an immunofluorescence assay (IFA) was performed. Vero cells were plated at a low density (1.5 ml of trypsinized cells in 25 ml media; in the usual plating 1 ml of trypsinized cells is mixed with 9 ml of medium) in 35 mm plates containing coverslips and were allowed to grow overnight. The cells were transfected using Lipofectamine 2000 (Invitrogen) according to manufacturer's recommendations with 5 µg of 1-277 RUB C or 1-88 RUB C (wt, R1A, R2A, 2RA, S46D, and S46E) cDNA. Transfection reagents were allowed to incubate on the cell cultures for at least 4 hours before removal and addition of growth medium and coverslips were then processed for IFA 2 days post-transfection. One set of cells was labeled for 30 minutes using MitoTracker® red (1:10,000) (Invitrogen) diluted in growth media prior to IFA using anti-FLAG antibodies.

Coverslips were processed for IFA as follows. Media was decanted and 1 ml of ice-cold methanol was added to the plate for 5 minutes. The plates were then washed 3 times with PBS, allowing the last wash to incubate for 15 minutes. Next, 100 µl of prepared primary antibody (1:1000 anti-FLAG, 1:333 anti-p32, 1:1000 Hoechst 33342 (Invitrogen), in PBS/1% BSA) was added to each coverslip and incubated in the dark for 30 minutes. After 3 washes with PBS, 100 µl prepared secondary antibody anti-mouse FITC (1:100 (Sigma) PBS/1% BSA) or anti-mouse FITC and anti-rabbit TRITC (1:100 (Sigma) (PBS/1% BSA) was added and incubated in the dark for 30 minutes. The coverslips were washed 3 times with PBS and mounted on glass slides with Entellan® new rapid mounting medium for microscopy (EMD). The coverslips were then observed using fluorescence microscopy using a Zeiss Axionplan 2 Imaging microscope.

2.3.8 CIP analysis of phosphorylation status of 1-88 RUB C mutant panel

Vero cells were plated in 35mm plates and allowed to grow overnight. The cells were transfected with the 1-88 RUB C wt or mutant panel cDNA 1 day after plating. The cells were transfected using Lipofectamine 2000 (Invitrogen) according to manufacturer's recommendations with 5 µg of 1-88 RUB C (wt, R1A, R2A, 2RA, S46D, and S46E) DNA. Transfection reagents were allowed to incubate on cell cultures for at least 4 hours before removal and addition of growth medium. Plates were harvested 2 days post-transfection.

Cells on the 35 mm plates were lysed in 400 µl PBS based lysis buffer (1.5mM NaCl, 1% Triton X-100, 0.1% SDS, 0.5% DOC in PBS) with complete, mini, EDTA-free protease inhibitor cocktail tablet (1 tablet/10ml buffer) (Roche) and clarified by centrifugation. Proteins were dephosphorylated using CIP according to manufacturer's recommendations (New England BioLabs) with modifications. Briefly, a 50 µl total reaction was done containing 1 µg/10 µl of

protein, two-fold excess CIP mixture and NEB buffer 2. The reaction was incubated at 37ºC for 30 minutes and then combined with 5X SDS PAGE loading buffer and boiled for 5 minutes prior to PAGE and Western blot analysis.

2.3.9 Western blot

Cells in 60 mm plates were lysed with 500 µl 1XRIP lysis buffer (10 mM Tris pH 8.0, 150 mM NaCl, 3 mM EDTA, 1% Triton X-100, 0.1% SDS, 0.5% DOC) with complete, mini, EDTA-free protease inhibitor cocktail tablet (1 tablet/10 ml buffer) (Roche) and lysates were clarified by centrifugation. Clarified cell lysates (20 µl) were combined with 5X SDS-sample buffer (250 mM Tris-HCl pH 6.8, 20 mM DTT, 10% SDS, 0.2% bromophenol blue, 50% glycerol) (5 µl), boiled for 5 minutes, and clarified by brief centrifugation. The cell lysates were electrophoresed in a 10% or 15% SDS-PAGE gel and transferred to a nitrocellulose membrane (Whatman) using 1X transfer buffer (100 ml 10X transfer buffer (250 mM Tris, 192 M glycine), 200 ml methanol, and 700 ml deionized water) and a mini-Protean II apparatus (BioRad) at 100V for 1 hour. The membranes were blocked in 5% non-fat dry milk in TBS (20 mM Tris-HCl pH 7.5 and 175 mM NaCl) and then probed with the appropriate primary and secondary antibody. Color development solution was added (10 ml alkaline phosphatase buffer (100 mM Tris, 100 mM NaCl, 50 mM $MgCl_2$-$6H_20$, pH 9.8), 33 µl NBT (Roche), and 33 µl BCIP (Roche)) to detect bound antibodies.

2.4 References

1. Beatch, M. D., J. C. Everitt, L. J. Law, and T. C. Hobman. 2005. Interactions between rubella virus capsid and host protein p32 are important for virus replication. J Virol 79:10807-20.

2. Beatch, M. D., and T. C. Hobman. 2000. Rubella virus capsid associates with host cell protein p32 and localizes to mitochondria. J Virol 74:5569-76.
3. Law, L. J., C. S. Ilkow, W. P. Tzeng, M. Rawluk, D. T. Stuart, T. K. Frey, and T. C. Hobman. 2006. Analyses of phosphorylation events in the rubella virus capsid protein: role in early replication events. J Virol 80:6917-25.
4. Law, L. M., J. C. Everitt, M. D. Beatch, C. F. Holmes, and T. C. Hobman. 2003. Phosphorylation of rubella virus capsid regulates its RNA binding activity and virus replication. J Virol 77:1764-71.
5. Tzeng, W. P., M. H. Chen, C. A. Derdeyn, and T. K. Frey. 2001. Rubella virus DI RNAs and replicons: requirement for nonstructural proteins acting in cis for amplification by helper virus. Virology 289:63-73.
6. Tzeng, W. P., and T. K. Frey. 2009. Functional replacement of a domain in the rubella virus p150 replicase protein by the virus capsid protein. J Virol 83:3549-55.

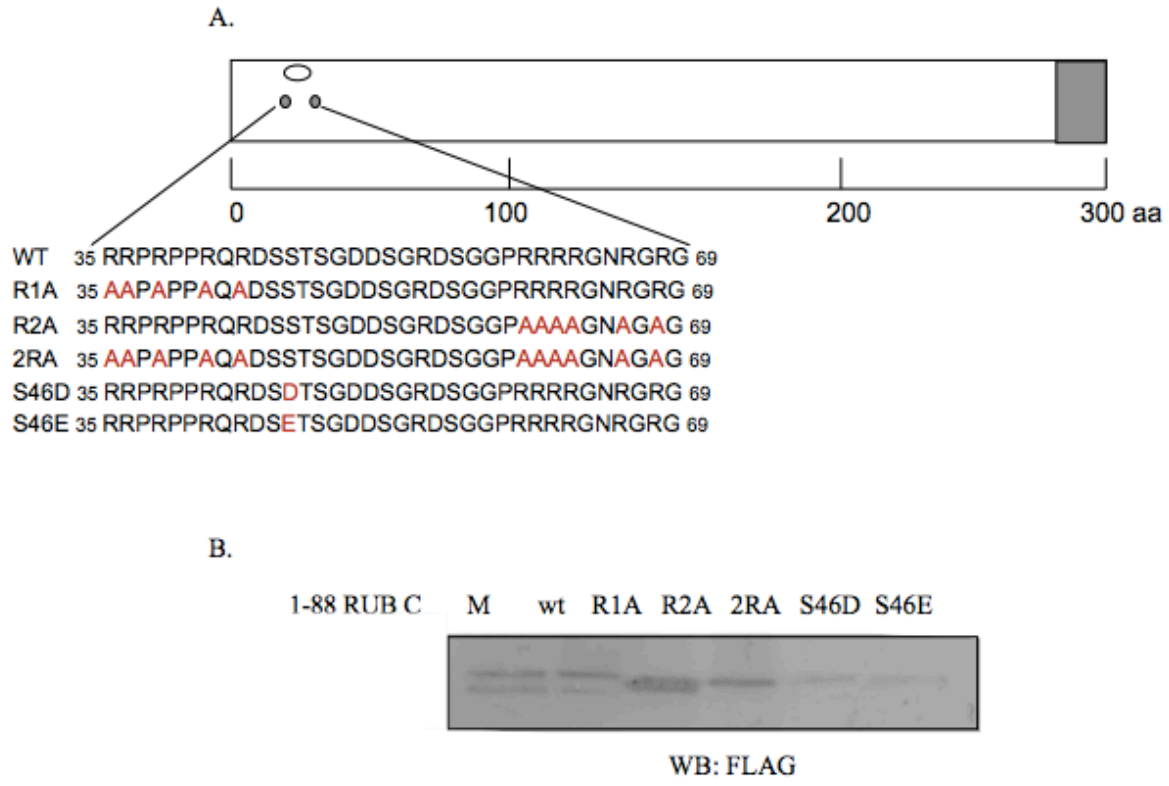

Figure 4. Expression of 1-88 RUB C and its mutants
A) Schematic of RUB C showing the two arginine clusters (gray circles), S46 primary phosphorylation site (white circle), and C-terminal E2 signal sequence (gray box). Below are shown aa 35 to 69 of RUB C with specific mutations introduced into 1-88 RUB C for this study in red. These include mutation of the first arginine cluster (R1A), second arginine cluster (R2A), both arginine clusters (2RA), and the primary phosphorylation site (S46D/S46E). B) Vero cells were mock-transfected (M) or transfected with 10 µg cDNA of 1-88 RUB C wt or one of the mutant panel 1 day after plating. Plates were lysed 2 days post-transfection and lysates were electrophoresed in a 15% SDS-PAGE gel and proteins were transferred to a nitrocellulose membrane. The membrane was then probed with primary antibody (anti-FLAG 1:400) and secondary antibody (anti-mouse AP conjugated 1:5000).

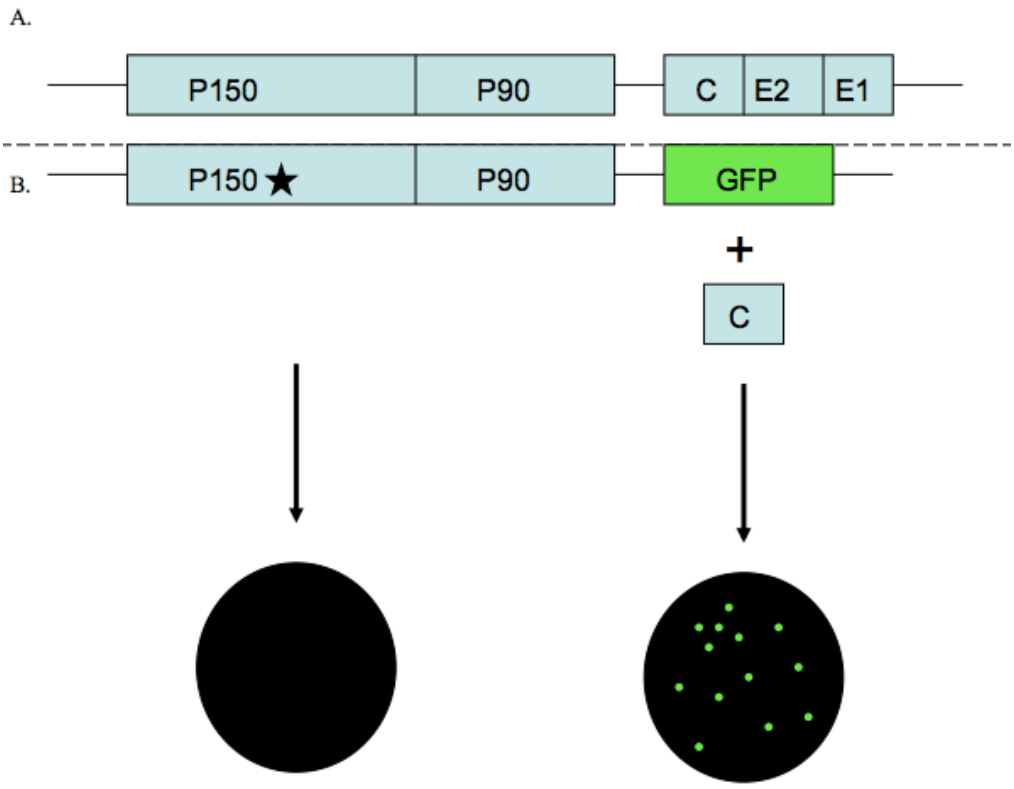

Figure 5. Diagram of RUBrep/GFP-ΔNotI rescue assay
A) The RUB virus genome with nonstructural ORF including P150 and P90, which form the viral replicase, and structural ORF including C, E2, and E1, which form the virion. B) RUBrep/GFP-ΔNotI rescue assay. The replicon contains an ~500 nt deletion between two in frame *Not*I restriction sites (*) and is replication deficient without RUB C. Replication of the replicon is monitored by the expression of GFP, which replaces the structural ORF. Mutant and wild type forms of RUB C were expressed in *trans* to determine if that form of RUB C rescued RUBrep/GFP-ΔNotI replication.

A.

	*Not*I day 1	*Not*I day 2	*Not*1 day 3
GFP day 2	-		
GFP day 3	+	+	
GFP day 4	++	+++	+

B.

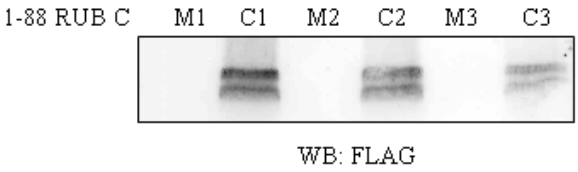

Figure 6. Optimization of RUBrep/GFP-ΔNotI rescue assay
Vero cells were transfected with 10 µg of 1-88 RUB C cDNA at day 1 and transfected with 6 µl of RUBrep/GFP-ΔNotI RNA transcripts on either day 1, 2, or 3. Plates that had been transfected with the replicon were examined for RUBrep/GFP-ΔNotI replication visualized as GFP expression using fluorescence microscopy at days 2, 3, and 4. A) Cells were transfected with 1-88 RUB C on day 1. In the table, "*Not*I day" is the day on which the cells were transfected with RUBrep/GFP- ΔNotI, "GFP day" is the day the plate was examined for GFP, and +/- represents the strength of the GFP signal. B) Western blot analysis of 1-88 RUB C expression was done on cells lysed on day 4. Lysates were electrophoresed in a 15% SDS-PAGE gel and proteins were transferred to a nitrocellulose membrane. The membrane was then probed with primary antibody (anti-FLAG 1:400) and secondary antibody (anti-mouse AP conjugated 1:5000). Cells were mock (M) or 1-88 RUB C (C)-transfected on day 1 and then transfected with RUBrep/GFP-ΔNot I RNA on day 1 (M1, C1), day 2 (M2,C2) or day 3 (M3,C3) followed by lysis on day 4 of the experiment.

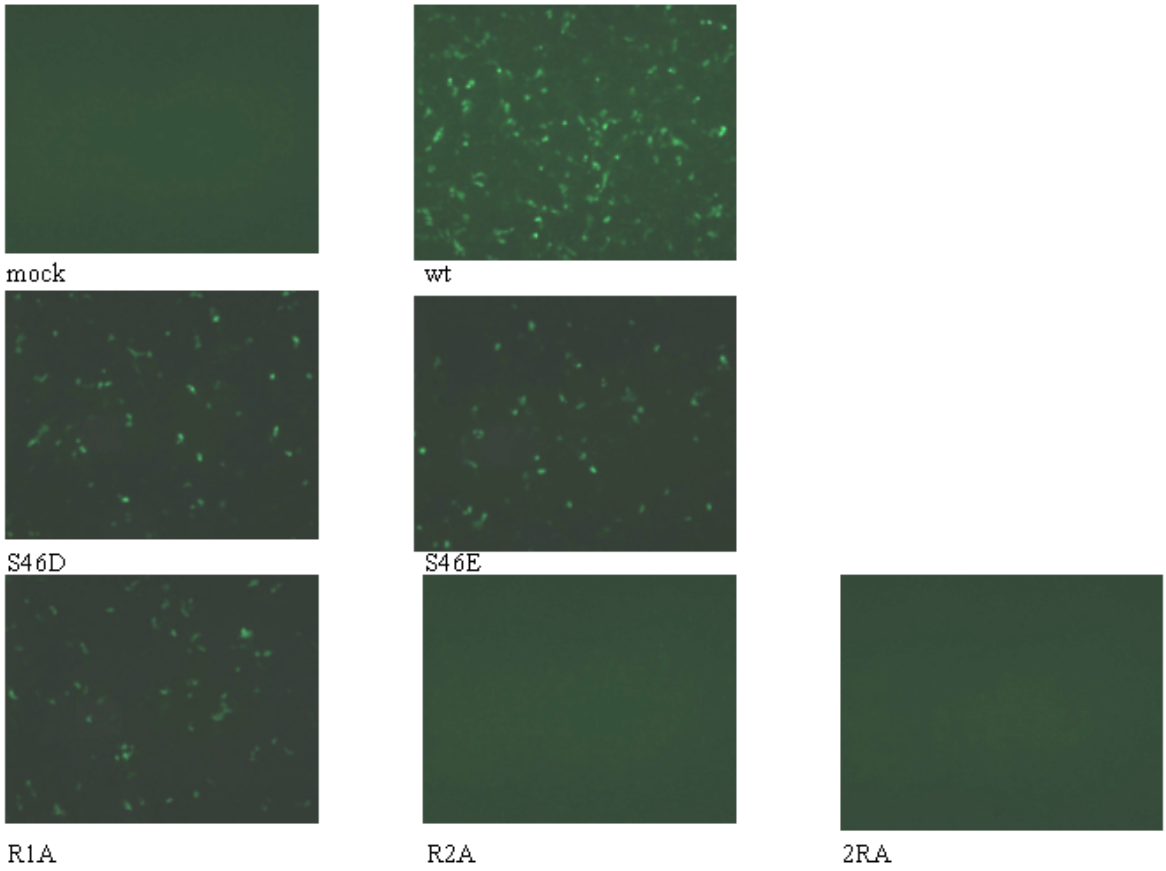

Figure 7. RUBrep/GFP-ΔNotI rescue by 1-88 RUB C and its mutants
Vero cells were transfected with 10 μg of 1-88 RUB C wt or mutant cDNA 1 day after plating and transfected with 6 μl of RUBrep/GFP-ΔNotI RNA 2 days after plating. All plates were examined for RUBrep/GFP-ΔNotI replication as visualized as GFP expression using fluorescence microscopy 4 days after plating at 10X magnification. The version of 1-88 RUB C expressed is denoted below each image.

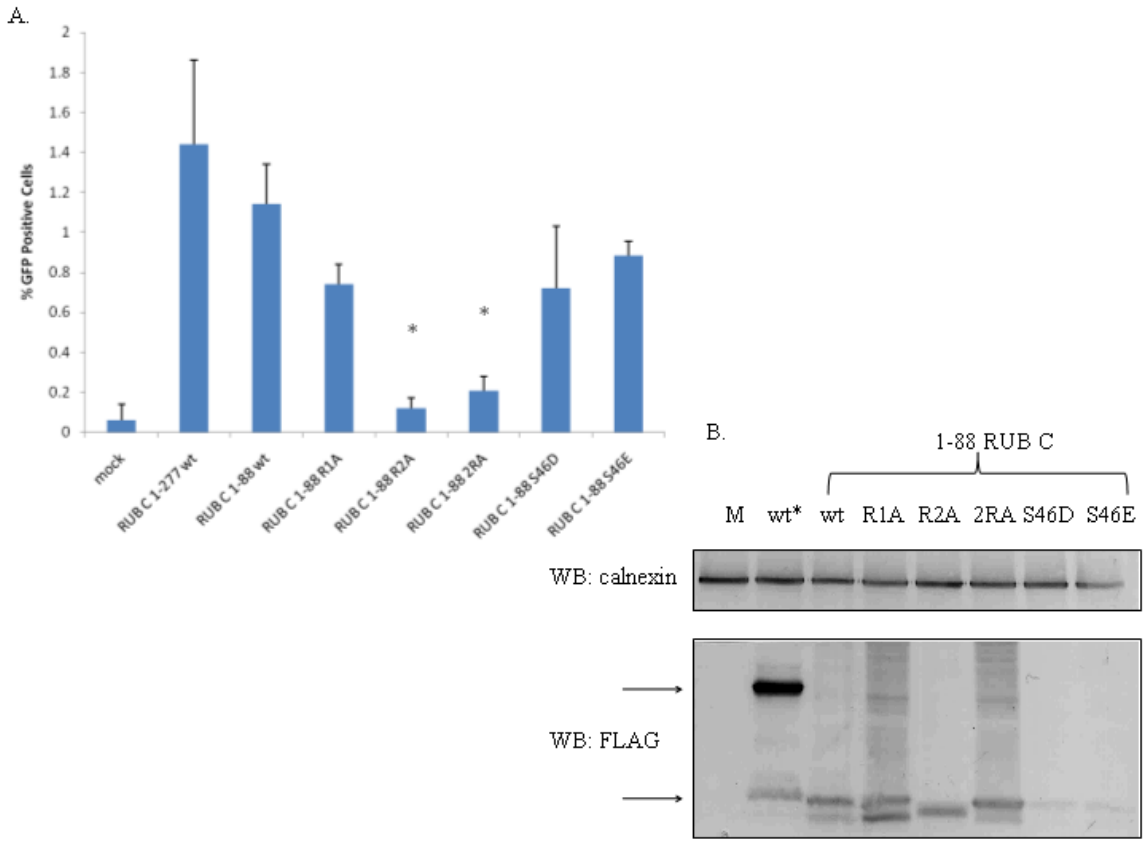

Figure 8. Quantification of RUBrep/GFP-ΔNotI rescue by 1-277 RUB C wt (*) or 1-88 RUB C and its mutants

Vero cells were transfected with 10 µg of 1-88 RUB C wt or mutant panel cDNA 1 day after plating and transfected with 6 µl of RUBrep/GFP-ΔNotI RNA 2 days after plating. Four days after plating, the cells were detached by trypsinization and divided into two aliquots. A) The first aliquot was examined for RUBrep/GFP-ΔNotI replication as measured by % GFP positive cells using FACS analysis. This experiment was repeated 3 times and the error bars represent the standard deviation. A) Student's *t* test was performed to determine significant differences. The * denotes $p < 0.05$ when compared to either wild type 1-277 RUB C or wild type 1-88 RUB C. B) The second aliquot was lysed and lysates were electrophoresed in a 10% (to probe for calnexin) or 15% (to probe for FLAG-tagged RUB C) SDS-PAGE gel and proteins were transferred to a nitrocellulose membrane. The membranes were then probed with primary antibodies (anti-calnexin 1:5000 or anti-FLAG 1:400) and secondary antibody (anti-mouse AP conjugated 1:5000). Arrows denote the migration of the 277 (wt*) and 88 amino acid forms of RUB C. The bands migrating higher than expected for the 1-88 RUB C samples could be dimers.

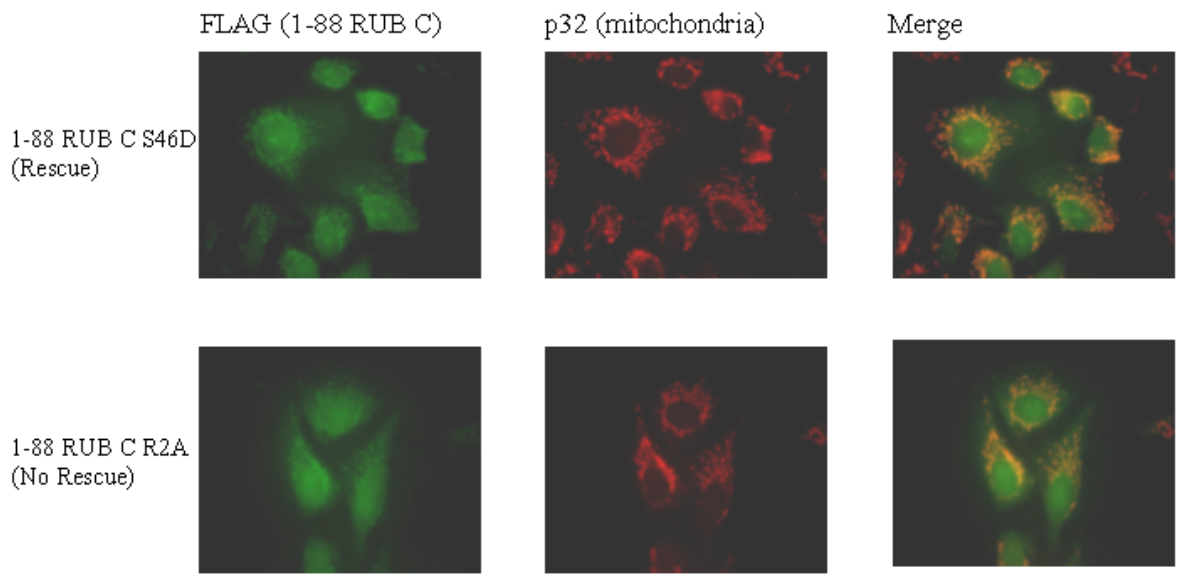

Figure 9. Intracellular localization of 1-88 RUB C and its mutants
Vero cells were transfected with 10 μg of 1-88 RUB C wt or mutant cDNA 1 day after plating. Two days after plating cells were examined by immunofluorescence staining of 1-88 RUB C with anti-FLAG (1:1000) and secondary anti-mouse FITC (1:100) and anti-p32 (1:333) and secondary anti-rabbit TRITC (1:100) and visualized. Fluorescence microscopy was performed using a 40X objective. Green corresponds to the FLAG-tagged 1-88 RUB C construct with denoted mutation and red corresponds to cellular mitochondrial protein p32. Representative images for a rescuing (S46D) and a non-rescuing form (R2A) of 1-88 RUB C are shown.

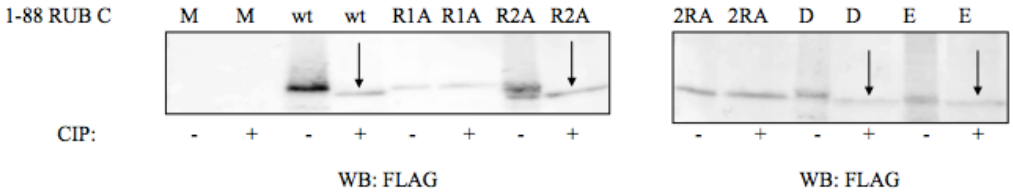

Figure 10. CIP dephosphorylation of 1-88 RUB C and its mutants
Vero cells were transfected with 5 µg of the 1-88 RUB C wt or mutant panel cDNA and lysed two days post-transfection. CIP-mediated protein dephosphorylation was done as described by the manufacturer's protocol (NEB) with the exception that a 30 minute incubation time was used. CIP treated (+) and untreated (-) lysates were electrophoresed in a 15% SDS-PAGE gel and proteins were transferred to a nitrocellulose membrane. The membrane was then probed with primary antibody (anti-FLAG 1:400) and secondary antibody (anti-mouse AP conjugated 1:5000). Differences in migration between untreated (-) and treated (+) lysates, indicative of phosphorylation, are indicated by arrows.

3 SPECIFIC AIM 2: DETERMINE THE STEP IN EARLY REPLICATION AT WHICH RUB C FUNCTIONS IN RESCUE.

3.1 Introduction

The mechanism behind the rescue of the RUB P150 Q domain by RUB C has been investigated, but not elucidated. RUB C is able to rescue the Δ*Not*I replicon at a step prior to the synthesis of detectable viral RNA (15). Packaged RUBrep/GFP-ΔNotI can also be rescued by RUB C provided within the virion (4), further supporting the notion that rescue occurs at an early step.

The early steps post-transfection at which C-mediated rescue of Δ*Not*I replicons could occur are outlined as follows:

1. Protection of the transfecting replicon RNA from the host cell RNA degradation machinery
2. Translation of the NS-ORF from the transfecting replicon RNA
3. Recruitment of the viral RNA, the viral replicase, and host cell factors to the RC
4. Establishment of the RC
5. Setting up an intracellular environment conducive to replication

We sought to investigate these early steps as follows:

The first hypothetical early step is protection of the incoming RNA from degradation by the host degradation machinery. Initially we hypothesized that the RNA binding activity of RUB C may be necessary for its rescue of the RUB P150 Q domain, but additional experimentation in our lab suggested that this was not the case. Drs. Zhou and Tzeng showed that the Δ*Not*I replicon was rescued by 1-277 RUB C wild type, S46A, S46D, and S46E (unpublished data) and we confirmed that this replicon is rescued by 1-88 RUB C wild type, S46D, and S46E in the previ-

ous aim. It had been previously reported that wild type and S46A RUB C bind RNA, while S46D and S46E RUB C do not (9). However, in the previous aim we found that the second arginine cluster of RUB C is important for the rescue phenomenon and this arginine cluster is required for RUB C binding of RNA (1). This suggests that the interaction between RUB C and the viral RNA, perhaps to prevent its degradation by the host cell machinery, could be the point in the life cycle critical for the rescue phenomenon. Thus, we sought to determine if RUB C protects the incoming viral RNA from degradation and if so, does this ability and the ability to bind the incoming viral RNA differ between rescuing and non-rescuing forms of RUB C as well.

The next step in the replication cycle of the RUB viral RNA upon introduction to the cytoplasm is the translation of the nonstructural ORF. There were no differences in translation of P150 between wild type and Δ*Not*I replicons in the presence or absence of RUB C at 6 and 24 hours post-transfection (17), suggesting that the rescue phenomenon occurs post translation. In this study, we revisited this experiment by examining additional time points post-transfection to confirm that RUB C functions at a point after the translation of the nonstructural ORF.

Finally, we tried to identify host proteins which interacted differentially with wt RUB C and its non-rescuing mutant, R2A. RUB C binding of a host protein could serve to recruit it to the RC. It is also possible that RUB C is needed to establish the proper host environment for replication via its interactions with host proteins. This could involve inactivation of a host innate defense mechanism or activation of a cell signaling pathway. In the previous aim we identified the R2 arginine cluster within RUB C to be required for the rescue of the RUB P150 Q domain. It has been reported that both arginine clusters are important for binding of cellular protein p32 (2). The identification of p32 as a RUB C binding partner was done using yeast two-hybrid screening of a cDNA library from CV1 cells, which are derived from African green monkey kid-

ney (2). As RUB virus is solely a human pathogen, the screening of a non-human library might be a pitfall of this study, although primates and humans have similar proteins. Subsequent efforts from this group identified p32 and poly(A)-binding protein (PABP) as RUB C binding partners by transfecting COS or HEK293T cells with a GST-tagged RUB C, performing GST pulldowns, and mass spectrometry (7). COS and HEK293T cells are derived from monkey kidney and human embryonic kidney cells respectively, so this screen was more relevant since human proteins were examined. Our study sought to examine known RUB C protein binding partners for differential interaction between rescuing and non-rescuing forms of RUB C, as well as to identify new host binding partners, including potentially more transient ones, by probing a human protein microarray.

RUB C also associates with the viral replicase, suggesting a possible mechanism for its involvement in RNA synthesis, namely recruitment of the replicase to the RC, although RUB C may need to bind to the replicase to perform its rescue function. Specifically, RUB C and RUB P150 have been shown to be associated by both co-immunoprecipitation (17) and colocalization (5, 8). The regions of RUB P150 and RUB C that are required for this association have been mapped by Dr. Tzeng to the first 31 amino acids of RUB C and the N terminus of RUB P150 (first 140 amino acids) (unpublished data).

3.2 Results

3.2.1 Analysis of 1-88 RUB C-RFP and 1-88 RUB C R2A-RFP with RUBrep/GFP-ΔNotI rescue assay and generation of stable cell lines

To study the RNA decay of RUB replicons, it was desirable to generate Vero cell lines that stably expressed the wt RUB C 1-88 or its R2A mutant. To this end, plasmids expressing 1-

88 RUB C wt and 1-88 RUB C R2A fused to RFP were constructed. These constructs were tested to ensure that the fusion to RFP did not disrupt ability the of these proteins to rescue or not rescue RUBrep/GFP-ΔNotI. Vero cells were transfected with 1-88 RUB C-RFP or 1-88 RUB C R2A-RFP 1 day after plating, transfected with RUBrep/GFP-ΔNotI 2 days after plating, and examined for GFP expression by fluorescence microscopy 4 days after plating. RUBrep/GFP-ΔNotI was rescued by 1-88 RUB-RFP, but was not rescued by 1-88 RUB C R2A-RFP as expected (Figure 11). Vero cells stably expressing 1-88 RUB C-RFP and 1-88 RUB C R2A-RFP were then generated. Robust expression of RFP was observed for both cell lines when assayed using both fluorescence microscopy and Western blot (Figure 12).

3.2.2 Early differential RNA decay of RUB replicons in the presence of RUB C

To test if a difference in replicon RNA stability could be detected in the presence of RUB C, Vero and C-Vero cells were transfected with replicon RNA transcripts and at 1, 6, and 12 hours post-transfection RNA was extracted and the amount of replicon RNA determined by qRT-PCR. As seen in Figure 13.A, at 1 hour post-transfection C-Vero cells contained significantly more RUBrep/GFP RNA than Vero cells, but there was no difference between the amount of replicon RNA in these two cell lines at 6 and 12 hours post-transfection. This trend was specific for RUB replicon RNA as there was no difference in RNA levels at any time point in Vero versus C-Vero cells when a corresponding SIN replicon, SINrep/GFP, was similarly examined (Figure 13.B). When cell lines stably expressing 1-88 RUB C-RFP and 1-88 RUB C R2A-RFP were used in this assay, there was significantly more RUBrep/GFP in 1-88 RUB C-RFP cells as compared to 1-88 RUB C R2A-RFP cells (Figure 14.A). This indicates that the second arginine cluster is important in this early protection of the RUB viral RNA.

To rule out the possibility that the lack of differences in RNA levels at the later time points could be due to RNA replication of RUBrep/GFP, we examined a replication defective RUB replicon, RUBrep/GFP-GDD*. The same trend of protection of the RUB viral RNA at the 1 hour time point in C-Vero and 1-88 RUB C-RFP cells, but not in Vero and 1-88 RUB C R2A-RFP cells seen with RUBrep/GFP was also seen with RUBrep/GFP-GDD* (Figure 13.C and Figure 14.B). Therefore, the lack of difference in RNA levels seen at the later time points is measuring the incoming *in vitro* transcript, and not newly replicated RNA. There was more RNA present in the experiment with RUBrep/GFP-GDD* (Figure 13.C) than RUBrep/GFP (Figure 13.A). Experimentation with these two replicons was undertaken at separate times with the RUBrep/GFP-GDD* experiments later, and therefore improved proficiency with RNA isolation with additional experience with the technique could explain this discrepancy.

3.2.3 Greater association of RUB replicon with 1-88 RUB C than 1-88 RUB C R2A

To determine if the greater stability of the replicon RNA at early times post-transfection in cells expressing versions of the wild type RUB C protein was due to a direct interaction between RUB C and the replicon RNA, protein-RNA complexes were immunoprecipitated to determine if there is a greater association of RUBrep/GFP RNA with 1-88 RUB C than 1-88 RUB C R2A. The 1-88 RUB C-RFP and 1-88 RUB C R2A-RFP stable cell lines were intended to be used for these experiments until it was discovered that anti-RFP could not immunoprecipitate the 1-88 RUB C-RFP fusion proteins. Instead, FLAG-tagged 1-88 RUB C and 1-88 RUB C R2A were transfected into Vero cells 1 day after plating and *in vitro* transcribed RUBrep/GFP transcripts were transfected 2 days after plating. One hour post-transfection, RNA protein complexes were crosslinked using formaldehyde, immunoprecipitated with anti-FLAG, and RNA was

isolated and quantified using qPCR. There was significantly more RUBrep/GFP RNA co-immunoprecipitated with 1-88 RUB C than 1-88 RUB C R2A (Figure 15). This suggests that the protection of RUB replicon RNA early after transfection occurs through physical interaction of the RNA with RUB C and that the R2 arginine cluster is important for the interaction between RUB C and RUB replicon RNA.

3.2.4 No differences in the translation of RUB P150 in RUB replicon transfected Vero and C-Vero cells

One of the initial events in both RUB virus and RUB replicon replication is the translation of the nonstructural proteins from the incoming RNA. Therefore, we examined the translation of a RUB nonstructural protein, P150, in Vero and C-Vero cells transfected RUBrep/GFP and RUBrep/GFP-ΔNotI at 1, 6, 12, and 24 hours post-transfection. There was no translation of P150 detected from either replicon in Vero or C-Vero cells at 1 hour post-transfection (Figure 16.A). There were no obvious differences between the translation of P150 from either replicon in Vero or C-Vero cells at 6, 12, or 24 hours post-transfection (Figure 16.B), indicating that translation is not the step early in replication enhanced by the presence of RUB C. This result was also seen in another study when the time points 6 and 24 hours post-transfection were examined (17).

3.2.5 RUB C and RUB P150 Q domain interact with cellular p32

We next explored if there was differential association of rescuing and non-rescuing forms of RUB C with cellular p32, a known binding partner of RUB C. Wild type and rescuing mutants of 1-88 RUB C were able to immunoprecipitate cellular p32, while non-rescuing mu-

tants, R2A and 2RA, of 1-88 RUB C were not able to immunoprecipitate cellular p32 (Figure 17.A). This finding contradicts the findings of Beatch et al. that both the R1 and R2 clusters are important for p32 binding (1). Encouraged that this interaction might be the basis for the rescue phenomenon, we next examined the wild type and appropriate mutants of RUB P150 Q domain for their interaction with cellular p32. Both wild type (does not require RUB C for replication) and its R_QQ mutant (Figure 17.B) in which the arginines in a poly-arginine cluster are mutated to glutamines, (does require RUB C for replication) were co-immunoprecipitated with p32 (Figure 17.C). Further, the interaction between the RUB P150 Q domain and cellular p32 was found to rely upon the presence of both of the two PxxPxR motifs within the Q domain as wt P150 Q domain or the P150 Q domain with either PxxPxR motif mutated individually (Mut1 or Mut 2; Figure 17.B) were co-immunoprecipitated with p32 while a construct with both motifs mutated (Mut1+2) was not (Figure 17.D). It is of note that the first two arginines in the poly-arginine cluster overlap the first PxxPxR motif and that RUBrep/GFP Mut1+2 does not require RUB C for replication (13). Taken together, this indicates that the interaction between RUB C and cellular p32 is not the basis of the rescue phenomenon.

*3.2.6 All forms of 1-277 RUB C mutant panel co-immunoprecipitate with RUB P200**

The formation of the replication complex (RC) is another early event in RUB virus and replicon replication that occurs before the accumulation of newly synthesized viral RNAs. We examined if rescuing and non-rescuing forms of RUB C differentially associated with the uncleaved NSP, P200. This was done by cotransfecting RUB C and a plasmid expressing a form of the NSP that cannot cleave (P200*). After many attempts it was determined that while 1-88 RUB C could not be co-immunoprecipitated with P200*, 1-277 RUB C could be, so the remain-

der of the experiments were done using the 1-227 RUB C mutant panel. Dr. Tzeng previously demonstrated that CAT-tagged 1-88 RUB C interacted with FLAG-tagged P150 when expressed from two different replicons (unpublished data). In addition to the mutant panel described and characterized in the previous aim of this dissertation, an additional 1-277 C mutant was constructed in which a predicted helix between residues 9 and 31 was disrupted (Figure 18), which was termed the helix mutant. Since Dr. Tzeng mapped the P150-binding region of C to between aa 1-31, we hypothesized that this helix may be important for protein-protein interactions. All forms of 1-277 RUB C could be co-immunoprecipitated with P200* (Figure 19), suggesting that the interaction between RUB C and P200 is not a factor in the ability of RUB C to rescue replication at an early step. The immunoprecipitation results were further confirmed by an immunofluorescence assay in cells cotransfected with GFP- tagged P200* and FLAG- tagged 1-277 RUB C and its mutants in which all forms of 1-277 RUB C colocalized with P200* (Figure 20 shows the colocalization between 1-277 RUB C wt and P200*).

3.2.7 RUB C and RUB P150 Q domain do not interact with Amph1 or Bin1

Recently several alphaviruses were found to interact with Amph1 and Bin1 via their P1 SH3 motif within nsP3. Interestingly, an arginine was found to be the critical reside within this motif for these interactions and the abrogation of these interactions by mutagenesis of the critical arginine to glutamic acid resulted in decreased RNA replication and viral titers (12). We therefore wanted to determine if RUB C or the RUB P150 Q domain interacted with either of these proteins and if so, if that interaction was mediated via the arginine clusters important for the rescue phenomenon. C-myc-tagged Amph1 and C-myc-tagged Bin1 appeared to pull down both wild type and R2A forms of 1-277 RUB C, but this interaction was not genuine as the same

bands were present in control beads-only (no anti-C-myc antibody) immunoprecipitation samples (Figure 21.C). Neither the wild type nor the R_QQ forms of the RUB P150 Q domain were co-immunoprecipitated with C-myc-tagged Amph1 (Figure 21.D left) or by C-myc-tagged Bin1 as bands present in the immunoprecipitation lanes were also present in the mock-transfected lane (Figure 21.D right). Therefore, neither 1-277 RUB C nor the P150 Q domain could be demonstrated to bind Amph1 or Bin1 and these cellular proteins are not implicated in the rescue phenomenon.

3.2.8 Purification of 1-88 RUB C and 1-88 RUB C R2A expressed from pFLAG-MAC using column chromatography

To determine if the C rescue phenomenon was mediated via its binding to a host protein, we sought to identify host protein binding partners for 1-88 RUB C that did not bind 1-88 RUB C R2A. Toward this aim, we induced expression of FLAG-tagged 1-88 RUB C and 1-88 RUB C R2A cloned into the bacterial expression vector pFLAG-MAC in *E. coli* BL21(DE3). Column purification of 1-88 RUB C was carried out using anti-FLAG M2 affinity gel and elution with FLAG peptide. This method successfully purified both 1-88 RUB C and 1-88 RUB C R2A (Figure 22.A and 22.B left panels). However, a significant portion of 1-88 RUB C did not bind to the anti-FLAG M2 affinity gel as evidenced in the intense band present in the flow-through lane of the Western blot (Figure 22.A right panel). FLAG-tagged 1-88 RUB C R2A was also purified using a similar purification strategy as for FLAG-tagged 1-88 RUB C, with modification. An increased amount of anti-FLAG M2 agarose was used, resulting in less protein lost in the flow-through fraction (Figure 22.B right panel). The protein was eluted with 0.1 M glycine pH 3.5 rather than FLAG peptide. The yield in the combined elution fractions for 1-88 RUB C

was 8.62 μg/ml and the molarity of the combined elution fractions was calculated to be 0.673 μM. The protein yield in the combined elution fractions for 1-88 RUB C R2A was 3.79 μg/ml and the molarity of the combined elution fractions was 0.310 μM. The amount of protein needed for the protein array experiment is 100 nM to 1 μM, so enough was eluted for each protein to continue to the protein array experiment.

3.2.9 Identification of potential host protein binding partners for 1-88 RUB C and 1-88 RUB C R2A

ProtoArray Human Protein Microarrays were used to identify host protein binding partners for FLAG-tagged 1-88 RUB C and 1-88 RUB C R2A by probing the array with 10 nM of these purified proteins and then probing with primary anti-FLAG and secondary anti-mouse AlexaFluor 647 before scanning the array. Complete ProtoArray analysis was completed twice for both 1-88 RUB C and 1-88 RUB C R2A and repeatable hits were considered for further analysis. Notably, there were 35 common hits for both 1-88 RUB C and 1-88 RUB C R2A (Table 1), 2 hits for 1-88 RUB R2A only, and a single hit for 1-88 RUB C only. The hits for 1-88 RUB C R2A only were guanylate cyclase 1, soluble, beta 3 (GUCY1B3) and DENN/MADD domain containing 1C (DENND1C). The hit for wild type 1-88 RUB C only was phosphatidylinositol transfer protein alpha isoform (PITPα).

3.2.10 PITPα binds both 1-88 RUB C and 1-88 RUB C R2A

To confirm that PITPα does bind 1-88 RUB C, but not 1-88 RUB C R2A, co-immunoprecipitation experiments were carried out. PITPα was not only co-immunoprecipitated with 1-88 RUB C, but also with 1-88 RUB C R2A (Figure 23.D). PITPα was not pulled down in

immunoprecipitation reactions excluding anti-FLAG (Figure 23.D), indicating that PITPα indeed binds both 1-88 RUB C and 1-88 RUB C R2A, rather than 1-88 RUB C only as suggested by the results of the protein array.

3.3 Methods

3.3.1 Cells and replicons

African green monkey kidney cells (Vero) were maintained in DMEM containing 5% FBS and gentamycin (10 μg/ml) at 35ºC and 5% CO_2. C-Vero cells (17) were maintained in DMEM containing 5% FBS and G418 sulfate (1.2 mg/ml).

Rubella replicons used in this study include RUBrep/GFP, RUBrep/GFP-ΔNotI, RU-Brep-HA/GFP, RUBrep-HA/GFP-ΔNotI, and RUBrep/GFP-GDD* (14, 17). A Sindbis replicon, SINrep/GFP was also used in this study (6). *In vitro* transcription of linearized replicon DNA templates was carried out in a 25 μl reaction containing 5 μl 5X transcription buffer (40 mM Tris-HCl (pH7.5), 6 mM $MgCl_2$, 2 mM spermidine) (Epicentre), 2.5 μl 100 mM DTT, 40 U RNasin Ribonuclease Inhibitors (Promega), 1 μl 25 mM NTPs (Amersham), 5 μl 10 mM cap analogue (m^7G(5')ppp(5')G) (New England BioLabs), 50 U SP6 DNA dependent RNA polymerase (Epicentre), and 2 μl 250 ng/μl linearized template incubated at 37ºC for 1 hr. The quality of the *in vitro* transcript was assayed by electrophoresing the product through a 1% agarose gel followed by staining with ethidium bromide.

3.3.2 Antibodies

The following antibodies were used in this study: monoclonal mouse anti-PITPα (Sigma), monoclonal mouse M2 anti-FLAG (Sigma), mouse monoclonal anti-HA (Roche), rabbit anti-calnexin (Sigma), polyclonal rabbit anti-32 (Santa Cruz), rabbit Living colors® A.v. peptide anti-GFP (Clontech), monoclonal mouse anti-C-myc (Roche), monoclonal mouse Living colors® anti-mCherry (Clontech). Secondary antibodies were goat or donkey anti-mouse IgG, AP-conjugated, and goat or donkey anti-rabbit IgG, AP-conjugated (Promega), and FITC- or TRITC-conjugated goat antibodies against mouse or rabbit (Sigma).

3.3.3 Generation of expression constructs and site-directed mutagenesis

To generate a 1-88 RUB C R2A construct fused to RFP, an asymmetric three round PCR strategy was employed as follows. The first round was performed using a 25 µl reaction containing 2.5 µl 10X buffer (Takara), 3.5 µl 2.5 mM dNTPs, 1µl of 200 ng/µl of reverse primer (5' GTTATCCTCGCCCTTGCTCACCATAGTTTCTTGCCGCTCCTCCGGGGG 3'), 2.5 U Ex Taq DNA polymerase (Takara), and 0.5 µl 1-277 RUB C R2A as a template. The PCR protocol used was 15 cycles of 98ºC for 30 sec, 55ºC for 20 sec, and 72ºC for 20 sec followed by incubation at 72ºC for 1 min. The second round was done in a 25 µl reaction as before using 1µl of 200 ng/µl of forward primer (5' GCGGGATATCATGGCTTCTACTACCCCCATCACCATGGA 3') and 2 µl of the first round product as template with the same PCR protocol as the first round. The third round was done in a 50 µl reaction containing 5 µl 10X buffer (Takara), 8 µl 2.5 mM dNTPs, 3 µl second round product as the forward primer, 1 µl of 200 ng/µl reverse primer (5' ACTAGAGGATCCCTAGTTTCCGGACTTGTACAGCTC 3'), 5U Ex Taq DNA polymerase (Takara), and 1 µl pCherry as a template for RFP. The PCR protocol used was 36 cycles of 98ºC

for 30 sec, 55ºC for 20 sec, and 72ºC for 1 min followed by incubation at 72ºC for 1 min. VR1062 and purified third round PCR products underwent restriction digestion using *Bam*HI and *Eco*RV restriction enzymes (New England BioLabs), followed by gel purification using QI-Aquick gel extraction kit (QIAGEN) and these fragments were ligated together using T4 DNA ligase (New England BioLabs) for 1 hour at room temperature. The ligation reactions were then transformed into competent *E. coli* DH5α. Resulting colonies were picked for miniprep plasmid DNA isolation that was then screened for the presence of both the insert and the vector by *Bam*-HI and *Eco*RV and agarose gel electrophoresis. Apparent positive constructs were confirmed by sequencing. The resulting construct was termed 1-88 RUB C R2A-RFP. 1-88 RUB C-RFP was previously constructed as described above by Dr. Jason Matthews (unpublished data).

Prolines were inserted into a predicted helix between residues 9 and 31 of RUB C to disturb the structure for 1-277 RUB. Specifically three prolines were inserted after L16 and three additional prolines were inserted after L23 (see Figure 18). This was accomplished using the same three step PCR strategy with the same experimental parameters employed in the creation of 1-88 RUB C R2A-RFP as described above. The first round used a forward primer (5' CTCCAGAAGGCCCTCCCGCCGCCGGAGGCACAATCCCGCGCCCTGCCGCCGCCGCG CGCGG AACTCGCC 3') containing sequences with the desired mutations and 1-277 RUB C as a template. The second round used a reverse primer (5' GTACTCTAGACTAGCGAGTTTC TTGCCGC 3') including a 3' *Xba*I restriction site, translation termination codon, and sequences complementary to the RUB C gene starting at codon 277 and the first round product as template. The third round used the second round product as the reverse primer, a forward primer including a 5' *Eco*RV restriction site followed by the 5' sequences of the RUB C gene (5' TAAGATATCC ATGGACTATAAGGACGACGACGACAAGGACTATAAGGACGACGACGACAAAGGCT

TCTACTACCCCCATCACCATGGAG 3'), and 1-277 RUB C as a template. pcDNA and purified third round PCR products underwent restriction digestion using *Eco*RV and *Xba*I restriction enzymes (New England BioLabs), followed by gel purification using QIAquick gel extraction kit (QIAGEN) and these fragments were ligated together using T4 DNA ligase (New England BioLabs) for 1 hour at room temperature. The ligation reactions were then transformed into competent *E. coli* DH5α. Resulting colonies were picked for miniprep plasmid DNA isolation that was then screened for the presence of both the insert and the vector by restriction with *Eco*RV and *Xba*I followed by agarose gel electrophoresis. Presumptive positive constructs were confirmed by sequencing. The resulting construct was termed 1-277 RUB C helix mutant.

The construction of the vectors expressing the Q domain of RUB P150 and its mutants have been previously described (13). Briefly, these were PCR-amplified from the corresponding HA-tagged RUB infectious cDNA clone (11). This was accomplished in a 50 µl reaction containing 5 µl 10X buffer (Takara), 8 µl 2.5mM dNTPs, 1 µl 200 ng/µl forward primer including a *Eco*RV restriction site in front of the P150 Q domain 5' sequences (5' GCCGATATCATGGCTC CCCGCTGCGACGTCCCGCGC 3'), 1 µl of 200 ng/µl reverse primer including a *Bam*HI restriction site in front of P150 Q domain 3' sequences (5' GGCGGATCCTCATGGGTCTGCCC TGGTTGACGTGGG 3'), 5U Ex Taq DNA polymerase (Takara), and 0.5 µl RUBrep-HA/GFP R_QQ, Robo 502/930 (containing a HA-tag) Mut1, Mut2, or Mut 1+2 as template. The PCR protocol used was 36 cycles of 98ºC for 30 sec, 55ºC for 20 sec, and 72ºC for 1 min followed by incubation at 72ºC for 1 min. VR1062 and purified PCR products underwent restriction digestion using *Eco*RV and *Bam*HI restriction enzymes (New England BioLabs), followed by gel purification using QIAquick gel extraction kit (QIAGEN) and these fragments were ligated together using T4 DNA ligase (New England BioLabs) for 1 hour at room temperature. The ligation

reactions were then transformed into competent *E. coli* DH5α. Resulting colonies were picked for miniprep plasmid DNA isolation that was then screened for the presence of both the insert and the vector by restriction with *Eco*RV and *Bam*HI and agarose gel electrophoresis. Presumptive positive constructs were confirmed by sequencing. The resulting constructs were termed RUB P150 Q domain wt, R_QQ, Mut 1, Mut 2, and Mut 1+2 Q domain.

1-88 RUB C and 1-88 RUB C R2A were cloned into bacterial expression vector pFLAG-MAC. 1-88 RUB C wt or R2A was PCR-amplified from 1-277 RUB C or 1-277 RUB C R2A (16) in a 50 µl reaction containing 5 µl 10X buffer (Takara), 8 µl 2.5 mM dNTPs, 1 µl 200 ng/µl forward primer which contained a *Hind*III restriction site and 2X FLAG tag in front of the 5' RUB C sequences (5' GCCAAGCTTCATGGACTATAAGGACGACGACGACAAGGACTAT AAGGACGACGACGACAAGGCTTCTACTACCCCCATCACCATGGAG 3') or a forward primer including a *Hind*III restriction site in front of the 5' RUB C sequences (5' GCCAAGCTT GCTTCTACTACCCCCATCACCATGGAG 3'), 1 µl of 200 ng/µl reverse primer containing a *Eco*RI restriction site in front of the complement of the RUB C sequences starting at aa 88 (5' G CCGAATTCGCGACTTTCTTGCCGCTCCTC 3'), and 5U Ex Taq DNA polymerase (Takara). pFLAG-MAC includes a stop codon after the multiple cloning site, so no stop codon was required in the reverse primer for PCR. The PCR protocol used was 36 cycles of 98ºC for 30 sec, 55ºC for 20 sec, and 72ºC for 1 min followed by incubation at 72ºC for 1 min. pFLAG-MAC and purified PCR products underwent restriction digestion using *Hind*III and *Eco*RI restriction enzymes (New England BioLabs), followed by gel purification using QIAquick gel extraction kit (QIAGEN) and these fragments were ligated together using T4 DNA ligase (New England BioLabs) for 1 hour at room temperature. The ligation reactions were then transformed into competent *E. coli* DH5α. Resulting colonies were picked for miniprep plasmid DNA isolation that

was then screened for the presence of both the insert and the vector by restriction digestion with *Hind*III and *Eco*RI and agarose gel electrophoresis, the presence of the desired sequences were confirmed by sequencing, and positive constructs were transformed into competent *E. coli* BL21(DE3).

Constructs expressing C-myc-tagged Amph1 and Bin1 were kindly provided by Dr. Tero Ahola and have been described previously (12).

3.3.4 Analysis of 1-88 RUB C-RFP and 1-88 RUB C R2A-RFP using RUBrep/GFP-ΔNotI rescue assay

Screening of 1-88 RUB C-RFP and 1-88 RUB C R2A-RFP for RUBrep/GFP-ΔNotI rescue was done as follows. Vero cells were plated in 60 mm plates and allowed to grow overnight. The cells were transfected with 1-88 RUB C-RFP or 1-88 RUB C R2A-RFP 1 day after plating and were transfected with RUBrep/GFP-ΔNotI *in vitro* transcribed RNA 2 days after plating. The cells were transfected using Lipofectamine 2000 (Invitrogen) according to manufacturer's recommendations with 10 μg of DNA of each RUB C construct or 6 μl of *in vitro* transcribed RNA. Transfection reagents were allowed to incubate on cell cultures for at least 4 hours before removal and addition of growth medium. Plates were observed for expression of GFP and RFP using fluorescence microscopy 4 days after plating.

3.3.5 Generation and screening of 1-88 RUB C-RFP and 1-88 RUB C R2A-RFP stable cell lines

Vero cells were plated in 100 mm plates and grown overnight. The cells were transfected using Lipofectamine 2000 (Invitrogen) according to manufacturer's recommendations

with 8 µl of miniprep cDNA of 1-88 RUB C-RFP or 1-88 RUB C R2A-RFP and 0.02 µg or 0.2 µg of pHyg. Transfection reagents were allowed to incubate on cell cultures for at least 4 hours before removal and addition of growth medium. One day post-transfection normal growth media was replaced with H media (DMEM, 5% FBS, 125 mg Hyg). H media was replaced on cells every three days until drug resistant colonies emerged, which were picked as follows. Plates were washed with PBS and colonies were isolated using cloning cylinders. The cylinders were filled with 100 µl of trypsin solution and allowed to incubate at room temperature for 10 minutes. The detached cells were then added to 2ml of H media in 35 mm plates. Plates with cell growth were then screened for the expression of 1-88 RUB C-RFP or 1-88 RUB C R2A-RFP using fluorescence microscopy or Western blot analysis two days after plating.

3.3.6 RNA degradation time course

Prior to RNA degradation time course experiments, *in vitro* transcribed RUBrep/GFP, SINrep/GFP, and RUBrep/GFP-GDD* RNAs were treated with 15 U of DNase I (Roche) per 25 µl of RNA for 1 hour at 37ºC to degrade the template DNA. Vero and C-Vero cells were plated in 60 mm plates and allowed to grow overnight. Cells were transfected with Lipofectamine 2000 (Invitrogen) according to manufacturer's instructions. Transfection reagent was combined with 6 µl of each *in vitro* transcribed RNA and replaced with growth medium 4 hours post-transfection. Plates were harvested at 1 hour, 6 hours, and 12 hours post-transfection and RNA was isolated.

The time course was also done in the 1-88 RUB C-RFP wt- and R2A-stable cell lines using RUBrep/GFP transcripts as described above.

3.3.7 RNA immunoprecipitation

To examine the association of 1-88 RUB C and 1-88 RUB C R2A with RUBrep/GFP Vero cells were plated in 100 mm plates and allowed to grow overnight. One day after plating cells were transfected with 1-88 RUB C or 1-88 RUB C R2A. Cells were transfected with Lipofectamine 2000 (Invitrogen) according to manufacturer's instructions. Transfection reagent was combined with 10 μg of DNA. Two days after plating cells were transfected with DNase-treated RUBrep/GFP RNA transcripts. Cells were transfected with Lipofectamine 2000 (Invitrogen) according to manufacturer's instructions. Transfection reagent was combined with 10 μl of *in vitro* transcribed RNA.

Protein-RNA complexes were crosslinked with 1% formaldehyde for 30 minutes at room temperature at 1 hour post-transfection followed by lysis with 600 μl 1XRIP buffer (10mM Tris pH 8.0, 150mM NaCl, 3mM EDTA, 1% TritonX-100, 0.1% SDS, 0.5% DOC) with complete, mini, EDTA-free protease inhibitor cocktail tablet (1 tablet/10 ml buffer) (Roche) and RNasin Ribonuclease Inhibitors (50 U/500 μl buffer) (Promega). Lysates were flash frozen, thawed, and sonicated (30 seconds on, 30 seconds off, high for 10 minutes using a Bioruptor sonicator) three times, with vortex mixing and centrifugation between sonications. Lysates were treated with DNase (400 U/500 μl) (Roche) for 10 minutes at 37ºC and this reaction was stopped by the addition of EDTA to 20 mM. Four μl of anti-FLAG antibodies was added and lysates were incubated at 4ºC overnight with rotation. Prewashed protein A-agarose (30 μl) (Roche) was added and incubated for 2 hours at 4°C with rotation. The beads were then washed four times with 0.5 ml 1XRIP buffer containing RNasin Ribonuclease Inhibitors (50 U/500 μl buffer) (Promega) and washed four additional times with 0.5 ml 1XRIP buffer with RNasin Ribonuclease Inhibitors (50 U/500 μl buffer) (Promega) and 1M urea to reverse the crosslinking between

the RNA-protein complexes. The beads were then suspended in 1 ml of TRI reagent (Molecular Research Center, Inc) to isolate RNA from these samples according to manufacturer's instructions.

3.3.8 RNA isolation, reverse transcription, and qPCR

RNA was isolated using TRI reagent (Molecular Research Center, Inc). Samples from RNA degradation time course experiments were resuspended in 150 µl of water while samples from RNA immunoprecipitation experiments were resuspended in 5 µl of water.

RNA samples were quantified using spectrometry for the RNA degradation time course experiments and 0.1 µg of RNA was diluted in 5 µl of water prior to reverse transcription. In the RNA immunoprecipitation experiments, the entire sample was reverse transcribed. Reverse transcription was done as follows. RNA samples were boiled for 5 minutes and placed on ice for 3 minutes. The appropriate reverse primer (200 ng) (see Table 2 antisense primers), 3 µl water, and 4 µl 2.5 M dNTP mix (Takara) were added while the sample remained on ice, and then was incubated at 55ºC for 8 minutes. The sample was returned to ice. Four µl 5X First-Strand Buffer (Invitrogen), 2 µl 0.1M DTT, 200 units SuperScript III Reverse Transcriptase (Invitrogen), and 40U RNasin Ribonuclease Inhibitors (Promega) were added and samples were incubated at 55ºC for 1 hour.

Real time quantitative PCR (qPCR) analysis of viral RNA levels were performed using a 20 µl reaction containing 2 µl of reverse transcription product or 2 µl of standard (serial dilutions of a known concentration of RUBrep/GFP-ΔNotI DNA), the appropriate primer pair (Table 2) (200 ng of each), and 10 µl Fast SYBR Green Master Mix (Applied Biosystems). Real time qPCR was done on a 7500 Fast Real-Time PCR System (Applied Biosystems) with the following

parameters: 95ºC for 20 sec (holding stage), 95ºC for 3 sec, and 60ºC for 30 sec (cycling stage) for 40 cycles. The RNA concentration was calculated though the use of a standard curve of known concentrations of RUBrep/GFP-ΔNotI DNA and normalized to levels of β actin.

3.3.9 Replicon translation time course

Analysis of the translation of RUB P150 from replicons was done as follows. Vero and C-Vero cells were plated in 35 mm plates and allowed to grow overnight. The cells were transfected with either RUBrep-HA/GFP or RUBrep-HA/ GFP-ΔNotI (both expressing a HA-tagged P150) *in vitro* transcribed RNA. The cells were transfected using Lipofectamine 2000 (Invitrogen) according to manufacturer's recommendations with 3 µl of *in vitro* transcribed RNA. Transfection reagents were allowed to incubate on cell cultures for at least 4 hours before removal and addition of growth medium. Plates were harvested at 1, 6, 12, and 24 hours post-transfection. The cells were lysed with 0.3 ml of PBS based lysis buffer (1.5mM NaCl, 1% Triton X-100, 0.1% SDS, 0.5% DOC in PBS) and lysates were examined using Western blot analysis probed with anti-HA antibody.

3.3.10 Immunoprecipitation and Western blot analysis

Vero cells were plated in 60 mm plates and allowed to grow overnight. The cells were transfected using Lipofectamine 2000 (Invitrogen) according to manufacturer's recommendations with 10 µg of DNA. Transfection reagents were allowed to incubate on cell cultures for at least 4 hours before removal and addition of growth medium. Cells on the 60 mm plates were lysed with 600 µl PBS based lysis buffer (1.5 mM NaCl, 1% Triton X-100, 0.1% SDS, 0.5% DOC in PBS) or 500 µl 1XRIP lysis buffer (10 mM Tris pH 8.0, 150 mM NaCl, 3 mM EDTA,

1% Triton X-100, 0.1% SDS, 0.5% DOC) with complete, mini, EDTA-free protease inhibitor cocktail tablet (1 tablet/10 ml buffer) (Roche) and lysates were clarified by centrifugation. The appropriate antibody (1-2 µl, or no antibody for the beads-only control) was added to 500 µl of clarified cell lysate and incubated for 3 hours at room temperature with rotation. Prewashed protein A-agarose (Roche) (30 µl) was added and incubated for 1.5 hours at room temperature with rotation. This mixture was washed once with PBS based lysis buffer or 1XRIP lysis buffer, washed twice with PBS based wash buffer (1.5 mM NaCl, 1% Triton X-100 in PBS) or RIP wash buffer (10 mM Tris pH 8.0, 150 mM NaCl, 1% Triton X-100), resuspended in 2X SDS-sample buffer (100 mM Tris-HCl pH 6.8, 20 mM DTT, 4% SDS, 0.2% bromophenol blue, 20% glycerol) (75 µl), boiled for 5 minutes, and clarified by brief centrifugation. Clarified cell lysates (20 µl) were combined with 5X SDS-sample buffer (250 mM Tris-HCl pH 6.8, 20 mM DTT, 10% SDS, 0.2% bromophenol blue, 50% glycerol) (5 µl), boiled for 5 minutes, and clarified by brief centrifugation.

Supernatants from immunoprecipitations and cell lysates were electrophoresed in 8%, 10%, or 15% SDS-PAGE gels and transferred to a nitrocellulose membrane (Whatman) using 1X transfer buffer (100 ml 10X transfer buffer (250 mM Tris and 192 M glycine), 200 ml methanol, and 700 ml deionized water) and a mini-Protean II apparatus (BioRad) at 100V for 1 hour. The membranes were blocked in 5% non-fat dry milk in TBS (20 mM Tris-HCl pH 7.5 and 175 mM NaCl) and then probed with the appropriate primary and secondary antibody. Color development solution was added (10 ml alkaline phosphatase buffer (100 mM Tris, 100 mM NaCl, 50 mM $MgCl_2$-$6H_20$, pH 9.8), 33 µl NBT (Roche), and 33 µl BCIP (Roche)) to detect bound antibodies.

3.3.11 Immunofluorescence assay

The localization of FLAG-tagged 1-277 RUB C and its mutants with respect to RUB P200* (10) were examined by IFA. Vero cells were plated at low density (1.5 ml cells in 25 ml media; in the usual plating1 ml of trypsinized cells is mixed with 9 ml of medium) in 35 mm plates containing coverslips and were allowed to grow overnight. The cells were transfected using Lipofectamine 2000 (Invitrogen) according to manufacturer's recommendations with 10 μg of each 1-277 RUB C construct (wt, R1A, R2A, 2RA, S46D, and S46A) cDNA with or without 10 μg RUB P200* cDNA. Transfection reagents were allowed to incubate on cell cultures for at least 4 hours before removal and the addition of growth medium and coverslips were then processed for IFA 1 day post-transfection.

Coverslips were processed for IFA as follows. Media was decanted and 1 ml of ice-cold methanol was added to the plate for 5 minutes. The plates were then washed 3 times with PBS, allowing the last wash to incubate for 15 minutes. Next, 100 μl of prepared primary antibody (1:1000 anti-FLAG, 1:1000 Hoechst 33342 (Invitrogen), in PBS/2% BSA) was added to each coverslip and incubated in the dark for 30 minutes. After 3 washes with PBS, 100 μl prepared secondary antibody (1:5000 AlexaFluor 594 (Molecular Probes) in PBS/2% BSA) was added and incubated in the dark for 30 minutes. The coverslips were washed 3 times with PBS and mounted on glass slides with Entellan® new rapid mounting medium for microscopy (EMD). The coverslips were then observed using a Zeiss Axionplan 2 Imaging microscope.

3.3.12 Purification of 1-88 RUB C and 1-88 RUB C R2A from pFLAG-MAC

One colony of *E. coli* BL21(DE3) transformed with pFLAG-MAC 1-88 RUB C or 1-88 RUB C R2A was picked for overnight growth at 37°C in 4 ml LB containing ampicillin (60

μg/ml). The overnight sample was diluted into 400 ml of LB and grown for 2 hours and induced with 4 ml 100 mM IPTG for 2 hours. The cells were collected by centrifugation, resuspended in 20 ml PBS with complete, mini, EDTA-free protease inhibitor cocktail tablet (1 tablet/10 ml buffer) (Roche) and lysed by 4 cycles of freeze- thawing. Lysates were clarified by centrifugation for 10 minutes and applied to a column prepared as follows. The empty column was rinsed 2 times with 1 column volume TBS. Anti-FLAG M2 affinity gel (200 μl) (Sigma) was applied to the column, rinsed with 3 column volumes 0.1 M glycine HCl pH 3.5, and washed with 5 column volumes of TBS. The lysate was applied to and allowed to pass through the column 3 times. The column was then washed with 10 column volumes of TBS containing dissolved complete, mini, EDTA-free protease inhibitor cocktail tablet (1 tablet/10 ml buffer) (Roche). 1-88 RUB C was eluted with 5 X 2 ml aliquots of TBS with 100 μg/ml 3X FLAG peptide (Sigma) and dissolved complete, mini, EDTA-free protease inhibitor cocktail tablet (1 tablet/10 ml buffer) (Roche). 1-88 RUB C R2A was eluted with 6 X 1 ml aliquots of 0.1 M glycine pH 3.5 and 1 M Tris pH 8.0 was added to the elution fractions until the pH was 7.0.

Aliquots from the various stages of the purification process were prepared for analysis. Twenty μl of each sample was combined with 5 μl of 5X sample buffer (250 mM Tris-HCl pH 6.8, 20 mM DTT, 10% SDS, 0.2% bromophenol blue, 50% glycerol) and boiled for 5 minutes. Once prepared, the samples were electrophoresed in a 15% SDS-PAGE gel and transferred to a nitrocellulose membrane (Whatman) for Western blot analysis or stained with GelCode Blue Stain Reagent (Pierce). The protein was quantified using the Bio-Rad protein microassay according to manufacturer's instructions.

3.3.13 ProtoArray human protein microarray

ProtoArray Human Protein Microarrays (Invitrogen) were used to identify host protein binding partners for 1-88 RUB C and 1-88 RUB C R2A as follows. Incubation trays and stock solutions were chilled overnight at 4°C. The microarray was equilibrated at 4°C for 15 minutes and incubated with freshly prepared and chilled blocking buffer, pH 7.5 (50 mM HEPES (pH7.5), 200 mM NaCl, 0.08% Triton X-100, 25% glycerol, 1X synthetic block (Invitrogen), 1 mM DTT) for 30 minutes under gentle circular agitation at 4°C. The blocking buffer was removed and the bottom and sides of the array were dried with a paper towel. The array was then probed with 10 nM of either purified 1-88 RUB C or 1-88 RUB C R2A in 120 µl of freshly prepared and chilled washing buffer (1X synthetic block (Invitrogen), 0.1% Tween 20, PBS) under a LifterSlip (Thermo Scientific) for 90 minutes at 4ºC. The array was washed 5 times for 5 minutes with washing buffer at 4ºC with gentle agitation, incubated for 1 hour and 15 minutes with anti-FLAG (1µg/ml final concentration) in 10 ml washing buffer at 4ºC with gentle agitation, washed 5 times for 5 minutes with washing buffer at 4ºC with gentle agitation, incubated for 1 hour and 15 minutes with anti-mouse AlexaFluor 647 (Molecular Probes)(1µg/ml final concentration) in 10 ml washing buffer at 4ºC with gentle agitation, and washed 5 times for 5 minutes with washing buffer (1X synthetic block (Invitrogen), 0.1% Tween 20, PBS) at 4ºC with gentle agitation. The array was then dipped into room temperature deionized water 3 times and dried by centrifugation at 200xg for 1 minute.

The array was scanned by a GenePix 4000B Microarray Scanner (Molecular Devices) using GenePix Pro 6.1 (Molecular Devices) for acquisition and analysis using the following settings: wavelength 635 nm, PMT gain 600, laser power 100%, pixel size 10 µm, lines to average 1.0, and focus position 0 µm. The data was further analyzed using ProtoArray Prospector 5.2.1

in protein-protein interaction (PPI) mode (Invitrogen). A hit in the PPI mode is defined as any protein where the two replicates of the protein have an average Z-score of greater than 3 and the coefficient of variation of the replicates is less than 0.5. Two ProtoArrays were probed for each protein and reproducible hits were considered for further analysis.

3.4 References

1. Beatch, M. D., J. C. Everitt, L. J. Law, and T. C. Hobman. 2005. Interactions between rubella virus capsid and host protein p32 are important for virus replication. J Virol 79:10807-20.
2. Beatch, M. D., and T. C. Hobman. 2000. Rubella virus capsid associates with host cell protein p32 and localizes to mitochondria. J Virol 74:5569-76.
3. Chey S, Claus C, Liebert UG (2010) Validation and application of normalization factors for gene expression studies in rubella virus-infected cell lines with quantitative real-time PCR. J Cell Biochem 110:118-128
4. Claus, C., W. P. Tzeng, U. G. Liebert, and T. K. Frey. 2012. Rubella virus-like replicon particles: analysis of encapsidation determinants and non-structural roles of capsid protein in early post-entry replication. J Gen Virol 93:516-25.
5. Fontana, J., W. P. Tzeng, G. Calderita, A. Fraile-Ramos, T. K. Frey, and C. Risco. 2007. Novel replication complex architecture in rubella replicon-transfected cells. Cell Microbiol 9:875-90.
6. Frolova, E. I., R. Z. Fayzulin, S. H. Cook, D. E. Griffin, C. M. Rice, and I. Frolov. 2002. Roles of nonstructural protein nsP2 and Alpha/Beta interferons in determining the outcome of Sindbis virus infection. J Virol 76:11254-64.
7. Ilkow, C. S., V. Mancinelli, M. D. Beatch, and T. C. Hobman. 2008. Rubella virus capsid protein interacts with poly(a)-binding protein and inhibits translation. J Virol 82:4284-94.
8. Kujala, P., T. Ahola, N. Ehsani, P. Auvinen, H. Vihinen, and L. Kaariainen. 1999. Intracellular distribution of rubella virus nonstructural protein P150. J Virol 73:7805-11.
9. Law, L. J., C. S. Ilkow, W. P. Tzeng, M. Rawluk, D. T. Stuart, T. K. Frey, and T. C. Hobman. 2006. Analyses of phosphorylation events in the rubella virus capsid protein: role in early replication events. J Virol 80:6917-25.
10. Matthews, J. D., W. P. Tzeng, and T. K. Frey. 2012. Determinants in the maturation of rubella virus p200 replicase polyprotein precursor. J Virol 86:6457-69.
11. Matthews, J. D., W. P. Tzeng, and T. K. Frey. 2009. Determinants of subcellular localization of the rubella virus nonstructural replicase proteins. Virology 390:315-23.
12. Neuvonen, M., A. Kazlauskas, M. Martikainen, A. Hinkkanen, T. Ahola, and K. Saksela. 2011. SH3 domain-mediated recruitment of host cell amphiphysins by alphavirus nsP3 promotes viral RNA replication. PLoS Pathog 7:e1002383.
13. Suppiah, S., H. A. Mousa, W. P. Tzeng, J. D. Matthews, and T. K. Frey. 2012. Binding of cellular p32 protein to the rubella virus P150 replicase protein via PxxPxR motifs. J Gen Virol 93:807-16.

14. Tzeng, W. P., M. H. Chen, C. A. Derdeyn, and T. K. Frey. 2001. Rubella virus DI RNAs and replicons: requirement for nonstructural proteins acting in cis for amplification by helper virus. Virology 289:63-73.
15. Tzeng, W. P., and T. K. Frey. 2003. Complementation of a deletion in the rubella virus p150 nonstructural protein by the viral capsid protein. J Virol 77:9502-10.
16. Tzeng, W. P., and T. K. Frey. 2009. Functional replacement of a domain in the rubella virus p150 replicase protein by the virus capsid protein. J Virol 83:3549-55.
17. Tzeng, W. P., J. D. Matthews, and T. K. Frey. 2006. Analysis of rubella virus capsid protein-mediated enhancement of replicon replication and mutant rescue. J Virol 80:3966-74.

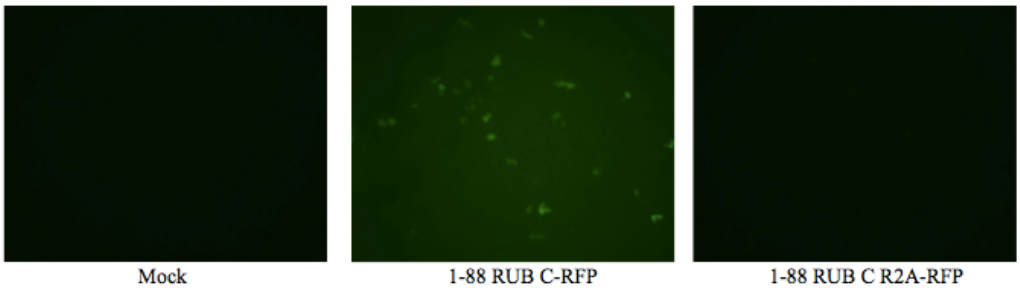

Figure 11. Analysis of 1-88 RUB C-RFP and 1-88 RUB C R2A-RFP-mediated RUBrep/GFP-ΔNotI rescue

Vero cells were transfected with 10 µg of 1-88 RUB C-RFP or 1-88 RUB C R2A-RFP cDNA 1 day after plating and transfected with 6 µl of RUBrep/GFP-ΔNotI RNA 2 days after plating. All plates were examined for GFP expression using fluorescence microscopy at (using a 10X objective) 4 days after plating.

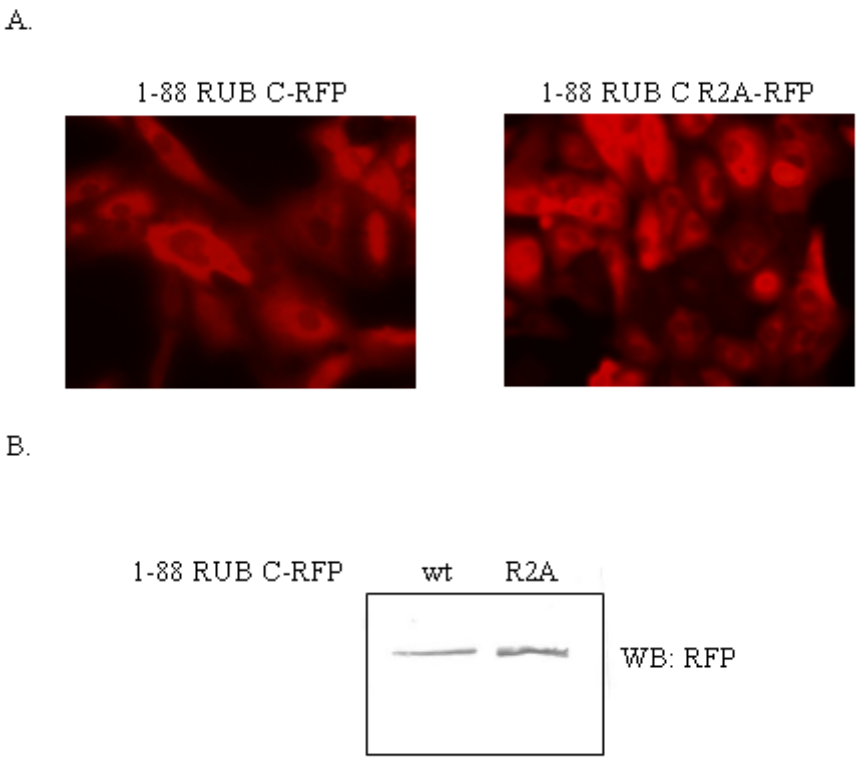

Figure 12. Expression of Vero cell lines stably expressing 1-88 RUB C-RFP and 1-88 RUB C R2A-RFP

Two days after plating, Vero cells stably expressing 1-88 RUB C-RFP or 1-88 RUB C 2RA-RFP were observed for RFP expression by A) fluorescence microscopy (40X objective) or B) Western blot analysis. In the Western blot analysis, after cell lysis and resolution of the proteins on a 15% SDS-PAGE gels, the blots were probed with primary antibody (anti-RFP 1:1000) and secondary antibody (anti-mouse AP conjugated 1:5000).

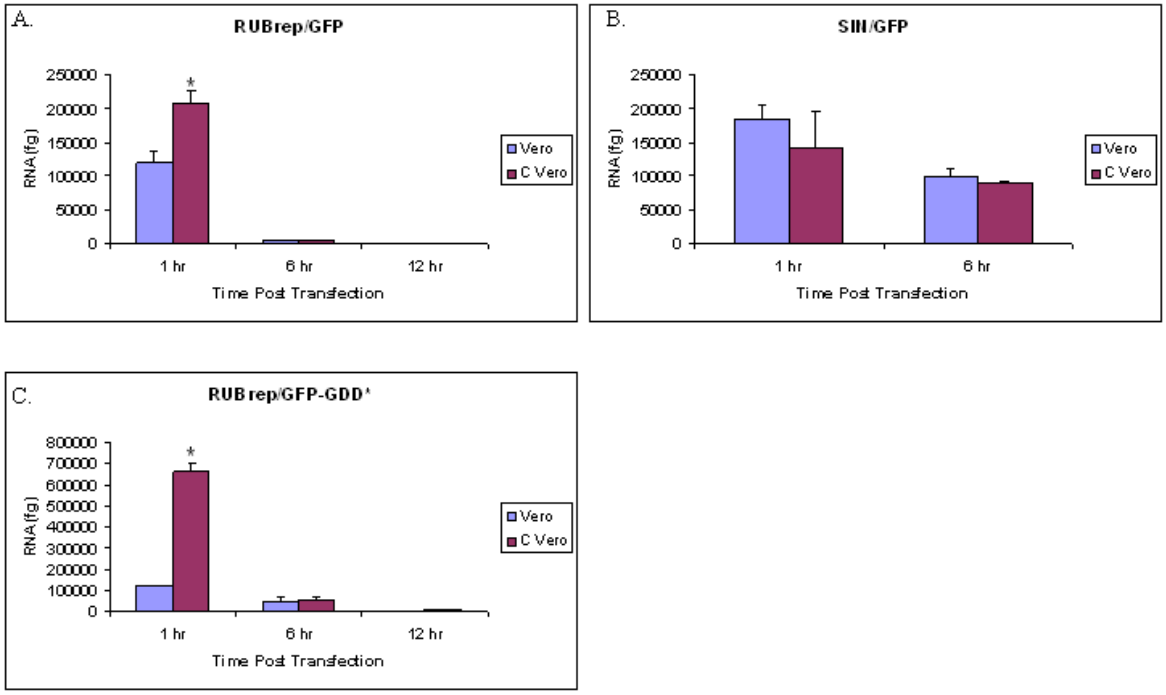

Figure 13. RNA decay of RUB and SIN replicons in the presence and absence of RUB C Vero and C-Vero cells were transfected with 6 µl of the appropriate replicon RNA, A) RUBrep/GFP, B) SINrep/GFP (a SIN replicon corresponding to RUBrep/GFP), and C) RUBrep/GFP-GDD*, a nonreplicating versions of RUBrep/GFP. RNA was extracted at 1, 6, or 12 hours post-transfection, reverse transcribed, and quantified using real time qPCR. The data shown are the average of three replicates representative of one of three separate experiments. Error bars represent the standard deviation and Student's *t* test was performed to determine significant differences (* represents p value < 0.05).

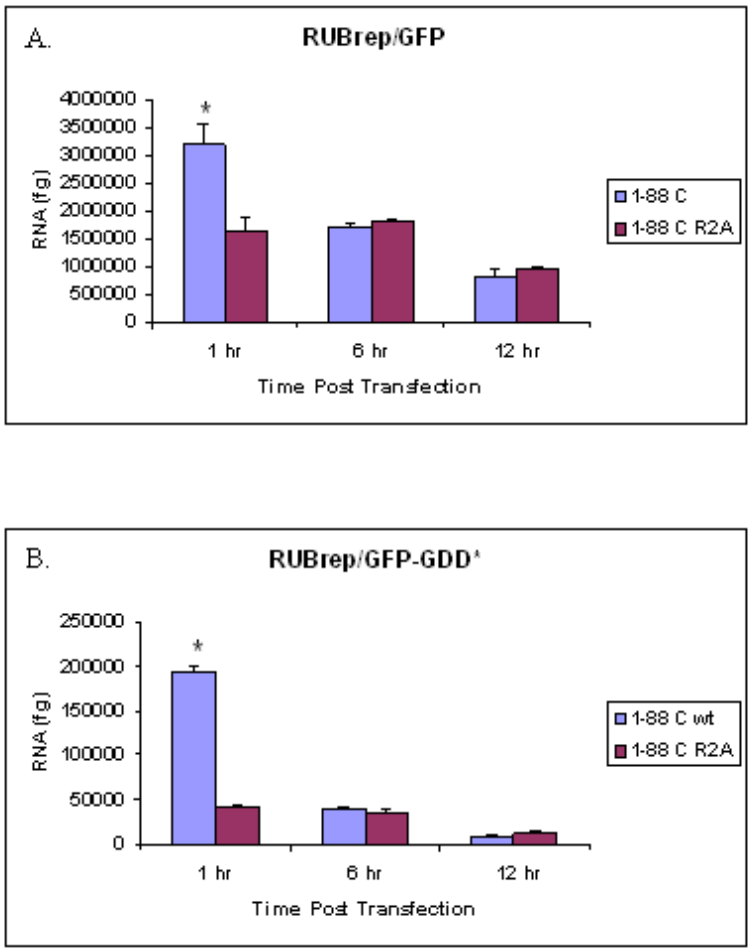

Figure 14. RNA decay of RUBrep/GFP and RUBrep/GFP-GDD* in 1-88 RUB C-RFP and 1-88 RUB C R2A-RFP cell lines

1-88 RUB C-RFP and 1-88 RUB C R2A-RFP Vero cells were transfected with 6 µl of the appropriate replicon RNA, either A) RUBrep/GFP or B) RUBrep/GFP-GDD*. At 1, 6, or 12 hours post-transfection RNA was isolated, reverse transcribed, and quantified using real time qPCR. The data shown here are the average of three replicates representative of one of three separate experiments. Error bars represent the standard deviation and Student's *t* test was performed to determine significant differences (* represents p value < 0.05).

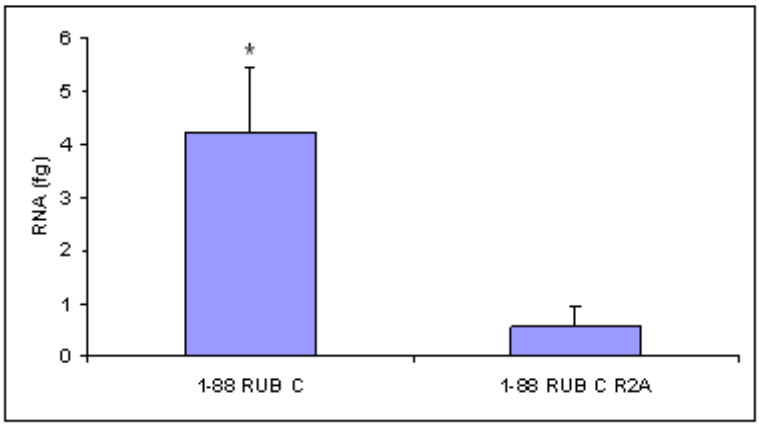

Figure 15. RNA immunoprecipitation of RUBrep/GFP by 1-88 RUB C and 1-88 RUB R2A Vero cells were transfected with 10 μg of 1-88 RUB C or 1-88 RUB C R2A cDNA 1 day after plating and 10 μl of RUBrep/GFP 2 days after plating. Protein-RNA complexes were crosslinked with formaldehyde at 1 hour post-transfection followed by lysis. Lysates were flash frozen and thawed, sonicated, and treated with DNase. Anti-FLAG antibody was added and protein-RNA complexes were immunoprecipitated and crosslinking was reversed. RNA was isolated, reverse transcribed, and quantified using real time qPCR. Each experiment was carried out 3 times. Error bars represent the standard deviation and Student's *t* test was performed to determine significant differences (* represents p value < 0.05).

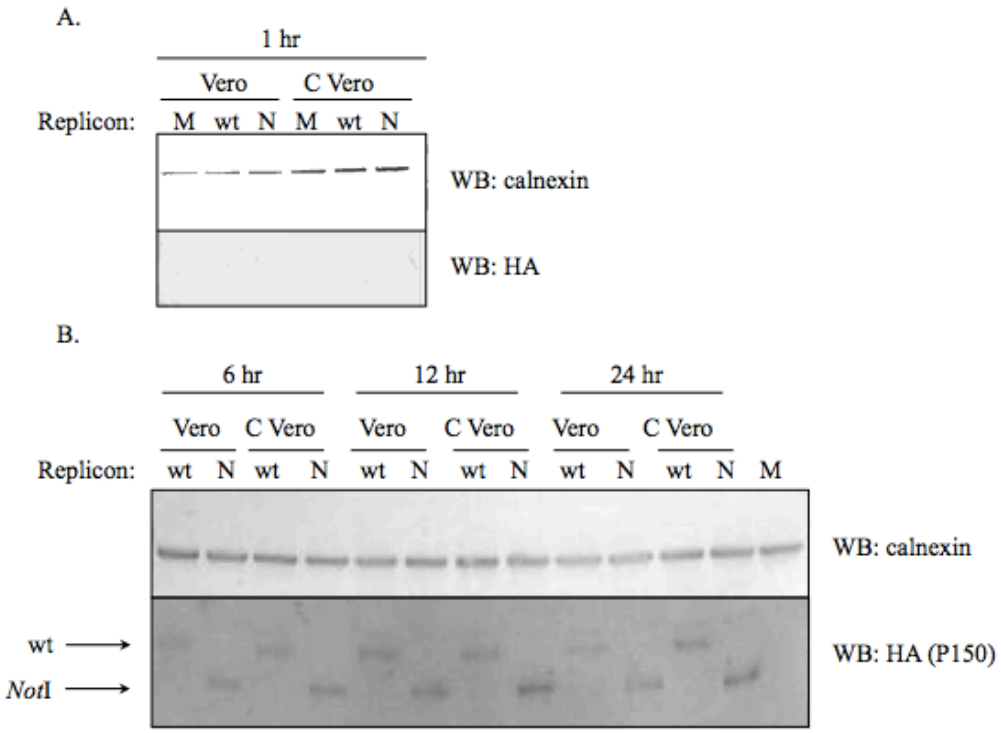

Figure 16. Translation time course of RUBrep/GFP (wt) and RUBrep/GFP-ΔNotI (N) in Vero and C-Vero cells

Vero or C-Vero cells were transfected with 6 µl of the appropriate HA-tagged-P150 replicon RNA, RUBrep/GFP or RUBrep/GFP-ΔNotI. The cells were lysed at 1 (A), 6, 12, and 24 (B) hours post-transfection. Lysates were electrophoresed in 8% (to resolve P150) and 15% (to resolve the calnexin loading control) SDS-PAGE gels and proteins were transferred to a nitrocellulose membrane. The membranes were then probed with primary antibody (anti-calnexin 1:5000 or anti-HA 1:1000) and secondary antibody (anti-mouse AP conjugated 1:5000). The wt and *Not*I forms of P150 are denoted; the *Not*I form is smaller because of the deletion. M stands for mock.

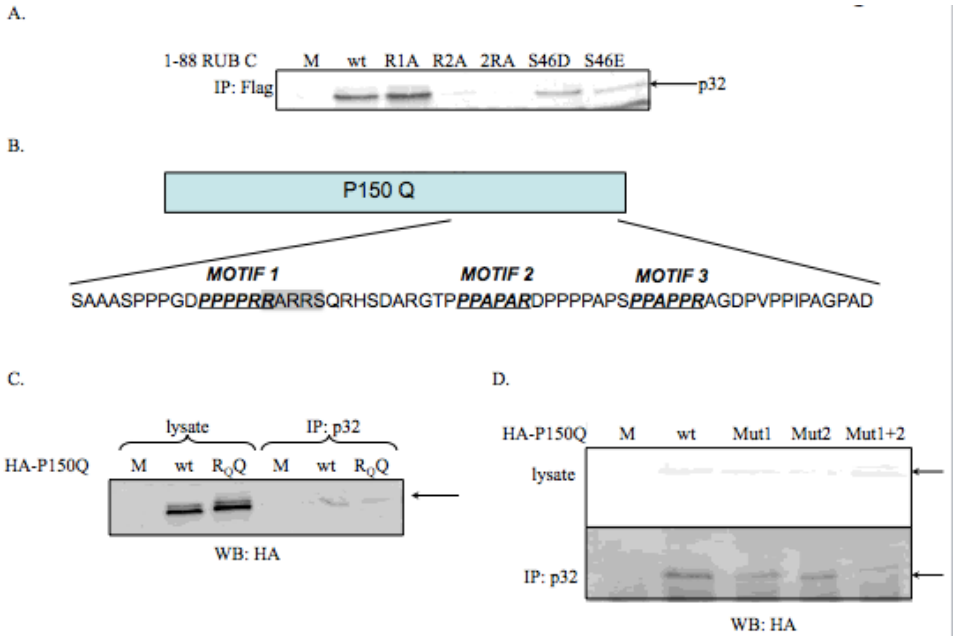

Figure 17. Co-immunoprecipitation of 1-88 RUB C and its mutants, the P150 Q domain and its mutants with cellular p32

A) Vero cells were mock transfected (M) or transfected with 10 µg of the 1-88 RUB C wt or one of a mutant cDNA panel. The plates were harvested at 2 days post-transfection, cells were lysed, and protein complexes were immunoprecipitated with anti-FLAG to pull down FLAG-tagged 1-88 RUB C and its mutants. Immunoprecipitated protein complexes were electrophoresed in a 15% SDS-PAGE gel and proteins were transferred to a nitrocellulose membrane. The membranes were then probed with primary antibody (anti-p32 1:500) and secondary antibody (anti-rabbit AP conjugated 1:5000). The arrow points to cellular p32. B) Schematic of RUB P150 Q domain. Below are shown aa residues 716 to 779 of RUB P150, with predicted SH3 motifs underlined and arginine cluster highlighted in grey. Mutations made to these motifs were as follows: Motif 1 (PPPRR to APPARR, termed Mut1), Motif 2 (PPAPAR to APAAAR, termed Mut2), and arginine cluster (RRARR to QQAQQ, termed R_QQ). C and D) Vero cells were transfected with 5 µg of the RUB P150 Q domain cDNA or cDNA encoding a Q domain mutant in the arginine rich domain or one of the PxxPxR sarc-homology domains. Plates were harvested at 1 day post-transfection, cells were lysed, and protein complexes were immunoprecipitated with anti-p32 antibody. Lysate aliquots and immunoprecipitated protein complexes were electrophoresed in a 10% SDS-PAGE gel and proteins were transferred to a nitrocellulose membrane. The membranes were then probed with primary antibody (anti-HA 1:1000) and secondary antibody (anti-mouse AP conjugated 1:5000). The arrow points to HA-tagged RUB P150 Q domain. M stands for mock.

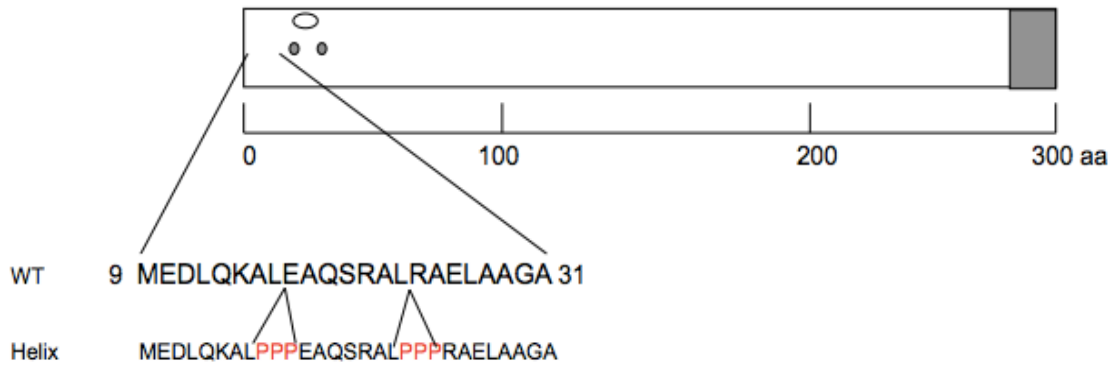

Figure 18. Predicted RUB C alpha helix and mutant
Schematic of RUB C showing the two arginine clusters (gray circles), S46 primary phosphorylation site (white circle), and C-terminal E2 signal sequence (gray box). Below are shown the residues of a predicted alpha helix, aa 9 to 31 of RUB C, with specific mutations introduced into 1-277 RUB C for this study in red. These inserted prolines were predicted to disrupt the predicted alpha helix in RUB C.

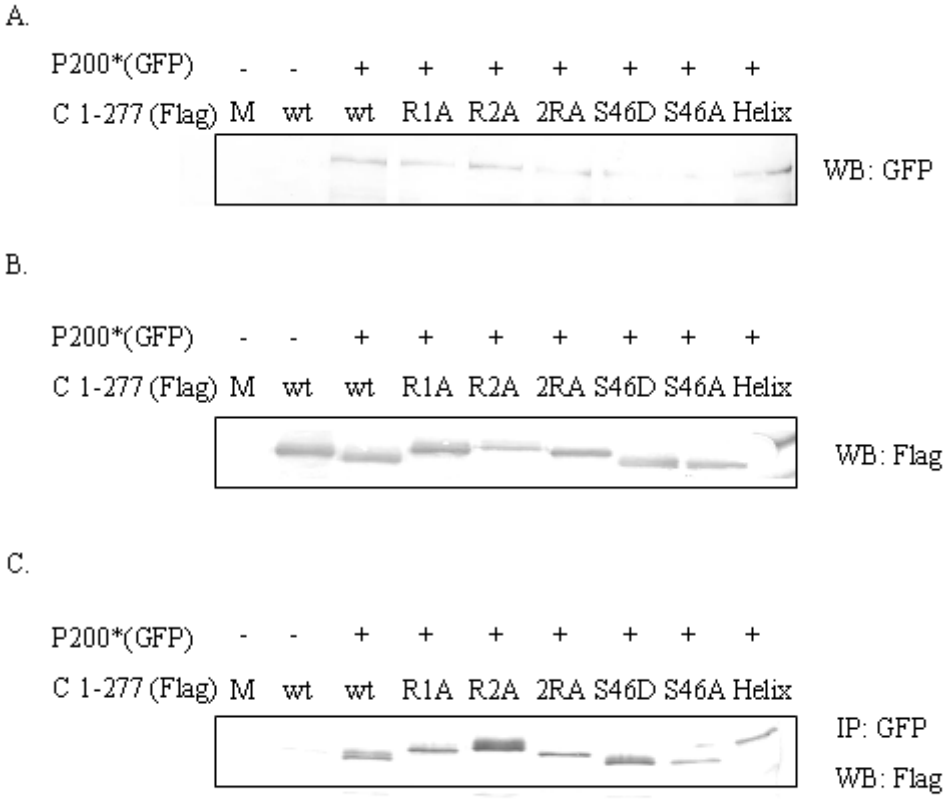

Figure 19. Co-immunoprecipitation of 1-277 RUB C and its mutants with P200*
Vero cells were transfected with 10 µg of the 1-277 RUB C wt or mutant cDNA and P200*. Plates were harvested at one day post-transfection, cells were lysed, and protein complexes were immunoprecipitated with anti-GFP antibody to pull down GFP-tagged P200*. Aliquots of the cell lysates (A-B) and immunoprecipitated protein complexes (C) were electrophoresed in 8% or 15% SDS-PAGE gels and proteins were transferred to a nitrocellulose membrane. The membranes were then probed with primary antibody (anti-GFP 1:2000; to detect GFP-tagged P150 or anti-FLAG 1:400; to detect FLAG-tagged RUB C or its mutants) and secondary antibody (anti-mouse AP conjugated 1:5000).

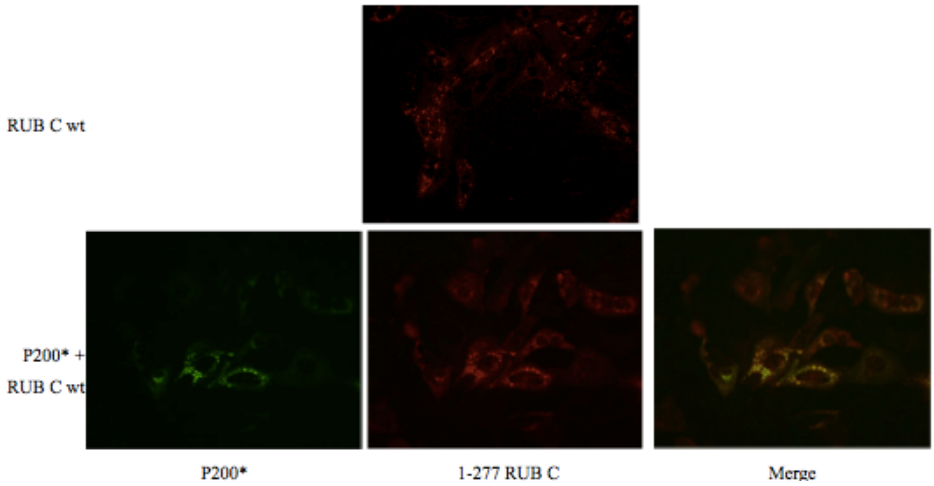

Figure 20. Co-localization of 1-277 RUB C and RUB P200*
Vero cells were transfected with 5 µg of RUB P200* (which is GFP tagged) cDNA and 5 µg of RUB C 1-277 wt or mutant cDNA 1 day after plating. Two days after plating cells were processed for immunofluorescence by staining 1-277 RUB C with anti-FLAG (1:1000) and secondary anti-mouse AlexaFluor 594 conjugated (1:5000). Coverslips were examined by fluorescence microscopy using a 40X objective. Green corresponds to GFP-tagged P200* and red corresponds to FLAG-tagged 1-277 RUB C. Representative imagines of cells transfected with P200* and wt 1-277 RUB C are shown. The results were similar for all of the 1-277 RUB C mutants.

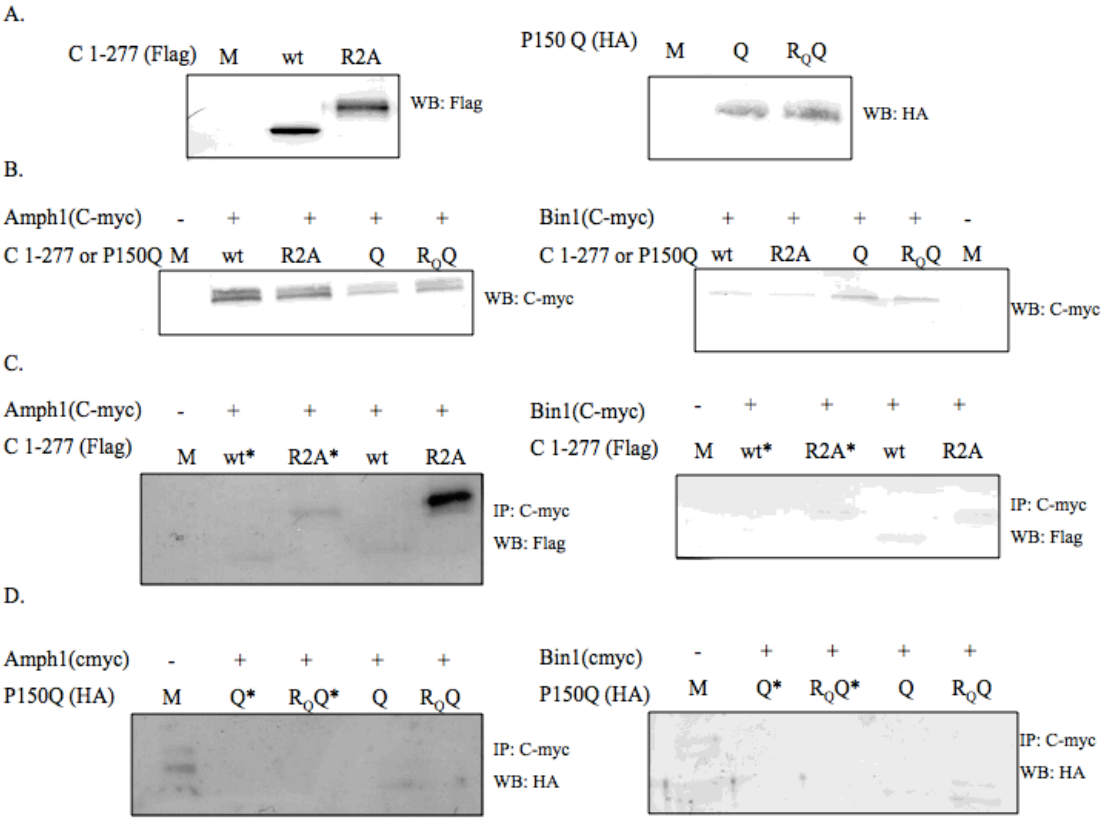

Figure 21. Co-immunoprecipitation of 1-277 RUB C and RUB P150 Q with Amph1 and Bin1

Vero cells were transfected with 10 µg of 1-277 RUB C or R2A or RUB P150 Q domain wt or R_QQ cDNA and 10 µg of either Amph1 or Bin1 cDNA. Plates were harvested at one day post-transfection, cells were lysed, and protein complexes were immunoprecipitated with anti-C-myc to pull down C-myc-tagged Amph1 or Bin1. Lysates (A-B) and immunoprecipitated protein complexes (C-D) were electrophoresed in 8% or 10% SDS-PAGE gels and proteins were transferred to a nitrocellulose membrane. The membranes were then probed with primary antibody (anti-C-myc 1:500, anti-HA 1:1000; to detect the Q domain, or anti-FLAG 1:400; to detect 1-277 RUB C) and secondary antibody (anti-mouse AP conjugated 1:5000). The * indicates a control sample in which the co-immunoprecipitation protocol was performed without antibody. M stands for mock.

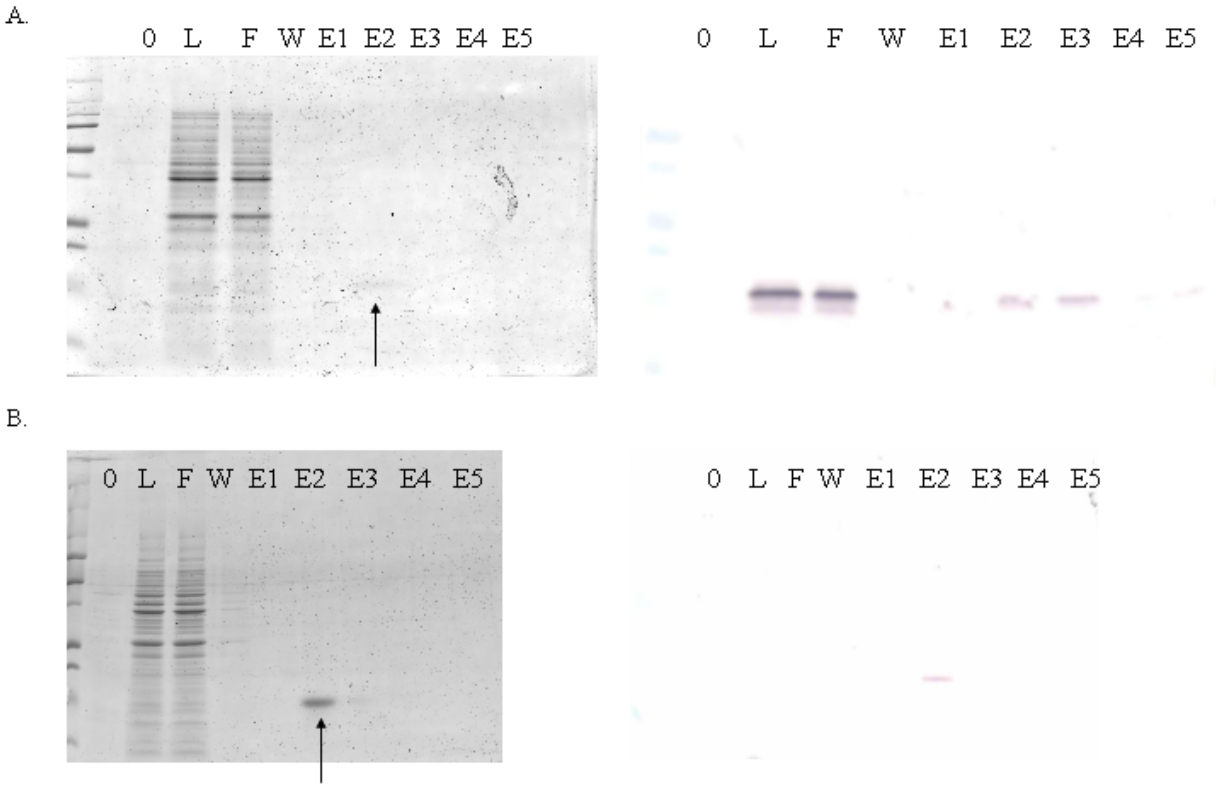

Figure 22. Large scale purification of 1-88 RUB C wt and 1-88 RUB C R2A bacterially expressed from pFLAG-MAC

A) *E. coli* BL21(DE3) cells transformed with RUB C 1-88 wt in pFLAG-MAC were grown overnight in 4 ml LB and ampicillin at 37°C. Four ml of each overnight culture was diluted in 400 ml of LB and allowed to grow 2 hours (0). The cultures were then induced with 4 ml of 100 mM IPTG. After 2 hours of growth, the cells were lysed (L), the lysate poured over a column of anti-FLAG M2 agarose. After collecting the flow-through (F) the agarose was washed (W) and FLAG-tagged RUB C 1-88 was eluted with 3XFLAG peptide (E1-35). Fractions were electrophoresed in a 15% SDS-PAGE gel and the gel was either stained with GelCode Blue (left) or subjected to Western blot analysis probed using anti-FLAG antibody (right). B) *E. coli* BL21(DE3) cells transformed with 1-88 RUB C R2A in pFLAG-MAC were grown overnight in 4 ml LB and ampicillin at 37°C. Four ml of each overnight culture was diluted in 400 ml of LB and allowed to grow 2 hours (0). The cultures were then induced with 4 ml of 100 mM IPTG. After 2 hours of growth, the cells were lysed (L), the lysate poured over a column of anti-FLAG M2 agarose. After the flow-through (F) was collected, the agarose was washed (W), and FLAG-tagged RUB C 1-88 R2A protein was eluted with 0.1 M glycine pH 3.5 (E1-5). Samples were electrophoresed in a 15% SDS-PAGE gel and the gel was either stained with GelCode Blue (left) or subjected to Western blot analysis probed using anti-FLAG antibody (1:400) (right). In both A and B, the fraction collected for use in probing the human protein array is marked with an arrow.

Table 1. Common hits from ProtoArray human protein array for 1-88 RUB C and 1-88 RUB C R2A

A hit was defined as any protein on the array where the two replicates of the protein yielded an average Z-score of greater than 3 and the coefficient of variation of the replicates is less than 0.5. Two ProtoArrays were probed for each protein and reproducible hits were considered for further analysis.

Hits for 1-88 RUB C and 1-88 RUB C R2A

chromosome 11 open reading frame 63 (C11orf63), transcript variant 2	general transcription factor IIB (GTF2B)
6-pyruvoyltetrahydropterin synthase (PTS)	protein kinase C, beta 1 (PRKCB1), transcript variant 1
Hematopoietic lineage cell-specific protein	cyclin G associated kinase (GAK)
dynein, cytoplasmic 1, intermediate chain 1 (DYNC1I1)	Nedd4 family interacting protein 1 (NDFIP1)
septin 5 (SEPT5)	interferon regulatory factor 6 (IRF6)
Ral GEF with PH domain and SH3 binding motif 2 (RALGPS2), transcript variant 1	excision repair cross-complementing rodent repair deficiency, complementation group 6-like (ERCC6L)
centaurin, beta 2 (CENTB2)	chromosome 1 open reading frame 62 (C1orf62)
protein phosphatase 2 (formerly 2A), regulatory subunit B", beta (PPP2R3B), transcript variant 2	RAS-like, family 11, member B (RASL11B)
actin binding LIM protein 1 (ABLIM1)	biogenesis of lysosome-related organelles complex-1, subunit 2 (BLOC1S2), transcript variant 1
sulfotransferase family, cytosolic, 1C, member 4 (SULT1C4)	Spindlin-2B
6-phosphofructo-2-kinase/fructose-2,6-biphosphatase 3 (PFKFB3)	Proteasome assembly chaperone 1
zinc finger, RAN-binding domain	v-akt murine thymoma viral oncogene homolog 2 (AKT2)
Aflatoxin B1 aldehyde reductase member 2	PWP1 homolog (S. cerevisiae) (PWP1)
calumenin (CALU)	Rho-associated, coiled-coil containing protein kinase 1 (ROCK1)
proteasome (prosome, macropain) subunit, alpha type, 4 (PSMA4), transcript variant 1	coiled-coil domain containing 75 (CCDC75)
SH2 domain protein 2A (SH2D2A)	zinc finger, RAN-binding domain containing 2 (ZRANB2)
6-pyruvoyl tetrahydrobiopterin synthase	serine/arginine repetitive matrix 2 (SRRM2)
6-phosphofructo-2-kinase/fructose-2,6-biphosphatase 1	

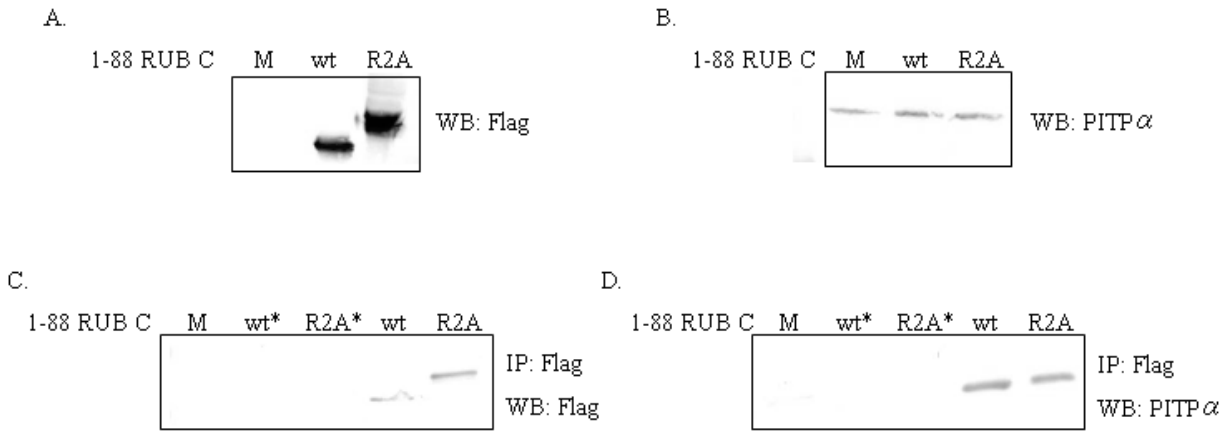

Figure 23. Co-immunoprecipitation of 1-88 RUB C and R2A with cellular PITPα
Vero cells were transfected with 10 μg of 1-88 RUB C or R2A cDNA. Plates were harvested at 2 days post-transfection, cells were lysed, and protein complexes were immunoprecipitated with anti-FLAG to pull down FLAG-tagged 1-88 RUB C. Lysates (A-B) and immunoprecipitated protein complexes (C-D) were electrophoresed in a 15% SDS-PAGE gel and proteins were transferred to a nitrocellulose membrane. The membranes were then probed with primary antibody (anti-PITPα 1:1000 or anti-FLAG 1:400) and secondary antibody (anti-rabbit AP conjugated 1:5000 or anti-mouse AP conjugated 1:5000). The arrow points to cellular PITPα. M denotes mock and * indicates a control in which the protocol was performed without antibody.

Table 2. qPCR primer pairs
Targets and the sense (s) and antisense (as) sequences are indicated. RUB P150 s primer corresponds to nt 3178 to 3197 while RUB P150 as primer corresponds to nt 3247-3266 (3).

Target	Sequence
Actin (s)	5'-TGACGGGGTCACCCACACTGTGCC-3'
Actin (as)	5'-CTAGAATTTGCGGTGGACGAT-3'
GFP (s)	5'-CTGAAGATCTTCATTACTTCTACAGCT-3'
GFP (as)	5'-ATATACTAGTATGGTGAGCAAGGGCG-3'
RUB P150 (s)	5'-TGACCGCGCCTATGTCAACC-3'
RUB P150 (as)	5'-GCCCGTAGACAACCACCTCG-3'

4 DISCUSSION

As summarized in the Introduction, virus core or capsid proteins have been found to play roles in the virus replication cycle in addition to comprising a structural component of the virus particle. The unique aspect of the role played by the RUB C is that it duplicates the role played by a domain within one of the virus nonstructural replicase proteins, namely the Q domain of P150. Indeed, this role was not apparent until deletion studies of P150 revealed that the Q domain could be deleted and rescued by RUB C. However, the function of the Q domain in RUB replication is unknown. Thus, in this study we sought to further understand the nonstructural role played by RUB C in the RUB life cycle that allows it to compensate for the function of the Q domain.

To this end, we first created a series of mutants that had been previously described in the literature within the context the first 88 amino acids of RUB C, the minimal region required for its rescue function, and screened them for their ability to rescue the replication of RUBrep/GFP-ΔNotI. We found that mutations to the primary phosphorylation site, S46, had no impact on the ability of 1-88 RUB C to rescue the Δ*Not*I replicon, indicating the phosphorylation status of RUB C did not control the rescue phenomenon. Similarly, mutation of the first arginine cluster (R1A) did not affect the ability of 1-88 RUB C to rescue the Δ*Not*I replicon, but mutation of the second (R2A) or both (2RA) arginine clusters in 1-88 RUB C led to a loss of the ability of RUB C to rescue the Δ*Not*I replicon, indicating that the arginine residues in the R2 cluster confer the ability of RUB C to rescue the loss of the Q domain in RUB P150. This finding was confirmed though the quantification of GFP-positive cells present in cells expressing the various 1-88 RUB C mutants and later transfected with RUBrep/GFP-ΔNotI as we found that the percentage of the population containing GFP-positive cells was significantly reduced in cells expressing 1-88 RUB

C harboring the R2A or 2RA mutations when compared to both wild type 1-277 and 1-88 RUB C.

The first possible explanation for this loss of ability to rescue the Δ*Not*I replicon that we explored was a change in the localization of 1-88 RUB C R2A. If this mutant localized to a different area of the cell, it could simply be unavailable to fulfill its compensatory function. However, this was not the case as all wild type and mutant forms of 1-88 RUB C localized to both the mitochondria and nucleus. We expected to observe 1-88 RUB C localized to the mitochondria as this localization has been previously noted in the literature (22), but the localization in the nucleus was unexpected because replication of RUB occurs in the cytoplasm. However, the nuclear localization of C-terminally truncated constructs of RUB C had been observed previously (35) and it was shown that the first four of the arginine residues of R2 served as a nuclear localization signal. When full length RUB C was expressed, nuclear localization was not observed and the ability of these arginine clusters to serve as nuclear localization signals thus appeared to be overridden in the context of the entire RUB C protein. Pools of capsid proteins of other RNA viruses that carry out their replication cycle completely in the cytoplasm have been observed to also localize to the nucleus and nucleolus and often this unexpected localization is associated with the ability of these capsid proteins to modulate the cell cycle, apoptosis, or host cell gene expression (13, 33, 45, 47, 48, 55, 57). RUB has been reported to induce apoptosis in cell cultures derived from fully differentiated cells (9, 10, 14, 27, 36). However, there is no evidence that this depends on nuclear factors.

Another possible explanation for the differences in the ability of the various RUB C mutants to rescue the Δ*Not*I replicon that we explored was differential phosphorylation. RUB C is a phosphoprotein (21), so it is possible that the ability to compensate for the lesion in P150 could

be regulated through the phosphorylation of RUB C. The phosphorylation status the mutant panel did not follow the demarcation of rescuing and non-rescuing forms of 1-88 RUB C as the wild type, R2A, S46D, and S46E mutants were phosphorylated while the R1A and 2RA mutants were not. S46D and S46E serve as phosphorylation mimic mutations and it was found that wild type, S46D, and S46E RUB C were all phosphorylated in a previous study (20), which agrees with our findings. This same lab showed that wild type, R1A, and R2A RUB C were phosphorylated but 2RA RUB C was not (1), while our analysis found that wild type and R2A RUB C were phosphorylated but R1A and 2RA were not. There are differences between this group's and our own experimental designs. Our study examined the first 88 amino acids of RUB C, while Beatch et al. used the entire coding region of RUB C along with the E2 signal sequence. Additionally, different techniques were used to determine phosphorylation status of the various forms of RUB C in the two studies (1). However, our findings possibly indicate that the R1 cluster serves as a phosphorylation signal.

We verified that the second arginine cluster in RUB C is important for the rescue phenomenon, which agrees with a previous study in our lab (49). That study also determined that an arginine-rich region of the P150 Q domain is required for viability and that mutations in this motif were rescued by RUB C. Thus, an arginine cluster appears to be the basis of function of the P150 Q domain which is rescued by RUB C. Arginine-rich motifs (ARMs) of other viral proteins have been found to be important in the virus life cycle through their interactions with viral RNA and/or host proteins. The P7a movement protein of beet black scorch virus (BBSV) contains an arginine-rich motif that is important for its localization to the nucleus and nucleolus via its interaction with cellular importin α. This motif is also required for the replication of viral RNA and productive infection (53). The Rev protein of HIV-1 contains an ARM that both binds

viral RNA and is needed for oligomerization (59), and this interaction is needed for nuclear export of viral RNAs containing introns. The ARM of the Flock House virus (FHV) coat protein is required for the targeting of this protein to RCs (52). The E1^E4 protein of human papillomavirus type 1 (HPV1) contains an ARM important for the ability of E4 to block cell cycle progression and inhibit host DNA synthesis (39).

Further analysis of the rescue of the P150 Q domain by RUB C could determine if this phenomenon could be regulated by arginine methylation. Arginine-rich proteins are often regulated through post-translational modification of the arginine residues. The methylation of arginine residues in the ARM of the nucleocapsid protein of HIV-1 inhibits its ability to anneal RNA primers and aid in reverse transcription (16). The methylation of the ARM of the HIV-1 Tat protein decreases its ability to interact with Tat transaction region (TAR) of the viral RNA and form Tat-TAR-cyclin T1 complexes, which in turn results in decreased transcriptional activation (56). Methylation of arginine residues of the RGG-box of ICP27 of herpes simplex virus type-1 (HSV-1) regulates its RNA binding, protein-protein interactions, and localization with hypomethylation resulting in inhibition of viral replication (58). Methylation of arginines within the L4-100K protein of adenovirus is required for efficient viral replication by impacting protein-protein and protein-RNA interactions (17). The arginine methylation of EBNA1 protein of Epstein-Barr virus (EBV) is required for proper localization (42). The helicase domain of NS3 of HCV is methylated at a critical arginine residue and it is hypothesized that this methylation regulates the binding of NS3 to viral RNA (37).

Throughout this study RUB replicon RNAs were employed rather than RUB infectious clone RNAs or virus. RUB replicons provide a convenient means to study the replication of the viral RNA and translation of the ORFs in isolation. However, replicons can be transfected into

cell lines that express the structural proteins of said virus, packaged into virus like particles (VLPs), and the VLP containing culture fluid can be passaged to fresh cells in order to introduce the replicon into the cells. This allows for the flexibility to add back the presence of the structural proteins and entry into the cell to the study if desired. The use of the RUB replicon in our study was appropriate as we were interested in the early rescue of RNA synthesis by the RUB structural protein capsid. The use of RUBrep/GFP allowed us to study early replication in the presence and absence of RUB C, which were provided in *trans* either stably expressed in the C-Vero or 1-88 RUB C-RFP cell lines or expressed from a plasmid.

In the second portion of our study we sought to determine which step in early replication RUB C acts to rescue the replication of RUBrep/GFP-ΔNotI using a Vero cell line, C-Vero, genetically engineered to express RUB C. The first step in the replication cycle studied was RNA transcript stability following transfection of Vero and C-Vero cells, which could reflect either RUB C stabilizing transcripts, possibly by protecting them from the cell's RNA degradation machinery, and/or recruitment of the transcript RNA to the RC. Indeed, more transcript RNA was present in cells harboring RUB C (C-Vero) than normal Vero cells one hour after RUBrep/GFP was transfected but both cell lines had similar levels of viral RNA at later time points, indicating that RUB C protects RUBrep/GFP at this early time point. This effect was specific for RUB viral RNA as no differences were seen at any time point in Vero versus C-Vero cells transfected with Sindbis virus replicon RNA. This specificity for RUB sequences may be conferred by the high GC content of the RUB genome or by specific secondary RNA structures. The similarity of RNA levels seen at 6 and 12 hours post transfection between Vero and C-Vero cells could not be attributed to newly synthesized viral RNA as similar decay kinetics were observed with RUBrep/GFP-GDD*, a replication defective RUB replicon. The same trend was seen when 1-88

RUB C was compared to its R2A mutant. At the one hour time point, cells expressing wild type 1-88 RUB C harbored significantly more RUBrep/GFP or RUBrep/GFP-GDD* than cells expressing the R2A mutant, but viral RNA levels were comparable at later time points. Thus, RUB C protects the incoming RUB RNA from degradation at an early time point and the second arginine cluster within RUB C is associated with this protective action. However, it must be noted that the introduction of RUB replicon RNA into the cell via transfection bombards the cell with a large amount of RNA that is not associated with protein, which could be detected by pattern recognition receptors or the host cell RNA decay machinery to activate the immune response or RNA degradation pathways. The introduction of the replicon RNA packaged into a virus like particle would more accurately mimic the introduction of RUB RNA into the cell during infection.

We next wanted to know if the differences in this early protection of the viral RNA could be attributed to differential interaction of the 1-88 RUB C wild type and R2A variants with the viral RNA at this early time point. RNA immunoprecipitation followed by qPCR one hour after transfection of RUB replicon RNA showed that significantly more replicon RNA associated with 1-88 RUB C than 1-88 RUB R2A. Another group reported that RUB C R2A expressed in the context of the complete protein bound RNA very weakly in comparison to RUB C wt or R1A as assayed by an *in vitro* RNA-binding assay (1), which is in line with our results. The approach we took cross-linked the viral RNA with RUB C in the cell prior to lysis, which we used to give a more accurate picture of RNA-protein interactions in the transfected cell. The association of RUB replicon RNA with RUB C via the second arginine cluster could either be a direct interaction or the second arginine cluster could bind a host cell protein, such as a protein involved in RNA stabilization, that directly binds the RUB replicon RNA. The formation of the protein-

RNA complex could then mask the replicon RNA from detection by cellular pattern recognition receptors or evade the cellular mRNA degradation pathways, ultimately stabilizing the RUB RNA. Alternatively, the early stabilization of RUB replicon RNA may involve the shutdown of the host RNA decay machinery via the second arginine cluster of RUB C.

As reviewed by Narayanan and Makino, viruses evade the cellular mRNA degradation pathways by attempting to make their RNAs appear to be like cellular mRNAs through cap structures and poly(A)-tails, by possessing stabilization sequences or structures within the viral RNA, or through association of the viral RNA with cellular RNA stabilization machinery (32). Additionally, virus proteins play a role in this process. Human T-lymphotropic virus type 1 (HTLV-1) protein Tax inhibits the nonsense-mediated mRNA decay (NMD) pathway, which in turn stabilizes the viral transcript (30). Several viruses inhibit the RNase L pathway to protect viral RNAs during replication (28, 38, 40, 41, 61). Some viruses prevent formation of stress granules or SGs (3, 11, 12, 31), which sequester RNA during times of cellular stress to be degraded or translated at a later point. For example, the poliovirus 3C proteinase cleaves several cellular proteins involved in deadenylation and stress granule (SG) pathways (8, 19, 54) while WNV and DENV redistribute other cellular proteins involved in SG pathways (11). The early protection provided by RUB C to the viral RNA suggests that RUB C may induce stress granule formation to protect the viral RNA early on. However, previous work in our lab has found that RUB does not induce the formation of SGs, but rather directs the redistribution of G3BP, a major SG component, into other clusters distinct from SGs (23).

Based on the differential RNA decay and association of wild type and R2A 1-88 RUB C with the viral RNA, we initially hypothesized that RUB C complexes with the incoming RUB viral RNA providing protection from the host cell RNA decay pathways. Once translated, the Q

domain of RUB P150 would take over this role of providing protection against decay, allowing for replication of the viral RNA. However, subsequent work suggests that this is not the case. As expected with this model, the P150 Q domain does bind transfected RUB replicon RNA when expressed in Vero cells, but the R_QQ P150 Q domain mutant, which requires RUB C for replication, is also able to bind RUB replicon RNA (data not shown). Additionally our model would predict that RUB C mutants that cannot rescue the replication of RUBrep/GFP-ΔNotI would not be able to prevent RUB RNA decay at the early time point or bind RUB RNA, and this is not the case. The R2 arginine cluster in RUB C contains six arginines (RRRRGNRGR). When the first of these arginines is changed to alanine (termed mutant 1811), RUB C loses its ability to rescue the Δ*Not*I replicon (Tzeng unpublished data). However, the 1811 1-88 RUB C mutant is able to prevent the early decay of RUB RNA and bind RUB RNA (data not shown). The R2 arginine cluster was previously shown to be important for RNA binding in an in vitro assay (1) and is thought to be important for genome encapsidation. We, therefore, hypothesize that the binding of transfected RUB replicon RNA by wt RUB C, but not its R2A mutant, and protection from degradation at early times post-transfection, is due to the encapsidation function of RUB C and is not involved in the Q domain rescue phenomenon. The encapsidation of the RUB genome does not depend upon an encapsidation signal, but rather long stretches of RUB RNA (5).

The next step of the replication cycle upon entry of the genomic RNA into the cytoplasm is the translation of the nonstructural polyprotein from the nonstructural ORF. Translation from RUBrep/GFP and RUBrep/GFP-ΔNotI containing an HA-tag within P150 did not differ at 1, 6, 12, or 24 hours post-transfection in Vero or C-Vero cells, indicating that the presence or absence of RUB C has no impact on the translation from RUB replicons and therefore translation is not the stage of the viral life cycle at which RUB C acts to rescue the Q domain of P150. This find-

ing agrees with previous findings from our lab where there was no difference in the translation of P150 from various replicons at 6 and 24 hours post-transfection into Vero and C-Vero cells (50).

Finally, we investigated the possibility that RUB C elicits its rescue function by binding to a cell protein, either to recruit the protein to the replication complex, to inhibit an innate cellular defense mechanism, or to otherwise mediate changes in the cellular environment to make it conducive to virus replication. For example, both RUB C and RUB P150 bind cellular protein p32 (a cell protein with a long history in the RUB literature), making the hypothesis that the interaction between this common binding partner is the duplicated function shared by these two viral proteins attractive. Interestingly, p32 was not co-immunoprecipitated by 1-88 RUB C R2A and 2RA, the non-rescuing mutants, while all the rescuing mutants of 1-88 RUB C were able to pull down p32. This result did not completely align with a previous study that found that wild type RUB C expressed in the context of the complete C protein but not the R1A, R2A, or 2RA mutants were co-immunoprecipitated with p32 (1). The results of our study also differed from this study concerning the RUB C R1A mutant's phosphorylation state as discussed above. Encouraged by this finding, we examined if variants of the P150 Q domain that either require RUB C for replication (the P150 R_QQ Q domain mutant) or do not require RUB C for replication (the wild type P150 Q domain) differentially interact with p32. Both wild type and R_QQ P150 Q domain were co-immunoprecipitated with p32, suggesting that the interaction with cellular p32 is not the duplicated function behind the rescue phenomenon between RUB C and the Q domain of RUB P150. Additional work done in our lab also supports the assertion that the interaction between cellular p32 and these viral proteins is not behind the rescue phenomenon as P150 expressed by a RUB replicon harboring two mutated PxxPxR motifs in the P150 Q domain does not bind p32 but does not require RUB C for its replication (44). In this paper it was also

demonstrated that p32 primarily colocalizes with P150 that is not associated with replication complexes (44), indicating that this interaction is not important for viral RNA synthesis. Virus and replicons with the two mutated PxxPxR motifs, which produce P150 that does not interact with p32, produced viral RNAs and GFP expressing cells to comparable levels as wild type sequences (44), providing further support that the interaction between p32 and RUB C does not underlie the rescue phenomenon as this rescue occurs at a stage prior to viral RNA accumulation. Additionally, as discussed above, the R2 arginine cluster in RUB C contains six arginines (RRRRGNRGR). When the first of these arginines is changed to alanine (termed mutant 1811), RUB C loses its ability to rescue the Δ*Not*I replicon (Tzeng unpublished data), but we found it is still able to bind p32 (data not shown). Taken together, this indicates that interactions between p32 and the RUB viral proteins P150 and RUB C are not the basis of the rescue phenomenon.

Another set of host proteins that we wanted to explore as potential common binding partners between RUB C and the Q domain of P150 were amphiphysins. The SH3 binding domain within these proteins was found to be important for the viral RNA accumulation of alphaviruses through its interaction with nsP3. We were further intrigued by these proteins as arginines were found to be the critical residues for this effect and interaction (34), since the critical residues associated with the common function of RUB C and the Q domain of P150 are also arginines. However, none of the wild type or arginine cluster mutant forms of 1-277 RUB C or the Q domain of RUB P150 examined bound either Amph1 or Bin1.

Efforts to identify host protein binding partners with RUB C in the past have been done using yeast two-hybrid screening or GST pulldowns. Although both approaches successfully identified RUB C host cell binding partners, there were pitfalls to these approaches. The yeast two-hybrid screening used an African green monkey kidney cell derived cDNA library (2),

which was not as ideal as a human library since RUB is a strictly human pathogen. The GST pulldowns were done in both monkey and human embryonic kidney derived cell lines (15), but more transient interactions may have been eliminated using this technique. We, therefore, screened a human protein library with 1-88 RUB C and 1-88 RUB C R2A. The human proteins spotted on this array were purified using a baculovirus expression system, meaning these proteins were expressed in insect cells and so could obtain post-translational modifications. A potential pitfall of our study is that we purified these probes after expression in bacteria and therefore without potentially important post-translational modifications. Perhaps more meaningful host protein binding partners would have been formed for these two forms of 1-88 RUB C had these proteins been expressed and purified from a mammalian system. It is also possible that interactions between RUB C and host proteins could be dependent upon the environment provided in the host cell that cannot be duplicated on an array, such as pH, proper folding and modification of the proteins, presence of lipids, or the requirement for multiple proteins and/or nucleic acids for the formation of a complex. Additionally, the interactions between RUB C and host proteins may be dependent upon active replication or the presence of the RUB RNA and/or other RUB proteins. Another limitation of this approach is that the human protein array selected for this study provided over 9000 potential cellular binding proteins to assay for potential interactions, which does not include all possible human proteins. However, this array did contain the most human proteins at the time of analysis and the number of protein spotted on this array has not changed since our analysis, therefore a more robust analysis using this methodology would not be possible using the currently available human protein microarrays. Instead, the expression of the rescuing and non-rescuing forms of RUB C in mammalian cells, followed by the identification of cellular binding partners using pull-down followed by mass spectrometry could over-

come the limitations of the protein microarray. More transient interactions could be captured with this method by crosslinking the protein-protein interactions prior to pull-down experiments.

The sole protein found to interact with the wild type form of 1-88 RUB C but did not interact with 1-88 RUB C R2A was phosphatidylinositol transfer protein alpha isoform (PITPα). However, PITPα was co-immunoprecipitated with both forms of 1-88 RUB C expressed in Vero cells and, therefore, was not the answer for the rescue phenomenon, but was still an intriguing newly identified RUB C binding partner as it fits into what is already known about RUB biology. PITPα binds, transfers, and exchanges phophatidylinositol (PI) or phosphatidylcholine (PC) to maintain proper lipid composition in cellular membranes. PI molecules in the plasma membrane can be differentially phosphorylated to generate second messengers important in cell signaling cascades (6), one of which is the phosphoinositide 3-kinase (PI3K)-Akt survival pathway. RUB infection results in the activation of the PI3K-Akt survival pathway and this activation is needed to decrease RUB-induced apoptosis and promote cell viability during RUB infection (7). The activation of the PI3K-Akt pathway has also been implicated in cell survival during respiratory syncytial virus (RSV) and coxackievirus B3 (CVB3) infection (47, 60), and the nucleocapsid of SARS-CoV is thought to play a role in the establishment of virus persistence through its induction of the PI3K-Akt and other pathways (29). Interestingly, PITPα can be regulated through phosphorylation by protein kinase C (51). We identified protein kinase C, beta 1 (PRKCB1), transcript variant 1 as a host protein that binds both the wild type and R2A forms of 1-88 RUB C through our protein array analysis, and although this interaction has not been verified, it further suggests a role for RUB C in cell signaling pathways. Previous studies in our lab have documented the association of all RUB NSPs with cellular membranes (26), so another potential role

for the interaction between RUB C and PITPα could be ensuring the proper cellular membrane composition required for RUB RCs.

A final interaction that could impact the ability of RUB C to rescue the P150 Q domain is that between RUB C and the nonstructural proteins. However, such an interaction could be necessary to localize RUB C to exert its rescue function rather than compensate for the Q domain function per se. RUB C and RUB P150 colocalize in RUB infected cells (18) and have been shown to co-immunoprecipitate when RUBrep/GFP containing an HA-tagged P150 was transfected into C Vero cells (50). We began this portion of the study with the intention of studying the interaction of the 1-88 RUB C mutant panel with RUB P200*, a form a P200 that is unable to cleave itself into P150 and P90, but we were unable to co-immunoprecipitate these two proteins. This was an unforeseen complication as previous work done in our lab showed that CAT-tagged 1-88 RUB C expressed from one replicon interacted with FLAG-tagged P150 expressed from another replicon when cotransfected into Vero cells (Tzeng unpublished data). One possible pitfall that could impact our study, but specifically could explain these differences is that our analysis we were overexpressing RUB proteins from a CMV driven promoter, which could result in the formation of protein aggregates or improper stoichiometry of P200* and 1-88 RUB C compared to when these proteins are expressed from RUB virus or RUB replicon. Instead, we examined the interaction of the 1-277 RUB C mutant panel with RUB P200*, both expressed from plasmids. All mutant forms of 1-277 RUB C were pulled down with RUB P200*, indicating that the residues affected by the mutations had no effect on the interaction between the nonstructural polyprotein and RUB C. RUB C contains a long alpha helix from aa 9 through 31 at its N-terminus and previous studies (Tzeng unpublished data) indicated that the binding of RUB C and P150 required aa 1 through 31 of RUB C, a region containing this alpha helix. However, proline

insertion mutants in 1-277 RUB C, designed to disrupt the alpha helix, still interacted with the P200 precursor, indicating that the interaction between RUB C and the RUB nonstructural protein precursor cannot explain the rescue phenomenon.

4.1 Conclusions and significance

The overarching goal of this dissertation was to elucidate the mechanism behind the rescue of the P150 Q domain by RUB C. RUB C and the Q domain of P150 share a similar function as RUB C can be substituted for the Q domain within P150. In both, this function centers on a critical arginine-rich motif. Both also share a similar structure, as the N-terminal third of RUB C, the region necessary for rescue, and the Q domain are both predicted to be highly disordered. This is a hallmark of proteins that act as RNA chaperones and the potential of RUB C to function as an RNA chaperone is attractive as it is able to rescue the replication 5' and 3' CAE mutants (4, 50). Recently, our lab also found that RUB C can rescue mutations in an N-terminal long alpha helix in P200 that is important for proteolytic cleavage of the nonstructural protein, proper subcellular targeting of the nonstructural proteins, RNA synthesis, and the interaction between P150 and P90 (24, 25). Specifically, RUB C is able to rescue the genomic RNA synthesis and increase the number of double-stranded RNA (dsRNA) containing cells (a marker for RCs) for many of the P200 alpha helix mutants tested. Taken together, these findings suggest to us a role for RUB C in the establishment of RCs. Our model is that RUB C mediates the interaction of the genomic RNA with the newly translated P200, possibly serving as a chaperone, to achieve the proper conformation of the RUB genomic RNA and P200 necessary for establishment of the RC and viral RNA synthesis (Figure 24). In this regard, it has been recently shown using a novel transcomplementation system developed for the alphavirus SFV that both the nonstructural replicase pro-

teins and the genomic RNA, as well as functional RNA synthesis, are necessary for generation of observable RCs in transfected cells (43). Our model is also proposed in conjunction with the studies in this dissertation, which found no differences in the early events post-transfection of RUB replicons that could explain RUB C-mediated rescue of P150 when RUB C was provided in *trans*. In terms of the infection cycle, we hypothesize that RUB C in the incoming virus particle plays a chaperone role in the establishment of the initial RCs and appears to be more efficient in this role than is the Q domain, given that wt replicon RNA synthesis is detectable earlier in C-Vero cells than in Vero cells. However, in the expansion of the number of RCs in the infected cell, translation of the genomic RNA may become disconnected from available RUB C protein and when this occurs, the Q domain plays this chaperone role. The question of evolutionary interest is why RUB would have evolved duplicate functions shared by its C protein and one of its replicase proteins when this does not appear to have occurred among other positive-sense RNA viruses, even its closest relatives.

The work described in this dissertation adds to the expanding breadth of knowledge concerning the nonstructural roles of capsid proteins. It is important to continue this work, as important parallels could be drawn between the function of RUB C and other viral capsid proteins in the RNA synthesis of their respective viruses. Small RNA viruses must be able to efficiently replicate with a limited number of viral proteins, and therefore often these proteins must be multifuctional. However, it is intriguing that in RUB, which produces only five mature proteins, that there would be the redundancy in function seen with RUB C and the P150 Q domain, suggesting the importance of this function in the RUB life cycle. The importance of this common function to the life cycle of RUB is further suggested by how many different ways RUB C can be provided to rescue the P150 Q domain, specifically that RUB C can be provided in *cis*, in *trans*, or from

the virion. Furthering the understanding of RUB replication is important because the mechanism behind CRS is still unknown. Aspects of RUB replication that contribute to its teratogenicity could also draw important parallels to other viral teratogens.

4.2 Future directions

Although strides have been reported in this dissertation to understand the basis of the rescue phenomenon, more work needs to be done to address this problem. We were able to identify an arginine cluster within RUB C that is critical for this protein's ability to rescue the replication of RUBrep/GFP-ΔNotI. This arginine cluster was also shown to be important for the early protection of the viral RNA against decay as well as for the binding of RUB C to the viral RNA. First, it could be determined if RUB C and/or the RUB P150 Q domain contain methylated arginines by immunoprecipitating RUB C or RUB P150 Q domain and probing the blot with antibodies to detect methylated arginine. If this proved to be the case, the next steps would be mapping the arginine residues within RUB C and/or the RUB P150 Q domain that are methylated as well as defining the protein arginine methyltransferase responsible for this post-translational modification. Additionally, it could be determined if this modification regulates the rescue of the Δ*Not*I replicon by RUB C.

Further investigation of the role of PITPα in the RUB viral life cycle would be another extension of this study. Particularly, it would be interesting to determine if RUB C does indeed play a role in the PI3K-Akt cell survival pathway that is induced by RUB infection. First, PITPα could be knocked down in cells using a specific siRNA or a nonspecific siRNA (as a control), those cells could be subsequently infected, and viral titers measured to determine if the expression of this protein impacts virus production. Knockdown of PITPα and infection with RUB fol-

lowed by examination of the PI3K-Akt cell survival pathway for activation would indicate if PITPα is required for the activation of this pathway in RUB infected cells. Next, similar experiments could be done to determine if RUB RNA synthesis or RUB protein translation is impacted by the absence of PITPα. The binding site for PITPα within the RUB C protein could be mapped and later mutated in the RUB infectious clone or replicon to determine if this interaction is important for the RUB life cycle.

To provide additional support to our final model, we would first need to confirm that RUB C and the P150 Q domain are RNA chaperones. Next, we could develop a transcomplementation system similar to the one developed for SFV (42) to determine the necessary components required for the establishment of RCs, including RUB RNA sequences and domains of the RUB C, P150, and P90.

4.3 References

1. Beatch, M. D., J. C. Everitt, L. J. Law, and T. C. Hobman. 2005. Interactions between rubella virus capsid and host protein p32 are important for virus replication. J Virol 79:10807-20.
2. Beatch, M. D., and T. C. Hobman. 2000. Rubella virus capsid associates with host cell protein p32 and localizes to mitochondria. J Virol 74:5569-76.
3. Borghese, F., and T. Michiels. 2011. The leader protein of cardioviruses inhibits stress granule assembly. J Virol 85:9614-22.
4. Chen, M. H., I. Frolov, J. Icenogle, and T. K. Frey. 2004. Analysis of the 3' cis-acting elements of rubella virus by using replicons expressing a puromycin resistance gene. J Virol 78:2553-61.
5. Claus, C., W. P. Tzeng, U. G. Liebert, and T. K. Frey. 2012. Rubella virus-like replicon particles: analysis of encapsidation determinants and non-structural roles of capsid protein in early post-entry replication. J Gen Virol 93:516-25.
6. Cockcroft, S. 2001. Phosphatidylinositol transfer proteins couple lipid transport to phosphoinositide synthesis. Semin Cell Dev Biol 12:183-91.
7. Cooray, S., L. Jin, and J. M. Best. 2005. The involvement of survival signaling pathways in rubella-virus induced apoptosis. Virol J 2:1.
8. Dougherty, J. D., J. P. White, and R. E. Lloyd. 2011. Poliovirus-mediated disruption of cytoplasmic processing bodies. J Virol 85:64-75.

9. Duncan, R., A. Esmaili, L. M. Law, S. Bertholet, C. Hough, T. C. Hobman, and H. L. Nakhasi. 2000. Rubella virus capsid protein induces apoptosis in transfected RK13 cells. Virology 275:20-9.
10. Duncan, R., J. Muller, N. Lee, A. Esmaili, and H. L. Nakhasi. 1999. Rubella virus-induced apoptosis varies among cell lines and is modulated by Bcl-XL and caspase inhibitors. Virology 255:117-28.
11. Emara, M. M., and M. A. Brinton. 2007. Interaction of TIA-1/TIAR with West Nile and dengue virus products in infected cells interferes with stress granule formation and processing body assembly. Proc Natl Acad Sci U S A 104:9041-6.
12. Fros, J. J., N. E. Domeradzka, J. Baggen, C. Geertsema, J. Flipse, J. M. Vlak, and G. P. Pijlman. 2012. Chikungunya virus nsP3 blocks stress granule assembly by recruitment of G3BP into cytoplasmic foci. J Virol 86:10873-9.
13. Hiscox, J. A., T. Wurm, L. Wilson, P. Britton, D. Cavanagh, and G. Brooks. 2001. The coronavirus infectious bronchitis virus nucleoprotein localizes to the nucleolus. J Virol 75:506-12.
14. Hofmann, J., M. W. Pletz, and U. G. Liebert. 1999. Rubella virus-induced cytopathic effect in vitro is caused by apoptosis. J Gen Virol 80 (Pt 7):1657-64.
15. Ilkow, C. S., V. Mancinelli, M. D. Beatch, and T. C. Hobman. 2008. Rubella virus capsid protein interacts with poly(a)-binding protein and inhibits translation. J Virol 82:4284-94.
16. Invernizzi, C. F., B. Xie, F. A. Frankel, M. Feldhammer, B. B. Roy, S. Richard, and M. A. Wainberg. 2007. Arginine methylation of the HIV-1 nucleocapsid protein results in its diminished function. Aids 21:795-805.
17. Koyuncu, O. O., and T. Dobner. 2009. Arginine methylation of human adenovirus type 5 L4 100-kilodalton protein is required for efficient virus production. J Virol 83:4778-90.
18. Kujala, P., T. Ahola, N. Ehsani, P. Auvinen, H. Vihinen, and L. Kaariainen. 1999. Intracellular distribution of rubella virus nonstructural protein P150. J Virol 73:7805-11.
19. Kuyumcu-Martinez, N. M., M. Joachims, and R. E. Lloyd. 2002. Efficient cleavage of ribosome-associated poly(A)-binding protein by enterovirus 3C protease. J Virol 76:2062-74.
20. Law, L. J., C. S. Ilkow, W. P. Tzeng, M. Rawluk, D. T. Stuart, T. K. Frey, and T. C. Hobman. 2006. Analyses of phosphorylation events in the rubella virus capsid protein: role in early replication events. J Virol 80:6917-25.
21. Law, L. M., J. C. Everitt, M. D. Beatch, C. F. Holmes, and T. C. Hobman. 2003. Phosphorylation of rubella virus capsid regulates its RNA binding activity and virus replication. J Virol 77:1764-71.
22. Lee, J. Y., J. A. Marshall, and D. S. Bowden. 1999. Localization of rubella virus core particles in vero cells. Virology 265:110-9.
23. Matthews, J. D., and T. K. Frey. 2012. Analysis of subcellular G3BP redistribution during rubella virus infection. J Gen Virol 93:267-74.
24. Matthews, J. D., W. P. Tzeng, and T. K. Frey. 2010. Analysis of the function of cytoplasmic fibers formed by the rubella virus nonstructural replicase proteins. Virology 406:212-27.
25. Matthews, J. D., W. P. Tzeng, and T. K. Frey. 2012. Determinants in the maturation of rubella virus p200 replicase polyprotein precursor. J Virol 86:6457-69.
26. Matthews, J. D., W. P. Tzeng, and T. K. Frey. 2009. Determinants of subcellular localization of the rubella virus nonstructural replicase proteins. Virology 390:315-23.

27. Megyeri, K., K. Berencsi, T. D. Halazonetis, G. C. Prendergast, G. Gri, S. A. Plotkin, G. Rovera, and E. Gonczol. 1999. Involvement of a p53-dependent pathway in rubella virus-induced apoptosis. Virology 259:74-84.
28. Min, J. Y., and R. M. Krug. 2006. The primary function of RNA binding by the influenza A virus NS1 protein in infected cells: Inhibiting the 2'-5' oligo (A) synthetase/RNase L pathway. Proc Natl Acad Sci U S A 103:7100-5.
29. Mizutani, T., S. Fukushi, K. Ishii, Y. Sasaki, T. Kenri, M. Saijo, Y. Kanaji, K. Shirota, I. Kurane, and S. Morikawa. 2006. Mechanisms of establishment of persistent SARS-CoV-infected cells. Biochem Biophys Res Commun 347:261-5.
30. Mocquet, V., J. Neusiedler, F. Rende, D. Cluet, J. P. Robin, J. M. Terme, M. Duc Dodon, J. Wittmann, C. Morris, H. Le Hir, V. Ciminale, and P. Jalinot. 2012. The human T-lymphotropic virus type 1 tax protein inhibits nonsense-mediated mRNA decay by interacting with INT6/EIF3E and UPF1. J Virol 86:7530-43.
31. Montero, H., M. Rojas, C. F. Arias, and S. Lopez. 2008. Rotavirus infection induces the phosphorylation of eIF2alpha but prevents the formation of stress granules. J Virol 82:1496-504.
32. Narayanan, K., and S. Makino. 2012. Interplay between viruses and host mRNA degradation. Biochim Biophys Acta.
33. Netsawang, J., S. Noisakran, C. Puttikhunt, W. Kasinrerk, W. Wongwiwat, P. Malasit, P. T. Yenchitsomanus, and T. Limjindaporn. 2010. Nuclear localization of dengue virus capsid protein is required for DAXX interaction and apoptosis. Virus Res 147:275-83.
34. Neuvonen, M., A. Kazlauskas, M. Martikainen, A. Hinkkanen, T. Ahola, and K. Saksela. 2011. SH3 domain-mediated recruitment of host cell amphiphysins by alphavirus nsP3 promotes viral RNA replication. PLoS Pathog 7:e1002383.
35. Pappas, C. L., W. P. Tzeng, and T. K. Frey. 2006. Evaluation of cis-acting elements in the rubella virus subgenomic RNA that play a role in its translation. Arch Virol 151:327-46.
36. Pugachev, K. V., and T. K. Frey. 1998. Rubella virus induces apoptosis in culture cells. Virology 250:359-70.
37. Rho, J., S. Choi, Y. R. Seong, J. Choi, and D. S. Im. 2001. The arginine-1493 residue in QRRGRTGR1493G motif IV of the hepatitis C virus NS3 helicase domain is essential for NS3 protein methylation by the protein arginine methyltransferase 1. J Virol 75:8031-44.
38. Rivas, C., J. Gil, Z. Melkova, M. Esteban, and M. Diaz-Guerra. 1998. Vaccinia virus E3L protein is an inhibitor of the interferon (i.f.n.)-induced 2-5A synthetase enzyme. Virology 243:406-14.
39. Roberts, S., S. R. Kingsbury, K. Stoeber, G. L. Knight, P. H. Gallimore, and G. H. Williams. 2008. Identification of an arginine-rich motif in human papillomavirus type 1 E1;E4 protein necessary for E4-mediated inhibition of cellular DNA synthesis in vitro and in cells. J Virol 82:9056-64.
40. Sanchez, R., and I. Mohr. 2007. Inhibition of cellular 2'-5' oligoadenylate synthetase by the herpes simplex virus type 1 Us11 protein. J Virol 81:3455-64.
41. Schroder, H. C., D. Ugarkovic, R. Wenger, P. Reuter, T. Okamoto, and W. E. Muller. 1990. Binding of Tat protein to TAR region of human immunodeficiency virus type 1 blocks TAR-mediated activation of (2'-5')oligoadenylate synthetase. AIDS Res Hum Retroviruses 6:659-72.

42. Shire, K., P. Kapoor, K. Jiang, M. N. Hing, N. Sivachandran, T. Nguyen, and L. Frappier. 2006. Regulation of the EBNA1 Epstein-Barr virus protein by serine phosphorylation and arginine methylation. J Virol 80:5261-72.
43. Spuul P, Balistreri G, Hellstrom K, Golubtsov AV, Jokitalo E, Ahola T (2011) Assembly of alphavirus replication complexes from RNA and protein components in a novel trans-replication system in mammalian cells. Journal of virology 85:4739-4751.
44. Suppiah, S., H. A. Mousa, W. P. Tzeng, J. D. Matthews, and T. K. Frey. 2012. Binding of cellular p32 protein to the rubella virus P150 replicase protein via PxxPxR motifs. J Gen Virol 93:807-16.
45. Surjit, M., B. Liu, V. T. Chow, and S. K. Lal. 2006. The nucleocapsid protein of severe acute respiratory syndrome-coronavirus inhibits the activity of cyclin-cyclin-dependent kinase complex and blocks S phase progression in mammalian cells. J Biol Chem 281:10669-81.
46. Surjit, M., B. Liu, S. Jameel, V. T. Chow, and S. K. Lal. 2004. The SARS coronavirus nucleocapsid protein induces actin reorganization and apoptosis in COS-1 cells in the absence of growth factors. Biochem J 383:13-8.
47. Thomas, K. W., M. M. Monick, J. M. Staber, T. Yarovinsky, A. B. Carter, and G. W. Hunninghake. 2002. Respiratory syncytial virus inhibits apoptosis and induces NF-kappa B activity through a phosphatidylinositol 3-kinase-dependent pathway. J Biol Chem 277:492-501.
48. Timani, K. A., Q. Liao, L. Ye, Y. Zeng, J. Liu, Y. Zheng, L. Ye, X. Yang, K. Lingbao, J. Gao, and Y. Zhu. 2005. Nuclear/nucleolar localization properties of C-terminal nucleocapsid protein of SARS coronavirus. Virus Res 114:23-34.
49. Tzeng, W. P., and T. K. Frey. 2009. Functional replacement of a domain in the rubella virus p150 replicase protein by the virus capsid protein. J Virol 83:3549-55.
50. Tzeng, W. P., J. D. Matthews, and T. K. Frey. 2006. Analysis of rubella virus capsid protein-mediated enhancement of replicon replication and mutant rescue. J Virol 80:3966-74.
51. van Tiel, C. M., J. Westerman, M. Paasman, K. W. Wirtz, and G. T. Snoek. 2000. The protein kinase C-dependent phosphorylation of serine 166 is controlled by the phospholipid species bound to the phosphatidylinositol transfer protein alpha. J Biol Chem 275:21532-8.
52. Venter, P. A., D. Marshall, and A. Schneemann. 2009. Dual roles for an arginine-rich motif in specific genome recognition and localization of viral coat protein to RNA replication sites in flock house virus-infected cells. J Virol 83:2872-82.
53. Wang, X., Y. Zhang, J. Xu, L. Shi, H. Fan, C. Han, D. Li, and J. Yu. 2012. The R-rich motif of Beet black scorch virus P7a movement protein is important for the nuclear localization, nucleolar targeting and viral infectivity. Virus Res 167:207-18.
54. White, J. P., A. M. Cardenas, W. E. Marissen, and R. E. Lloyd. 2007. Inhibition of cytoplasmic mRNA stress granule formation by a viral proteinase. Cell Host Microbe 2:295-305.
55. Wurm, T., H. Chen, T. Hodgson, P. Britton, G. Brooks, and J. A. Hiscox. 2001. Localization to the nucleolus is a common feature of coronavirus nucleoproteins, and the protein may disrupt host cell division. J Virol 75:9345-56.

56. Xie, B., C. F. Invernizzi, S. Richard, and M. A. Wainberg. 2007. Arginine methylation of the human immunodeficiency virus type 1 Tat protein by PRMT6 negatively affects Tat Interactions with both cyclin T1 and the Tat transactivation region. J Virol 81:4226-34.
57. Yang, M. R., S. R. Lee, W. Oh, E. W. Lee, J. Y. Yeh, J. J. Nah, Y. S. Joo, J. Shin, H. W. Lee, S. Pyo, and J. Song. 2008. West Nile virus capsid protein induces p53-mediated apoptosis via the sequestration of HDM2 to the nucleolus. Cell Microbiol 10:165-76.
58. Yu, J., B. Shin, E. S. Park, S. Yang, S. Choi, M. Kang, and J. Rho. 2010. Protein arginine methyltransferase 1 regulates herpes simplex virus replication through ICP27 RGG-box methylation. Biochem Biophys Res Commun 391:322-8.
59. Zapp, M. L., T. J. Hope, T. G. Parslow, and M. R. Green. 1991. Oligomerization and RNA binding domains of the type 1 human immunodeficiency virus Rev protein: a dual function for an arginine-rich binding motif. Proc Natl Acad Sci U S A 88:7734-8.
60. Zhang, H. M., J. Yuan, P. Cheung, H. Luo, B. Yanagawa, D. Chau, N. Stephan-Tozy, B. W. Wong, J. Zhang, J. E. Wilson, B. M. McManus, and D. Yang. 2003. Overexpression of interferon-gamma-inducible GTPase inhibits coxsackievirus B3-induced apoptosis through the activation of the phosphatidylinositol 3-kinase/Akt pathway and inhibition of viral replication. J Biol Chem 278:33011-9.
61. Zhao, L., B. K. Jha, A. Wu, R. Elliott, J. Ziebuhr, A. E. Gorbalenya, R. H. Silverman, and S. R. Weiss. 2012. Antagonism of the interferon-induced OAS-RNase L pathway by murine coronavirus ns2 protein is required for virus replication and liver pathology. Cell Host Microbe 11:607-16.

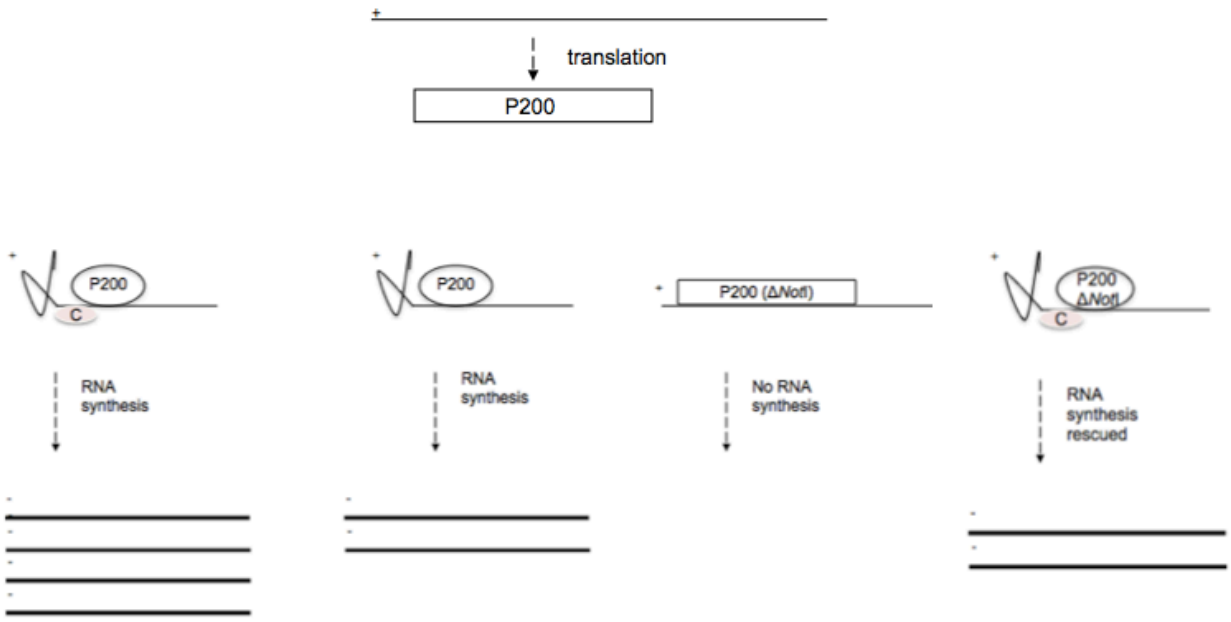

Figure 24. Model of RUB C enhancement and rescue of RNA synthesis